UNIVERSIDADE DE LISBOA

FACULDADE DE CIÊNCIAS

DEPARTAMENTO DE QUÍMICA E BIOQUÍMICA

Solute Carrier Transporters (SLCs) as Possible Drug Targets for Cystic Fibrosis

Íris Lameiro Petinga

Mestrado em Bioquímica

Especialização em Bioquímica Médica

Dissertação orientada por:

Professora Doutora Margarida D. Amaral

2017

Acknowledgments/Agradecimentos

Ao concluir este trabalho não posso deixar de agradecer a todas as pessoas que contribuíram de alguma maneira para a sua realização.

Em primeiro lugar gostaria de agradecer à professora Margarida Amaral não só por me ter recebido no seu laboratório e grupo de investigação, mas também por toda a orientação e acompanhamento e acima de tudo confiança depositada.

Não podia deixar também de agradecer ao professor Carlos Farinha por se ter mostrado sempre disponível para me ajudar, por toda a atenção, paciência e por me ter cativado para a área do estudo da Fibrose Quística desde muito cedo.

Agradeço a todos os meus colegas de laboratório que sempre se mostraram disponíveis para me ajudar, todos eles à sua maneira.

Primeiramente gostaria de agradecer à Verónica que tornou todos os infindáveis "Colony PCR" mais divertidos e me ajudou a seguir em frente quando tudo corria mal.

À Sara cuja paciente infinitiva em me ensinar a trabalhar na cultura e grande parte das outras técnicas que utilizei neste trabalho, para além de responder sempre com boa disposição a todas as minhas dúvidas e questões que foram enumeras e muitas delas sem nexo, por vezes.

À Madalena e aos seus maravilhosos cadernos de laboratório, sem dúvida a minha fonte de inspiração, mesmo longe esteve sempre disponível para responder às minhas dúvidas por mais chatas e aborrecidas que fossem e me fez crer desde o primeiro dia que seria possível. Um obrigado ainda pela sua leitura das versões mais provisórias da minha tese e por todo o investimento de tempo depositado para que ficasse muito melhor.

Á Arsénia por tornar sempre os meus dias mais divertidos e por me fazer acreditar que tudo tem sempre um lado positivo mesmo quando nada funcionava! À nossa Lab manager, Sofia por ter estado sempre lá para mim e por todos os fenomenais cafés. À Margarida Quaresma por ter se sempre mostrado disponível para me ouvir e me ensinar; à Susana por toda a paciência e boa disposição, ao João por todas as conversas sobre a "terrinha" e todos os concelhos dados; à Catarina que foi como uma mãe para mim, sempre disponível e com vontade de ajudar, ao Miqueias pela paciência infinita e por ter sido fundamental na reta final deste trabalho; à Filipa pela sua loucura e boa disposição, à Iris por ter feito sempre pressão para eu continuar a escrever e por partilhar o mesmo nome; ao Luís Sousa pela tranquilidade transmitida; ao Luís Marques pela paciência, pelas horas perdidas com o meu trabalho e por ajudar a torná-lo muito mais bonito. I also want to thank Nikhil, for all his help and be always available to taught me. Gostaria também de agradecer ao Hugo Botelho pela sua disponibilidade em me ajudar sempre que necessário.

Agradeço também a todas as minhas "Petit Gatêus" Diana, Clara, Beatriz, Inês e Sofia que me acompanharam nestes últimos 6 anos e por serem sem dúvida a minha nova família. Obrigado por me fazerem acreditar que era possível, por me animarem sempre que necessário e por todos os momentos que passámos.

Queria também agradecer às minhas amigas de sempre e para sempre à Soraia, Nadine e Jéssica por todo o apoio e por desculparem sempre as minhas ausências. Um muito obrigado por tudo!

Um obrigado muito especial ao João, por me conhecer tão bem por ter estado sempre lá e por me tentar animar nos momentos mais difíceis. Sem ti não teria sido o mesmo!

A toda a minha família, um muito obrigado por acreditarem em mim por terem estado sempre lá em todas as minhas vitórias e por me apoiarem incondicionalmente nas minhas decisões, sem eles nada disto teria sido possível. Obrigado ao meu pai, que é o exemplo que com muito trabalho tudo se consegue e que me motiva sempre a dar o meu melhor. Obrigado à minha mãe, por todo o carinho e por acreditar incondicionalmente em mim. Obrigado à minha maninha por ser tão maluca e por sempre mostrar o orgulho que tem em mim.

Não podia deixar de deixar um especial obrigado à minha tia Carla que é incansável para nos ver felizes e aos meus avós por tudo.

Obrigado a todos!

Abstract

Cystic Fibrosis (CF) is the most lethal autosomal recessive disorder in the Caucasian population, affecting 1: 25,00-6,000 new-borns and with about 85,000 affected people worldwide.

CFTR gene encodes a cAMP regulated chloride (Cl^-) and bicarbonate (HCO_3^-) anion channel expressed in apical membrane of epithelial cells of a variety of tissues. Mutations in the CFTR gene affect the normal processing, trafficking and function of CFTR. F508del, deletion of phenylalanine at position 508, is the most common mutation in CF patients and it is also associated with a severe clinical phenotype.

CFTR protein pays a key role in the regulation of Cl^- and HCO_3^- transport. Additionally, CFTR regulates other ion channels, such as the Epithelial Sodium (Na^+) Channel (ENaC) and it is also described as a regulator of several SLC26A family members.

SLC26 proteins are a large family of anion transports encoded by 11 genes, SLC26A1-SLC26A11, found in all forms of life. These proteins can act as anion exchangers and/or channels of a variety of substrates in epithelial cells, where they have an essential role in the composition and pH regulation of secreted fluids.

The most recent studies have identified and highlighted the role of these transporters in lung physiology, which makes these transporters novel candidates as pharmacological targets for CF. Among the most promising ones are SLC26A4/pendrin and SLC26A9.

SLC26A4 acts as an electroneutral anion exchanger of several substrates, but the Cl^-/HCO_3^- exchange mode is described as the most predominant. Although both pendrin and CFTR have the ability to transport HCO_3^-, it was recently proposed that pendrin controls the composition and pH of secreted fluids, while CFTR regulates the rate of secreted fluid.

In contrast, SLC26A9 functions as Cl^- channel with minimal HCO_3^- conductance and it was reported that it regulates the activity of CFTR, namely leading to an increase in Cl^- currents after stimulation with forskolin when both channels are expressed vs CFTR alone. Furthermore, it was also proposed that the presence of CFTR is essential for SLC26A9 activity. However, the physical and functional interactions between SLC26A4/A9 and CFTR are not completely understood.

The main objective of this MSc project was to identify novel regulators of the two above members of SLC26 family describe above (SLC26A4 and SLC26A9), and to study their functional interaction with CFTR. To achieve these goals, five tasks were proposed: *i)* to determine the influence of the CFTR genotype on SLC26A4/A9 mRNA levels and also on therespective protein subcellular localization in CF patients materials; *ii)* To generate double-tagged SLC26A4/SLC26A9 constructs to be used as traffic reporters; *iii)* To produce inducible novel cell lines stably expressing these double-tagged constructs to develop microscopy-based traffic assays; *iv)* To use such assays in siRNA microscopy screens to identify novel genes involved in regulating the traffic of these proteins that may constitute potential drug targets for CF; and finally *v)* to look for physical and functional interactions with normal and mutant CFTR by determining the localization and function of the protein upon overexpression and downregulation of CFTR.

The localization of both proteins in lung tissue from CF and non-CF individuals was analysed by immunostaining and the results showed that the localization of SLC26A4 and SLC26A9 - mostly at the plasma membrane (PM) – does not seem to be affected by the presence of wt- or mutant CFTR. Quantitative (q)RT-PCR was employed to determine whether the CF genotype affects the transcript levels of SLC26A4 and SLC26A9 in nasal cells from CF and non-CF individuals and also in CFBE stably expressing wt- or F508del-mCherry-Flag-CFTR. Data shown here indicate that although mRNA levels of both transporters seem to be slightly elevated in the lung of CF vs non-CF individuals (and those of SLC26A9 in F508del-CFTR CFBE cells), these differences are not statistically significant.

The double tagged constructs were produced for both proteins and their influence on the normal trafficking and processing of the proteins to the PM was assessed. Although an original construct of SLC26A9 did not expose the 3xHA to the extracellular space, in a second attempt this was successful and it was possible to detected PM expression of both constructs in CFBE cells by transient transfections.

The identification of traffic regulators (task 3) was completed for SLC26A9. The double-tagged construct was cloned into the lentiviral vector pLVX-TRE3G with inducible (Tet-ON) expression and three different CFBE cells lines overexpressing eGFP-3xHA-SLC26A9 3-HA were produced, namely: 1) parental CFBE; and co-expressing either 2) wt-mCherry-Flag-CFTR; or 3) F508del-mCherry-Flag-CFTR. These three novel eGFP-3xHA-SLC26A9 expressing CFBE cells were characterized by both immunostaining and Western Blot techniques. Inducible eGFP-3xHA-SLC26A9 was found to be expressed at the PM and our data also show that its expression does not appear to be dependent on CFTR expression.

Finally, a siRNA microscopy screen using a small siRNA library targeting 206 genes, reported as enhancers of F508del traffic or to interact with CFTR, was performed for CFBE eGFP-3xHA-SLC26A9 cells. Data from this siRNA screen suggest that SLC26A9 traffic to the plasma membrane is affected by genes involved in several biological processes like signal transduction, ion transport, cytoskeleton organization, programmed cell death, positive regulation of cell communication, among others.

Moreover, additional studies and further validation of these results could potentially constitute a new approach for CF therapy involving alternative Cl^- channels.

Key words: Cystic Fibrosis; CFTR; SLC26A4; SLC26A9; alternative Cl^- channels

Resumo

A fibrose quística (FQ) é a doença genética autossómica recessiva mais comum na população caucasiana afetando cerca de 1 em 25,000-6,000 recém-nascidos e com cerca de 85,000 pessoas afetadas em todo o mundo. Esta doença é causada por uma mutação no gene que codifica para a proteína CFTR, (do inglês *Cystic fibrosis transmembrane conductance regulator).* De entre as 2000 mutações encontradas no gene da CFTR, a mais comum e mais severa, é a deleção da fenilalanina na posição 508, com uma incidência de aproximadamente 85 % nos pacientes com FQ.

A CFTR é uma proteína responsável pelo transporte de cloreto (Cl^-) e bicarbonato (HCO_3^-) na membrana apical de várias células epiteliais, tendo um papel fundamental na regulação de processos de secreção e absorção na superfície do epitélio. Para além da sua função no transporte de aniões, a CFTR tem um papel importante no controlo de outros canais iónicos, destacando-se a regulação inibitória da absorção de sódio pela interação com a proteína ENaC, (do inglês *Epithelial Na^+ channel).*

Nos pacientes com fibrose quística, a presença de CFTR não funcional conduz a um desequilíbrio na secreção de cloreto e na absorção de sódio. Consequentemente, ocorre uma desidratação do líquido superficial das vias respiratórias (do inglês *airway surface liquid* (ASL)) com um progressivo aumento da viscosidade do muco e redução do batimento dos cílios. Desta forma, fica comprometido o processo de remoção de bactérias e outros patógenos. Os pacientes apresentam recorrentes infeções bacterianas que progressivamente se traduzem numa inflamação crónica, sendo esta a principal causa de mortalidade dos pacientes com FQ (80 %). Para além disso, os pacientes apresentam elevada concentração de cloreto no suor, sendo esta caraterística usada como método de diagnóstico na clínica. Frequentemente, exibem também outros fenótipos como: insuficiência pancreática e infertilidade masculina. Com menos frequência destaca-se o aparecimento de diabetes relacionada com FQ, ileus meconial e obstrução intestinal e hepática.

Para além da regulação da proteína ENaC, a CFTR regula outros canais iónicos na superfície do epitélio, tais como: os canais de Cl^- ativados por cálcio (CaCC) e os transportadores pertencentes à família SLC26A *(do inglês solute carrier).*

As proteínas SLC26 são uma grande família de transportadores iónicos que codifica 11 genes, SLC26A1-SLC26A11, encontrados em todos os organismos. Estas proteínas apresentam elevada semelhança estrutural apesar da notável diferença no padrão de expressão. Funcionam como canais e/ou trocadores aniónicos de uma grande variedade de substratos na superfície das células epiteliais, tendo um papel essencial na composição e regulação do pH dos fluidos secretados.

Os estudos mais recentes realçam o papel destes transportadores no controlo do transporte iónico na superfície do epitélio, bem como a sua interação e ação recíproca com a proteína CFTR. Consequentemente, no âmbito da fibrose quística dois membros desta família, SLC26A4, também conhecida como Pendrina, e SLC26A9 surgiram como canais alternativos à CFTR e potenciais alvos farmacológicos.

A proteína SLC26A4 funciona como um trocador aniónico eletroneutro antiporte de uma grande variedade de substratos, sendo, no entanto, a troca de Cl^- e HCO_3^- o modo de função predominante. Apesar da CFTR e o SLC26A4 poderem ambos transportar HCO_3^-, o papel de cada um deles é especifico: a pendrina assegura o controlo da composição e pH do líquido secretado enquanto a CFTR regula a taxa de secreção do líquido.

Por outro lado, a proteína SLC26A9 funciona como um canal de Cl^- com mínima condutância para o HCO_3^-. A interação e regulação entre a CFTR e a SLC26A9 tem sido

vastamente estudada e sabe-se que o SLC26A9 aumenta o transporte de Cl^- dependente da ativação da proteína cinase A da CFTR. Para além disso, a presença de SLC26A9 aumenta a expressão de CFTR na membrana plasmática, o que poderá indicar um papel deste canal iónico na biogénese e/ou estabilidade da CFTR.

SLC26A9 é também descrito como um gene modificador de FQ. Nomeadamente, um polimorfismo no gene SLC26A9 está associado com uma maior suscetibilidade e severidade de patologias associadas com a fibrose quística, como ileus meconial, diabetes relacionada com FQ e destruição pancreática pré-natal.

O principal objetivo deste trabalho é a identificação de novos reguladores destes dois membros da família SLC26A, SLC26A4 e SLC26A9 bem como estudar a interação destes transportadores com a CFTR. Desta forma o trabalho foi dividido em cinco tarefas principais: *i)* determinar a influência do genótipo da CFTR nos níveis de mRNA bem como na respetiva localização subcelular em amostras de pacientes; *ii)* Produção de constructos destas proteínas com dois tags para serem usados como reporters de tráfego iii) Produção de novas linhas celulares que expressem os constructos desenvolvidos para o uso em ensaios de microscopia de fluorescência *high-throughput*; iv) Usar *screens* com bibliotecas de siRNAs para identificar novos genes envolvidos na regulação destas proteínas e que possam ser novos e potenciais fármacos no tratamento de FQ; v) Estudar as interações funcionais entre estas proteínas e a CFTR na sua versão normal ou mutada através da localização e função das proteínas em condições de presença ou ausência de CFTR.

A localização das proteínas em amostras de pacientes com FQ ou control (sem FQ) foi analisada por imunofluorescência e os resultados mostram que a localização de SLC26A4 e SLC26A9, na membrana plasmática, não é afetada pela presença de CFTR normal ou mutada. O estudo do efeito do genótipo nos níveis transcricionais de SLC26A4 e SLC26A9, realizado por quantitativo (q)RT-PCR em CFBE wt- ou F508del-mCherry-Flag-CFTR e em células nasais de indivíduos com FQ e sem FQ, mostra que, embora os níveis de mRNA pareçam ser ligeiramente elevados em pacientes com fibrose quística essa diferença não é significativa.

Os construtos com dois tags foram produzidos para ambas as proteínas e o seu estudo no tráfego e processamento das proteínas para a membrana plasmática foi avaliado. Embora com o construto original de SLC26A9 não fosse possível detetar a expressão na membrana plasmática, devido à ausência do tag 3-HA no espaço extracelular, numa segunda tentativa foi possível detetar a expressão na membrana plasmática de ambos os construtos em células CFBE.

A terceira tarefa foi apenas concluída para a proteína SLC26A9. O construto foi clonado no vetor lentiviral pLVX-TRE3G e foram produzidas três linhas celulares que sobreexpressam eGFP-3xHA-SLC26A9: 1) CFBE parental; e co-expressão com 2) wt-mCherry-Flag-CFTR; ou 3) F508del-mCherry-Flag-CFTR SLC26A9 3-HA GFP, sob controlo de um promotor indutivel (Tet-ON).

Estas novas linhas celulares que sobre-expressam o construto eGFP-3xHA-SLC26A9 foram analisadas por técnicas de imunofluorescência e por Western Blot. A expressão de eGFP-3xHA-SLC26A9 na membrana plasmática foi detetada em todas as linhas celulares, concluindo-se assim não ser dependente da expressão de CFTR.

Por fim, foi feito um *screen* preliminar de uma pequena biblioteca de siRNAs que afetam 206 genes conhecidos por aumentar o tráfego da proteína F508del-CFTR para a membrana e genes que codificam para proteínas que fazem parte do interactoma da CFTR, usando as células

que sobre-expressam apenas eGFP-3xHA-SLC26A9. De entre os 81 genes que afetam o tráfego da proteína SLC26A9 para a membrana plasmática: 52 deles aumentam a expressão desta proteína na membrana plasmática enquanto os restantes 29 inibem a sua expressão. Os resultados do *screen* mostram que o tráfego da proteína SLC26A9 para a membrana plasmática é afetado por genes envolvidos em diversos processos biológicos tais como: vias de transdução de sinal, transporte iónico, organização do citoesqueleto, morte celular programada, regulação positiva da comunicação célula-célula, entre outros. Para além disso, estes resultados demonstram que muitos dos genes envolvidos no controlo do tráfego da proteína CFTR também afetam o tráfego da proteína SLC26A9 sugerindo assim uma corelação entre as vias de tráfego destas proteínas.

Posteriores validações dos resultados obtidos podem futuramente potenciar uma nova estratégia para o desenvolvimento de novas terapias para a FQ com recurso a canais de Cl^- e HCO_3^- alternativos. Para além disso, o melhor conhecimento do normal funcionamento e regulação destes dois membros, SLC26A4 e SLC26A9, poderá evidenciar novas vias de regulação que poderão compensar a ausência de CFTR.

Palavras chave: Fibrose quística, CFTR, SLC264; SLC26A9; canais de Cl^- alternativos

Table of contents

Index of figures and tables

Abbreviations

ABC	ATP-binding cassette
AE	Anion exchanger
ASL	Airway surface liquid
Asn	Asparagine
ATP	Adenosine triphosphate
BSA	Bovine serum albumin
C-terminal	Carboxly-terminal
CaCC	Ca^{2+} activated chloride channel
$CaCl_2$	Calcium chloride
cAMP	Cyclic adenosine monophosphate
CAL	CFTR associated ligand
CAP-1	CFTR associated ligand
CAP-70	CFTR associated protein -70
cDNA	Complementary DNA
CF	Cystic Fibrosis
CFBE 41 o^- / CFBE	Cystic fibrosis bronchial epithelial cells
CFTR	Cystic fibrosis transmembrane conductance regulator
Cl^-	Chloride
CO_2	Carbon dioxide
COPD	Chronic obstructive pulmonary disease
DMEM	Dulbecco's Modified Eagle Medium
Dox	Doxycycline
DTDST	Diastrophic dysplasia sulphate transporter
E-Cad	Epithelial cadherin
ECL	Extracellular loop
eGFP	Enhanced green fluorescente protein
EMEM	Eagle’s minimum essential medium
ENaC	Epithelial sodium channel
ER	Endoplasmic reticulum
ERQC	ER quality control
FBS	Fetal bovine serum
F508del	Deletion of phenylalanine (F) residue at position 508
eGFP	Enhanced Green fluorescent protein
HBE	Human bronchial epithelial (cell line)
HCO_3^-	Bicarbonate
HEK	Human embryonic kidney (cell line)
IL	Interleukin
IVS	Intervening sequence
KDa	KiloDalton
MCC	Mucociliary clearance
$MgCl_2$	Magnesium chloride
MSD1/2	Membrane-spanning domain 1/2
NaCl	Sodium chloride
NBD1/2	Nucleotide binding domain 1/2
N-terminal	Amino-terminal
NHERF	Sodium-proton exchange regulatory factor

NMD	Non-sense mediated decay
OHC	Outer hair cells
ORCC	Outwardly rectifying chloride channel
PAGE	Polyacrylamide gel electrophoresis
PBS	Phosphate buffer saline
PBS-T	Phosphate buffer saline with Tween
PCR	Polymerase chain reaction
PDZ	PDS-95, Disc-large, and ZO-1
PFA	Paraformaldehyde
PKA	Protein kinase A
PM	Plasma membrane
PTC	Premature termination codon
PVDF	Polyvinylidene fluoride
(q)RT-PCR	(Quantitative) reverse transcriptase polymerase chain reaction
RD	Regulatory domain
RNA	Ribonucleic acid
RT	Room temperature
RT-PCR	Reverse transcription polymerase chain reaction
Sat-1	Sulphate anion transporter 1
SDS	Sodium dodecyl sulphate
siRNA	Small interfering RNA
SLC	Solute carrier
STAS	Sulphate transporter and anti-sigma factor antagonist
TM	Transmembrane (segment)
TMED	Tetramethylethylenediamine
TMEM16 (ANO)	Transmembrane protein 16 (Anoctamin)
TNF-α	Tumor necrosis factor alfa
Tris	Tris(hydroxymethyl)aminomethane
UV	Ultraviolet
VRAC	Volume-regulated anion channel
wt	wild type

1. Introduction

1.1) Cystic fibrosis and CFTR

1.1.1) Cystic fibrosis disease

Cystic fibrosis (CF) is the most common life-limiting autosomal recessive disorder in the Caucasian population. CF has a carrier frequency of 1 in 25-40 individuals, and it affects around 85,000 worldwide[1]. CF incidence is higher in individuals of Northern European ancestry, affecting 1 in 2,500-3,000 new-borns, and it is lower in Southern Europe (1: 4,000-6,000) and Asian-Americans, (1:30,000)[2]. Dorothy Andersen published the first article describing CF of the pancreas and its relation to celiac disease, a gastrointestinal pathology, in 1938[3]. Only 50 years later, in 1989, at the hospital for Sick Children in Toronto the gene responsible for CF was identified and named Cystic Fibrosis Transmembrane Conductance Regulator (CFTR)[4].

CFTR encodes a cAMP-regulated chloride (Cl^-) and bicarbonate (HCO_3^-) anion channel expressed in the apical membrane of epithelial cells from a variety of tissues. To date there are ~2,000 mutations reported in the CFTR gene which cause different defects by affecting protein synthesis, folding, intracellular trafficking, channel gating, Cl^- conductance and/or plasma membrane stability [5,6]. However, the basic defect associated with all disease-causing mutations leads to the same consequence, i.e., decreased or absent anion conductance at the apical membrane of epithelial cells.

CFTR is a key regulator of secretion and absorption in several tissues, including the airways, gastrointestinal and reproductive tracts and secretory glands. Besides controlling Cl^- and HCO_3^- transport, CFTR regulates other non-CFTR channels[7]. One of these is the Epithelial Sodium (Na^+) Channel (ENaC) having CFTR an inhibitory effect on ENaC and, consequently on Na^+ transport [8]. Thus, in CF patients, where CFTR is non-functional, besides reduced Cl^- secretion, there is Na^+ hyperabsorption[9].

This imbalance in ion transport found in all CF patients leads to the dehydration of airway surface liquid (ASL) which consequently enhances mucus viscosity and decreases mucociliary clearance (MCC) leading to mucus accumulation and increased airway obstruction [10]. The removal of bacteria and other pathogens is thus compromised. Additionally, the absence of CFTR-mediated HCO_3^- secretion leads to an acidification of the ASL pH which compromises the innate immune system ability to kill bacteria[9]. Therefore, there is an exacerbated and chronic inflammatory response characterized by an increase in pro-inflammatory cytokines such as IL-8, IL-6, tumour necrosis factor alfa (TNF- α) and arachidonic acid metabolites, leading to impaired lung regeneration and progressive damage[11–15]. Recurring respiratory infections especially by *Pseudomonas aeruginosa* is a hallmark of CF and a leading cause of morbidity in people with CF[16].

In addition to recurrent pulmonary infections and chronic inflammation, elevated Cl^- concentration in sweat is another characteristic of CF patients, which led to the establishment of the elevated sweat Cl^- as the most widespread diagnosis biomarker. Moreover, meconium ileus, infertility (principally in male [17]) and pancreatic insufficiency (affecting 85% of CF patients[6]) are also very common CF symptoms.

1.1.2) CFTR – Gene, protein and mutations

Gene and mutation

CFTR gene is localized at the long arm of chromosome 7 (7q31.2) and consists of 27 exons and a TATA-less promoter, spanning over 190 kb that after transcription results in an mRNA of 6.5 kb[18].

Among the 2,000 mutations which were so far reported[19], only 10% (200~) are associated with disease liability at the CFTR2 Clinical and Functional Translation of CFTR database[20]. Deletion of a phenylalanine in the position 508 (F508del) located in the first nucleotide binding domain (NDB1), is the most common CF-causing mutation, with an incidence of about 85 %, and it is associated with a severe phenotype[21,22].

CFTR mutations have been distributed in seven classes according to the molecular and cellular defect they cause on CFTR protein (Fig.1). **Class I** mutations abolish protein production, including nonsense or premature termination codon (PTC) mutations. These mutations lead to a truncated mRNA which is consequently degraded by the RNA non-sense mediated decay (NMD) surveillance mechanism; **Class II** mutations lead to the synthesis of a misfolded protein, and consequently affect CFTR processing and traffic; **Class III** mutations result in a dysfunctional CFTR protein due to a defect in gating; **Class IV** represents mutations that lead to a CFTR channel with defective conductance; **Class V** mutations result in decreased protein synthesis; and **Class VI** mutations, lead to a protein with high turnover at the apical surface, due to increase CFTR endocytosis or to its decreased recycling to the cell surface[23]. Recently a new class has been proposed: Class VII also known as "unrescuable" mutations, due to the absence of mRNA transcription, englobes, e.g., large deletions/insertions that cannot be pharmacologically rescued[24].

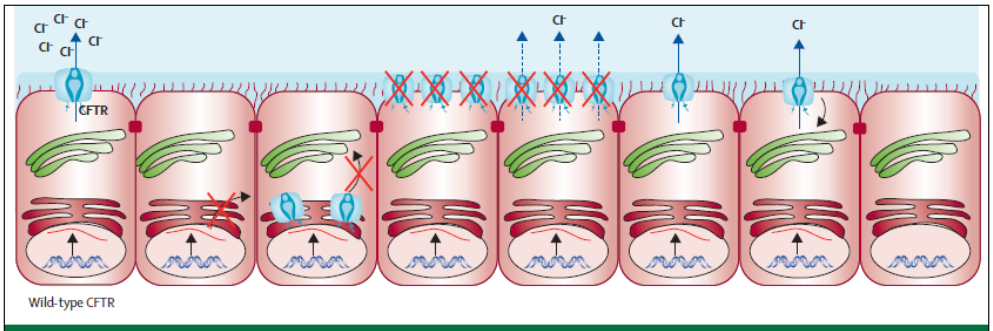

	Class I	Class II	Class III	Class IV	Class V	Class VI	Class VII
CFTR defect	No protein	No traffic	Impaired gating	Decreased conductance	Less protein	Less stable	No mRNA
Mutation examples	Gly542X, Trp1282X	Phe508del, Asn1303Lys, Ala561Glu	Gly551Asp, Ser549Arg, Gly1349Asp	Arg117His, Arg334Trp, Ala455Glu	Ala455Glu, 3272-26A→G, 3849+10 kg C→T	c. 120del23, rPhe508del	dele2,3(21 kb), 1717-1G→A

Figure 3.1 The seven classes of CFTR mutations [Adapted from [24]].

CFTR protein- Structure and function

CFTR is a transmembrane protein with 1,480 amino acids residues expressed in the apical membrane of epithelial cells. It is a member of the **A**TP-**b**inding **c**assette (ABC) transporters proteins, but it is the only one that acts as an ion channel rather than as an active transporter. CFTR shares the structure of ABC family members, that consists of two membrane-spanning domains (MSD1 and MSD2) each comprising 6 transmembrane (TM) segments that form the channel pore; two nucleotide-binding domains (NBD1 and NBD2), which form a "head-to-tail" dimer that binds and hydrolyses ATP; and a regulatory domain (RD), intrinsically unstructured which regulates channel opening and closing by phosphorylation/ dephosphorylation at its multiple PKA phosphorylation sites.

The N- and C-terminus of CFTR are both cytoplasmic. In the C-terminus there is a PDZ binding domain (D/E)T(R/K)L that has been shown to be essential for CFTR stability at the PM and where several other protein with PDZ-binding domains have been shown to bind, such as the Na^+–proton exchange regulatory factor (NHERF), CFTR-associated protein-70 (CAP70), and CFTR associated ligand (CAL)[25].

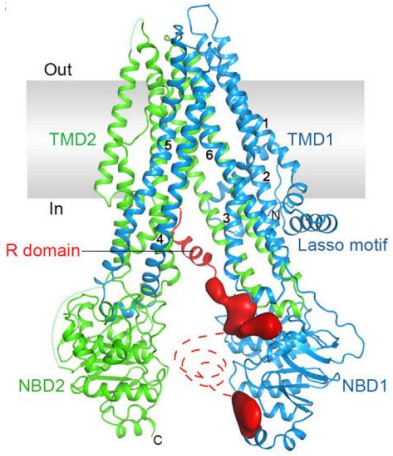

Figure 1.4 Structure of human CFTR in the closed (ATP-free) conformation [Adapted from [26]].

CFTR is synthesized in the cytoplasm and enters the endoplasmic reticulum (ER), where it starts its assembly and folding to follow the secretory pathway to reach the PM. In the ER lumen, CFTR is core-glycosylated at two Asn residues located in the 4th extracellular loop (ECL) undergoing then trafficking to the Golgi complex, where it is fully-glycosylated thus acquiring its mature form that is trafficked to the cell surface. CFTR folding is constantly monitored by ER quality control (ERQC) machinery[27].

In addition to its own function as a channel, CFTR also plays a significant role in the regulation of other channels (see below). CFTR has also been described to be involved in other processes such as regulation of vesicle trafficking, ATP release, and expression of inflammatory mediators (IL-8, IL-10 and nitric oxide synthase)[28], although these roles have not been confirmed.

1.1.3) CFTR as a major regulator of other epithelial ion channels

As already stated, CFTR has been described to control the activity of other channels and transporters in epithelial cells. Among these channels are ENaC, calcium (Ca^{2+})-activated Cl^- channels (CaCCs)[29], namely TMEM16A; outwardly rectifying Cl^- channels (ORCCs)[30], potassium (K^+) channels (such as ROMK2)[25], volume-regulated anion channels (VRACs)[29] and members of the solute carrier channels and transporters family (SLC26A).

CFTR was described to interact with several SLC26A family members, but while it has been reported as essential for the activity of the SLC26A's, the opposite does not appear to occur, i.e., CFTR activity does not rely on the expression of SLC26A's. However, the presence of SLC26A members was described to increase the activity of CFTR[31–33].

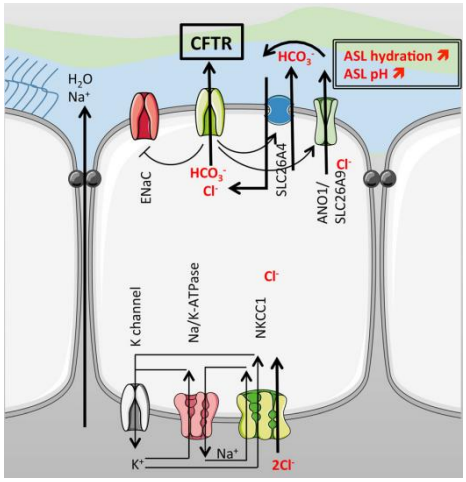

Figure 1.3 Ion transport in the airways. CFTR interacs at the apical membrane with ENaC, SLC26A4, SLC26A9 and ANO1. [Adapted from [7].]

1.1.4) Current advances in therapy development

The advances in therapy development in the last decade have revolutionized the approach to treat CF and increased dramatically the quality of life of CF patients. Until recently only the standardized symptomatic treatments existed, which included: antibiotics to prevent and control lung infections; mucolytics to make the mucus less thick and sticky; anti-inflammatory drugs to deal with chronic inflammation; oral pancreatic enzymes to compensate for the absence of their physiological secretion and a hypercaloric diet to maintain a good nutritional status[34].

However, the novel drugs that are becoming available are mainly focused on correcting structural and functional abnormalities of CFTR[2]. This new group of drugs are called CFTR modulators and in 2012 the first CFTR potentiator was approved, known as Ivacaftor (VX-770), for CF patients with a gating mutation (Class III)[9].This CFTR potentiator (developed by Vertex Pharmaceuticals) increases the function of CFTR at the plasma membrane (PM). In 2015 a CFTR corrector Lumacaftor (VX-809), was approved for patients with the F508del mutation (Class II). This drug acts by correcting protein folding and thus increases the quantity of protein that traffics to the PM. More recently, a combination of both drugs was approved for patients that are homozygous for the F508del mutation, and the results show a higher CFTR function when compared with the effect of each drug alone[24]. Despite these positive results, only a limited number of mutations can be treated with this approach.

Other therapies have been in development with a growing importance in the last years. Examples of these are read-through agents, that can benefit all patients with premature stop codon mutations (Class I), and targeting non-CFTR channels[35]. This non-CFTR approach can be used as an alternative route for Cl^-/HCO_3^- transport which can compensate for CFTR dysfunction in the airway epithelia. The manipulation of other ion channels can be a treatment for patients with "unrescuable" mutations (Class VII) as such therapy would apply to all CF patients, being thus as 'mutation-agnostic' therapy.

Among non-CFTR Cl^- channel candidates that could serve as drug targets for CF, are SLC26A4/pendrin and SLC26A9, two solute carrier transporters[36]; the CaCC anoctamin 1 (ANO1/TMEM16A)[37–39] and the epithelial Na^+ channel, ENaC[36].

1.2) SLC26 gene family of anion transporters and channels

1.2.1) Solute Carrier Family, SLC26A family

In the late 1990s, the SLC26 gene family emerged as structurally distinct from the classic SLC4 anion exchanger (AE) gene family, with similar transport functions[40]. The SLC26 gene family belongs to a highly conserved superfamily of amino acid-polyamine organocation APC transporters and encodes 11 genes, SLC26A1-A11, with SLC26A10 being a pseudo-gene[41]. The SLC26 proteins, also known as SulP proteins, constitute a large family of anion transporters which are ubiquitously expressed in all forms of life, demonstrating an essential importance of these membrane proteins in biology[42,43]. All family members are well conserved in the number and size of exons and protein amino acids length, but have noticeably different tissue expression patterns and function[44].

Structure

The human SLC26A proteins are comprised of 606 (SLC26A11) to 970 (SLC26A8) amino acids. All proteins share a similar structure characterized by two major domains: a NH_2-terminal membrane domain with 10-14 transmembrane domains, and a STAS (sulphate transporter and anti-sigma factor antagonist) domain in the C-terminus localized in the cytosol[45]. In addition, some C-terminus regions exhibit PDZ recognition motifs[46].

The N-terminus of SLC26 transporters represents two-thirds of the protein. It is mainly hydrophobic and it is where the anion binding and pore are thought to be localized. It is difficult to predict with accuracy the exact number of SLC26 transporter transmembrane spans. However, many algorithms have shown that SLC26 transports span the lipid bilayer 10 to 14 times[41,42].

The STAS domain localized at the C-terminus of SLC26 transporters was found to be similar to the anti-sigma factor antagonists SpoIIAA from *Bacillus subtilis*[45,47]. Namely, the core structure of isolated STAS domain of several bacterial members also resemble the STAS domain from SpoIIAA proteins, which suggests that the SpoIIAA and SLC26 STAS domains have similar structures[45].

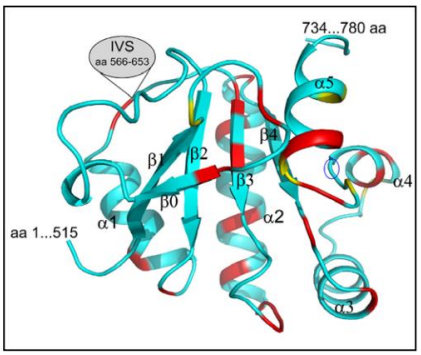

Figure 1.4 STAS domain structure [adapted from [46]].

More recently it has been shown that STAS domains of divergent amino acid sequence exhibit a conserved structure characterized by a central core of 4 β strands flanked by 5 α helices, as represented in Fig 1.4. However, the mammalian STAS domains are distinct from the bacterial STAS domains by a large insertion, intervening sequence (IVS) region, between the first helix and the third strand of the SLC26 STAS domain[45,46].

The bacterial STAS domain has been intensively studied and it was reported to have a key role in the regulation of the large family of sigma factors that bind to the RNA polymerase, which consequently controls the specificity of the target gene[46]. In mammalians, the STAS domain has been hypothesized to be a protein-protein interaction domain. To support this idea, the STAS domains of human and mouse SLC26A3 and SLC26A6 were described to interact with the RD of CFTR[48] and with NHERF2/CAP70[49,50], NHERF1/2[51], respectively. Although further studies are needed, the data already described suggest that the STAS domain is important for membrane targeting and function of the transporters.

Additionally, the linking region between the final transmembrane segment and the beginning of STAS domain has been shown to have a significant role, namely for SLC26A3, in the normal folding and exit from the ER[52].

Recent studies have suggested that SLC26 proteins organize in functional homo-oligomeric structures, more specifically homodimers or homotetramers[53]. However, each subunit is thought to constitute its own anion translocation entity[54].

Function, cellular localization and related diseases

The SLC26 family members act as anion exchangers or channels of a variety range of substrates, such as Cl^-, HCO_3^-, iodide (I^-), bromide (Br^-), hydroxide (OH^-), sulphate (SO_4^{2-}), oxalate, formate and glyoxylate, across the apical or basolateral membranes of polarized cells[41,54,55].

Altogether, the SLC26 proteins are widely expressed in epithelial cells where they contribute to the composition and pH regulation of secreted fluids.

SLC26 transporters have been shown to be electroneutral[56–59] or electrogenic[59,60], depending on the SLC26 protein and substrate and perhaps also on the tissue or expression system.

The functional diversity of the SLC26 proteins makes it difficult to predict their function from sequence homology[41]. Most of SLC26 family members catalyse Cl^-/ HCO_3^- and function as anion

exchangers. Only SLC26A7 and SLC26A9 have been reported to function additionally or exclusively as anion channels.

SLC26 proteins can be organized in three main groups based on the function and similarities described until now. Class 1 includs sulphate (SO_4^{2-}) transporters, SLC26A1 and SLC26A2; in class 2 are the Cl^-/HCO_3^- exchangers SLC26A3, SLC26A4 and SLC26A6, and the Class 3 includes the anion channels, SLC26A7 and SLC26A9[41].

SLC26A1 is the first member of the human SLC26 transporters and it is known as the sulphate anion transporter 1 (Sat-1). Besides sulphate transport, SLC26A1 also mediates the transport of oxalate and HCO_3^-. The uptake of sulphate is increased by acidic extracellular pH and by extracellular low concentrations of halides[41,43]. SLC26A1 is widely expressed in liver, pancreas and brain[61]. SLC26A2 functions as an electroneutral anion exchanger of sulphate, oxalate, I^-, OH^-, Br^- and NO_3^-. In opposition to SLC26A1, SLC26A2 appears to function as a SO_4^{-2}/Cl^- exchanger[62]. SLC26A2 is the gene responsible for diastrophic dysplasia and consequently is also known as diastrophic dysplasia sulphate transporter (DTDST)[63].

Class 2 proteins are mainly found in the luminal membrane of secretory epithelia where they have a key role in Cl^- absorption and HCO_3^- secretion. SLC26A3 is expressed mainly in the intestine where the exchange activity is coupled to NHE^{3-} mediated Na^+/H^+ exchange to generate electroneutral NaCl reabsorption across the intestinal mucosa. SLC26A3 is the gene responsible for congenital chloride diarrhoea[64]. SLC26A6 can act as electroneutral or electrogenic exchanger depending on the substrate. It is reported ta have a key role as a component of the pH buffering system essentially in the kidney and lung. Besides that, it is known to play an important function in sperm capacitation by increasing intracellular pH. SLC26A4, also known as pendrin, is an electroneutral anion exchanger with a broad anion substrate selectivity, including $Cl^–$, $HCO_3^–$, $I^–$, formate, nitrate, and $SCN^–$ [65,66]. Pendrin has a key role in regulation of pH and composition of the secreted fluid. Mutations in SLC26A4 are clinically associated with Pendred syndrome, characterized by deafness due to the loss of transport function. Moreover, pendrin is also known as a disease-causing gene for autosomal recessive non-syndromic deafness (DFN4)[67].

SLC26A7 is expressed in high endothelial venules, kidney, stomach, nasal epithelium, and epididymal ducts[68–71]. SLC26A7 was firstly described as an anion exchanger of Cl^-/HCO_3^- based on phi measurements in *Xenopus* oocytes[68]. However, SLC26A7 has recently been described as a highly selective $Cl^–$ channel with minimal $HCO_3^–$ permeability. The physiological role of this protein has not been already identified, but it is predicted to function as a sensor of pH in the cell[69]. SLC26A9 is highly expressed in the apical membrane of the airway epithelia and gastric parietal cells. Similarly to SLC26A7, it was first identified as a Cl^-/HCO_3^- exchanger, but it was later reported as a highly selective Cl^- channel with minimal HCO_3^- permeability[60,72].

SLC26A5, SLC26A8 and SLC26A11 are not well studied as the remaining family members, and consequently they were not inserted in any class. SLC26A5 is the gene responsible for the motility of outer hair cells (OHCs) in the cochlea. Instead of acting as an anion transporter, SLC26A5 undergoes a conformational change in response to alteration of intracellular Cl^- levels[73,74]. SLC26A8 is found in male germ line and brain, and has been suggested to function as a sulphate or I^- transporter. Due to its expression in testis it was predicted to have a role in male fertility[75–77]. Finally, SLC26A11 was described as a $Cl^–$, $SO_4^{2–}$ and oxalate exchanger. It is mainly expressed in kidney, brain and placenta but its physiological role is not currently understood[78].

Besides the functional diversity between the members of the SLC26 family, recent studies have identified and highlighted the role of these transporters in lung physiology. These findings make these transporters new biomarkers for airway disease and promising novel pharmacological targets.

For CF, the focus is in the SLC26A4/pendrin and SLC26A9 as alternative routes, respectively for HCO_3^- and Cl^-secretion in airway epithelia.

1.2.2) SLC26A4 (Pendrin)

Pendrin is a membrane protein with 780 amino acid residues and two putative glycosylation sites in ECL2, Asn 167 and Asn 172. As the other members of the SLC26A family, pendrin has both N- and C- termini in the cytoplasm and a STAS domain in the C terminus. Recent studies, suggest that SLC26A4 has 14 transmembrane domains[79].

Pendrin functions as an electroneutral anion exchanger with a variety of substrate selectivity such as, Cl^-, HCO_3^-, I^-, formate, NO_3^- and thiocyanate (SCN^-). Even though pendrin can act in different modes, the Cl^-/ HCO_3^- exchange mode is described as the predominant one[65,80].

The SLC26A4 gene product is expressed at the apical membrane of airway epithelial cells[65,81–83], salivary ducts[84], thyrocytes (follicular cells)[85]and renal collecting duct type B intercalated cells[85]. In addition, it is also expressed in cochlear epithelial cells of the spiral prominence, root cells and in spindle cells of the *stria vascularis* of cochlear duct[86].

The function of pendrin seems to be tissue-specific. In the inner ear pendrin has a key role in maintaining Cl^- and HCO_3^- homeostasis, which is crucial for normal hearing[87]. In the thyroid gland, pendrin mediates the transport of I^- which is fundamental for thyroxine biosynthesis[88]. In the kidney pendrin activity is linked to ENaC and it is described as having a key role in the regulation of acid-base balance and extracellular volume by mediating Cl^- and Na^+ reabsorption and HCO_3^- secretion[89,90]. In the airways, pendrin is reported to have a key role in acid-base homeostasis by functioning as a Cl^-/HCO_3^- exchanger[91].

A recent study reported that the activity and substrate affinity of pendrin is regulated by intracellular and extracellular pH[92]. Namely, it was described an increase on pendrin activity with low intracellular or extracellular pH. These results suggest that pendrin has an extracellular and an intracellular proton regulatory site. Interestingly, pendrin glycosylation seems to be essential for pendrin sensitivity to extracellular pH but not for the correct traffic of the protein to the PM[89].

Besides Pendred syndrome and DFN4, pendrin is also associated with a range of respiratory diseases, including asthma, COPD, rhinovirus infection, rhinitis and chronic rhinosinusitis[90,93–95]. Indeed, pendrin overexpression was reported in asthma and COPD models. In subsequent work, it was described the link between inflammatory cytokines, IL-4, IL-17 and IL-13 and pendrin overexpression[95–97]. Moreover, it was reported that IL-4 stimulated Cl^-/SCN^- exchange delivers SCN^- substrate to lactoperoxidase for the synthesis of hypothiocyanite ($OSCN^-$), which has antimicrobial properties[98]. In addition, pendrin overexpressing in the airways has been shown to lead to neutrophil recruitment and mucus overexpression, due to the increase of HCO_3^- that facilitates the solubilisation and transport of macromolecules, namely of mucins, the major components of mucus[83,95].

Until recently, CFTR was the only pathway described for HCO_3^- secretion. However, recent studies have reported that SLC26A4 has a key role in HCO_3^-secretion in cells also expressing CFTR. However, the relative role of CFTR and pendrin in HCO_3^- secretion is not established. A recent study in airway serous cells expressing SLC26A4 and CFTR shows that pendrin is responsible for the

composition of secreted fluid and consequently pH, while CFTR predominately controls the rate of liquid secretion[91].

These data suggested that pendrin has a critical role in transcellular HCO_3^- secretion and consequently in maintaining the pH homeostasis, which highlights pendrin as possibly being able, upon stimulation, to bypass the absence of CFTR-mediated HCO_3^- secretion in CF patients.

1.2.3) SLC26A9

SLC26A9 is a membrane protein with 791 amino acid residues and two putative glycosylation sites in ECL2, Asn 153 and Asn 156. It is predict that SLC26A9 has both N- and C-termini localized in the cytoplasm and 12 transmembrane domains[42]. In the C-terminus, the STAS domain is followed by a PDZ- motif type II, PSD95-Dlg1-Zo-1[99,100].

SLC26A9 is robustly expressed in the apical membrane of airway epithelial cells[77] as well as in the gastric mucosa and to a less extent in the kidney, brain and reproductive tracts[101,102]. SLC26A9 function is still controversial. Firstly, a Cl^-/HCO_3^- exchange activity was described in HEK cells stably expressing SLC26A9[103]. Later, another group reported that SLC26A9 acts as a Cl^- channel with minimal HCO_3^- permeability in both *Xenopus* oocytes and HEK cells transiently transfected with SLC26A9[99].

Additionally, the physiological role of SLC26A9 is not completely understood. SLC26A9 was proposed to mediate the HCO_3^- secretion needed for protection of the gastric mucosa against injury[104]. In the lung, SLC26A9 is up-regulated in Th2-mediated airway inflammation and it was suggested that it can mediate Cl^- secretion, preventing airway mucus plugging when there is mucus hypersecretion[105,106]. However, the knowledge on the regulation of SLC26A9 in the airway epithelia remains limited.

Physical interaction between CFTR and SLC26A9 has been well documented and confirmed by co-immunoprecipitation in HEK and HBE (human bronchial epithelial) cells co-expressing both proteins[103,107,108]. Interestingly, it was described that SLC26A9 can co-immunoprecipitate with both mature and immature CFTR, thus suggesting that these proteins interact at an early stage in their biogenesis, quite possibly in the ER[107]. This interaction has been shown to affect the activity of CFTR, being reported that SLC26A9 enhances CFTR Cl^- conductance[72,109]. Bertrand *et al* demonstrated that the magnitude of the current observed after stimulation with forskolin is higher in cells co-expressing SLC26A9 and CFTR when compared to cells expressing each channel individually[103,107]. Also, the magnitude did not correspond to the sum of both currents, which suggests a reciprocal regulatory interaction[103].

Moreover, it was found that the expression of CFTR is not essential for SLC26A9 PM localization, but appears to be required for SLC26A9 activity[110]. In addition, the levels of CFTR expressed at the PM (but not of F508del-CFTR) seem to be increased when SLC26A9 is co-expressed, what seems suggestive of a role of SLC26A9 in biogenesis and/or stability of CFTR[110,111]. Furthermore, co-expression of CFTR and SLC26A9 in mammalian epithelial cells provided evidence that SLC26A9 enhances PKA-activated CFTR Cl^- conductance[111–113].

Strikingly, SLC26A9 was also described as a CF modifier gene. Namely, it was described that SLC26A9 polymorphisms, specifically rs7512462, are associated with the severity of CF-associated pathologies, such as meconium ileus, CF-related diabetes and prenatal pancreatic damage in patients with CF. This indicates that SLC26A9 Cl^- channels may compensate for deficient CFTR-mediated Cl^- secretion in a variety of organs affected by CF, a multi-organ disease[111]. Moreover, in a patient heterozygous for F508del, two SLC26A9 mutations (R575W; V486I) were found and they were both

shown to disrupt SLC26A9 traffic to the PM[114]. Recent functional studies in mice demonstrated that SLC26A9-mediated Cl^- secretion is essential to prevent airway mucus obstruction due to mucin hypersecretion in airway inflammation[106].

More recently, the rs751246 variant in SLC26A9 has been shown to modulate the response to therapies. Specifically, it was described that patients with rs7512462*C allele have a better response to Ivacaftor and Lumacaftor[109].

Altogether, these data highlight the physiological relevance of SLC26A9 in the regulation of Cl^- fluxes in airway epithelia. Also, this suggests that this protein is a disease modifier and a novel candidate therapeutic target for CF as an alternative Cl^- channel to compensate for impaired functional CFTR, and improve mucus transport in patients with CF and potentially other muco-obstructive airways diseases.

1.2.4) CFTR and SLC26A family

Co-localization between CFTR and SLC26A transporters was found in various epithelia such as lung, trachea, stomach, pancreatic ducts and sweat gland[29,72,115]. The physical and functional interaction between SLC26A family members and CFTR was already described. Firstly, two members of SLC26A family (SLC26A3 and SLC26A6) were reported to interact with CFTR in *Xenopus* oocytes and in HEK cells[48,116].

Based on this work, a model for this physical interaction was proposed (Fig 1.5). Firstly, the SLC26A member and CFTR interact by their PDZ domains with a common scaffold protein. This first interaction brings them together and allows direct interaction between the RD of CFTR and the STAS domain of the SLC26A transporter. In addition, this interaction appears to be enhanced by the PKA-mediated phosphorylation of the RD[48,115,116].

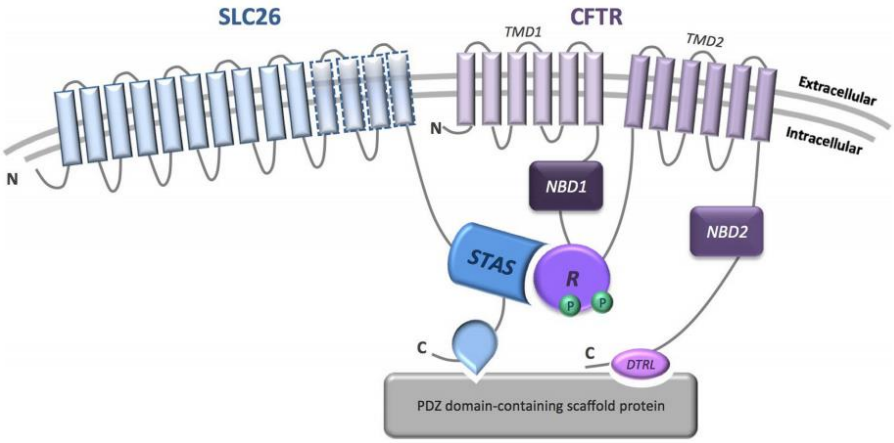

Figure 1.5 Model of physical interaction between SLC26A family proteins and the CFTR channel.
[Adapted from [72]].

Following this discovery, others members have been reported to bind to CFTR, such as SLC26A4, SLC26A5, SLC26A8 and SLC26A9[48,103,116–119]. This common mechanism shared by SLC26A members suggests that this interaction can be essential for their function.

However, the consequences of these interactions are not well established. For SLC26A3 and SLC26A6 it is known that their activity (and also that of CFTR) increases when co-expressed[116]. In turn, when wt-CFTR (but not F508del-CFTR) is overexpressed, there is an increase in the activation of SLC26A4 or SLC26A5, but the absence of these transporters does not seem to affect the activity of

CFTR[66,91,119]. These results highlight the selective role in the anion transport of the SLC26A transporters even when they are expressed in the same tissue.

The interaction between SLC26A4 and CFTR has been already reported: CFTR overexpression increases pendrin function in HEK cells. However, the absence of SLC26A4 has no significant effect in CFTR function[60,66,116].

The interaction between SLC26A9 and CFTR has been well studied but the functional consequences of this interaction are still controversial and are thought to be cell type dependent. Namely, it was described that this interaction is different in polarized airway epithelial cells than in non-polarized HEK 293 cells. In polarized airway epithelial cells SLC26A9 has a stimulatory effect in CFTR activity[99,103,120]. In opposition, in non-polarized cells there is no consensus in the results obtained from different labs [103,120].

A recent work has shown that SLC26A9 can bind PDZ-domain proteins that are known to have a crucial role in CFTR trafficking and biogenesis, namely Na^+/H^+ exchanger-3 regulatory factor 1 (NHERF-1) and CFTR-associated ligand (CAL)[107].

The evidence for the CFTR/SLC26A interaction and the increasing knowledge of the behaviour of SLC26A4 and SLC26A9 highlight the importance of these transporters as possible alternative pharmacological targets to correct the basic defect of CF. SLC26A9 may serve as an alternative Cl- channel by a double mechanism, i.e., by associating intrinsic Cl^- transport and also by activating any residual PKA-related CFTR Cl^- transport. SLC26A4 could be an important source of HCO_3^- and in the control of the magnitude and composition of the secreted fluid.

1.3) Objectives of the present work

The main goal of this MSc project is to identify novel regulators of two solute carrier transporters, SLC26A4 and SLC26A9, and to characterize their functional interaction with wild-type and mutant CFTR.

To achieve this objective five main tasks were proposed:

1. To determine the influence of the CFTR genotype on SLC26A4/A9 mRNA levels and also on the respective protein subcellular localization in CF patients materials;
2. To generate double-tagged (3HA and GFP) constructs of SLC26A4 and SLC26A9 cloned into an inducible lentiviral vector (pLVX-tet On/pLVX- TRE3G) to be used as traffic reporters to determine the levels of total and PM-localized protein by fluorescent microscopy;
3. To generate inducible novel stable cell lines expressing the inducible double-tagged constructs through lentiviral transduction and perform their functional characterization;
4. To use the above tools to perform siRNA microscopy screens to identify genes involved in regulating the traffic of SLC26A4 and SLC26A9 as potential drug targets for CF;
5. To look for physical and functional interactions with normal and mutant CFTR by measuring the localization and function of the protein upon overexpression and downregulation of CFTR.

The identification of SLC26A4/A9 interactors will shed light of our understanding of the physiological function of the transporters and will give us insight into its possible role in CF.

2. Results and discussion

2.1) SLC26A4 and SLC26A9 expression in nasal epithelial cells and wt and F508del-CFTR CFBE cells

As possible alternative targets with compensatory roles for anion conductance in CF, it is important to understand if the transcriptional levels of SLC26A4/SLC26A9 are related to CFTR genotype. For this purpose, SLC26A4 and SLC26A9 transcript levels were analysed by qRT-PCR in unpolarised wt- or F508del-mCherry-Flag-CFTR CFBE cells and in nasal epithelial cells from CF patients and non-CF healthy controls.

Although the CFBE cells are a useful and good model to represent the processes occurring in CF, CFBE wt or F508del mCherry CFTR are overexpressing CFTR. Thus, the use of freshly isolated nasal epithelial cells from CF patients homozygous for F508del-CFTR and non-CF healthy individuals constitute the best resource available to study changes in the levels of both SLC26A's occurring in CF.

In CFBE cells the mRNA levels of SLC26A4 and SLC26A9 were normalized to an internal control, β-Actin. Our data show that the transcript levels of these anion transporters were not significantly different between CF and non-CF cells (Fig. 2.1), although the SLC26A9 mRNA levels are slightly, but not significantly, increased in F508del- vs wt-CFTR expressing cells.

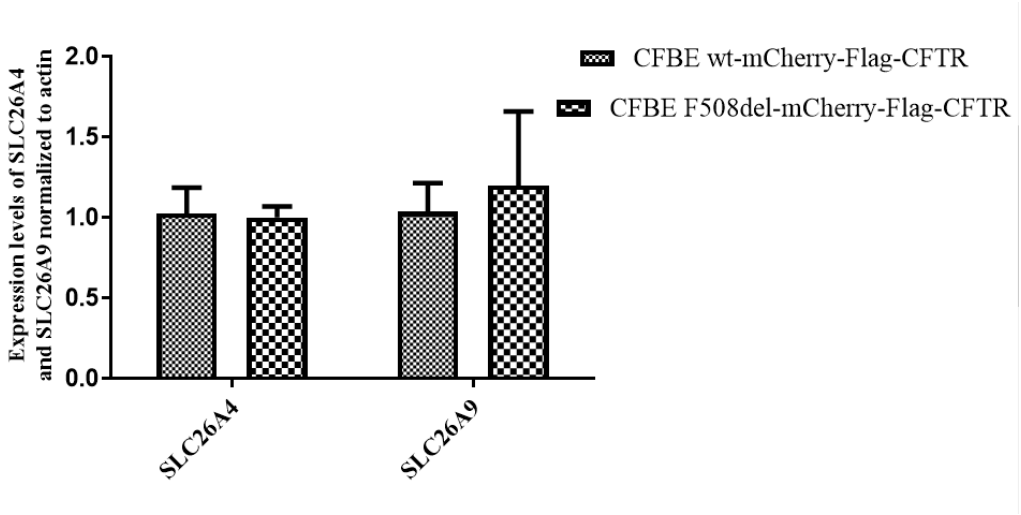

Figure 2.1 Expression of SLC26A4 and SLC26A9 in non-polarized CFBE cells. Levels of SLC26A4 and SLC26A9 mRNA expression were analysed by qRT-PCR in non-polarised CFBE cells stably expressing wt- or F508del-mCherry-Flag-CFTR. Fold expression of mRNA levels was obtained by relative quantification (ddCt) method and was normalized to an internal control (β-Actin) and compared with CFBE parental. Data plotted are mean ± SE, number of experiments (n=3).

The mRNA levels of SLC26A4 and SLC26A9 were measured in nasal epithelial cells from 5 non-CF healthy individuals and 5 patients homozygous for F508del-CFTR. Despite the small increase observed on the levels of both transporters in samples from CF patients, no significant differences were found (Fig 2.2).

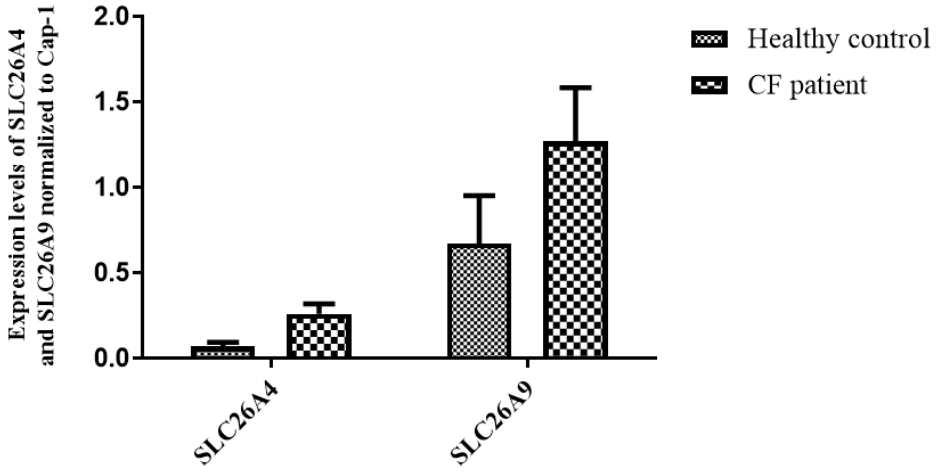

Figure 2.2 Expression of SLC26A4 and SLC26A9 transcripts in nasal epithelial cells. SLC26A4 and SLC26A9 expression was analysed by qRT-PCR in freshly nasal epithelial cells from 5 non-CF individuals and 5 CF patients homozygous for F508del-CFTR. Fold expression of mRNA levels was obtained by relative quantification ddCt method and was normalized to an internal control, Cap-1. (see Methods). Data plotted as the mean ± SE, (n) = number of experiments, (n=5).

There are no published data on the SLC26A4 mRNA levels in CF cellular models or individuals. Even though it is known that the expression of CFTR affects the activity of SLC26A4, the mRNA levels do not seem to be correlated with the CFTR genotype. Nevertheless, the results obtained for SLC26A9 were consistent with the results already published in CF mouse models[121].

Additionally, the results for these anion transporters were similar to the published data for other alternative channels such as ANO1 (TMEM16A) also in nasal epithelial cells from CF patients vs no-CF individuals[122].

2.2) Analyses of SLC26A4 and SLC26A9 expression pattern in human lung of CF vs non-CF individuals

Tissue explants from CF patients are an excellent resource to study the molecular changes occurring in disease. In addition, the use of this tissue makes this study closer to an *in vivo* situation.

It is reported that, in lung tissue from non-CF individuals, there is a pseudostratified (simple epithelium but appear to have two or more cell layers) columnar epithelium composed by ciliated, basal and goblet cell, al l adjacent to the basement membrane. However, this structure typically found in control tissue was lost in tissues from CF patients. In contrast, in CF lungs it is described that there are several layers of undifferentiated cells that result from the proliferation of basal cells[123]. Previous results in our laboratory have demonstrated that the observed structural changes are associated with loss of airway differentiation. These results were achieved by comparison of the expression of epithelial and mesenchymal markers in both tissues (unpublished data – Margarida Quaresma).

Furthermore, in the same work and in published data[123] it is demonstrated that there are changes in CFTR pattern expression. In normal epithelia, CFTR expression is restricted to the apical compartment of epithelial ciliated cells, while in CF, CFTR accumulates in the cytosol of epithelial cells[123]. These results are already validated by a member of the group (unpublished data – Margarida Quaresma).

SLC26A4 and SLC26A9 patterns of expression were analysed in control (non-CF) and CF lung bronchial tissue in order to understand if the localization of these membrane proteins is affected by the loss of differentiation and by the loss of membrane localized CFTR.

Direct general comparison can be made between the expression pattern in CF and control respiratory epithelium. In healthy non-CF tissue, SLC26A4 expression was observed to be at the apical component of the epithelium, although some internalization of the protein is also noticeable (Fig.2.3). In CF tissue, even though there is a clear decrease in the signal intensity of SLC26A4 (Fig.2.4) when compared with the signal obtained in non-CF tissue (Fig. 2.5), the protein is expressed in the apical membrane as well as in the cytoplasm of the epithelial cells in both tissues. Thus, the pattern expression of SLC26A4 observed in CF and non-CF is very similar and a change in the localization of the protein associated with the dysregulated CFTR expression and/or loss of airway differentiation is not clear. The decreased signal intensity observed can be due to the loss of the integrity of the tissue and to a reduced number of epithelial cells observed in CF tissue when compared with non-CF tissue.

SLC26A9 seems to be mostly localized in the cytoplasm of the cells in the control epithelium (Fig. 2.5) even though it is possible to detect its expression at the apical membrane. Unfortunately, in the CF tissue the epithelial cell layer is almost absent which may be due to the preservation process or to the obtainment of the cryocut in the cryostat. In this way, it is not possible to conclude if the localization of this protein is correlated with the CF genotype.

However, it is important to highlight that the pattern of expression observed for SLC26A4 and SLC26A9 in non-CF tissue is not consistent with the localization of the protein described in the literature. Both SLC transporters are described to be mainly localized at the apical membrane of epithelial cells[41].In this way, a strong signal at the apical membrane was expected, which was not observed for both proteins. The loss of specific apical signal can be due to limited quality and availability of non-CF tissue. Moreover, the control tissue used in this work belonged to a drug user, making it not a true healthy control. Additionally, other factors, such as inflammation, can change the localization of the proteins in the cell, as already reported for CFTR[124].

Figure 2.3. SLC26A4 pattern expression in control lung bronchial tissue. Tissue was stained for SLC26A4, used an Ab anti-SLC26A4 (see Methods). Nuclei were stained with DAPI. In merge pictures, nuclei are depicted in cyan and protein in green. Scale bar represents 50 μm.

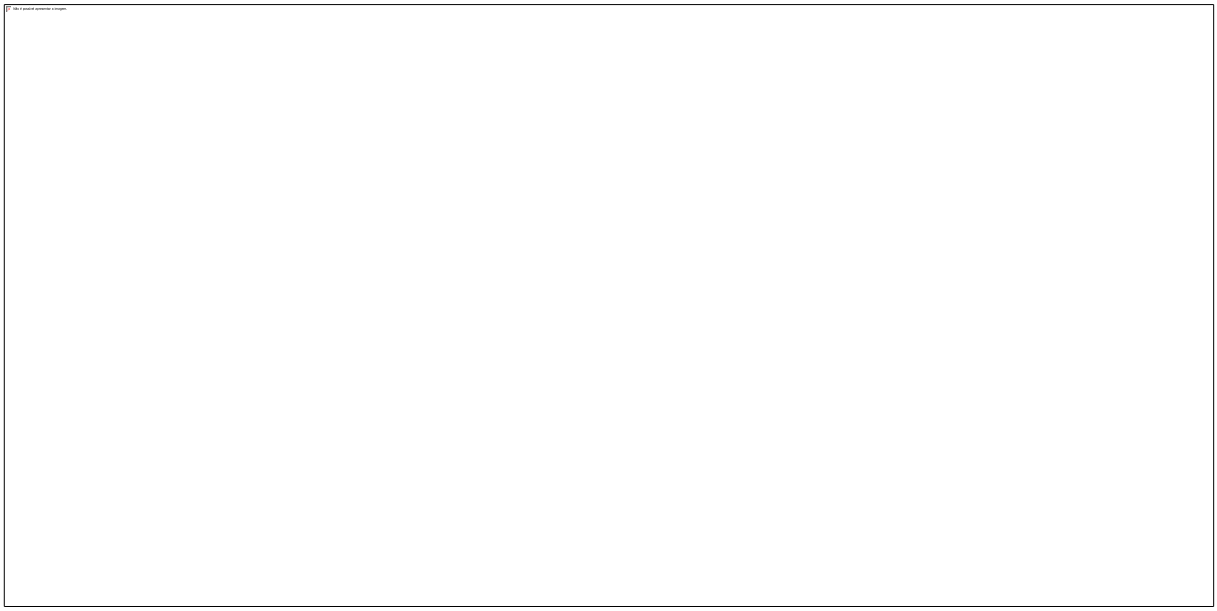

Figure 2.4. SLC26A4 pattern expression in CF lung bronchial tissue. Tissue was stained for SLC26A4, used an Ab anti-SLC26A4 (see Methods). Nuclei were stained with DAPI. In merge pictures, nuclei are depicted in cyan and protein in green. Scale bar represents 50 μm.

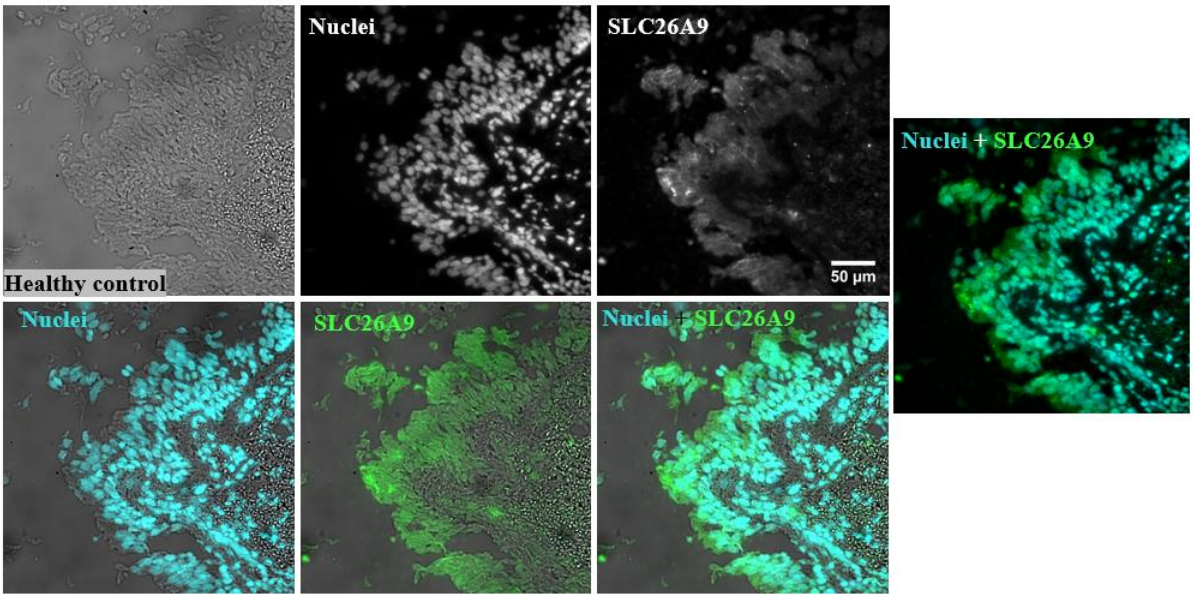

Figure 2.5. SLC26A9 pattern expression in control lung bronchial tissue. Tissue was stained for SLC26A9, used an Ab anti-SLC26A9 (see Methods). Nuclei were stained with DAPI. In merge pictures, nuclei are depicted in cyan and protein in green. Scale bar represents 50 μm.

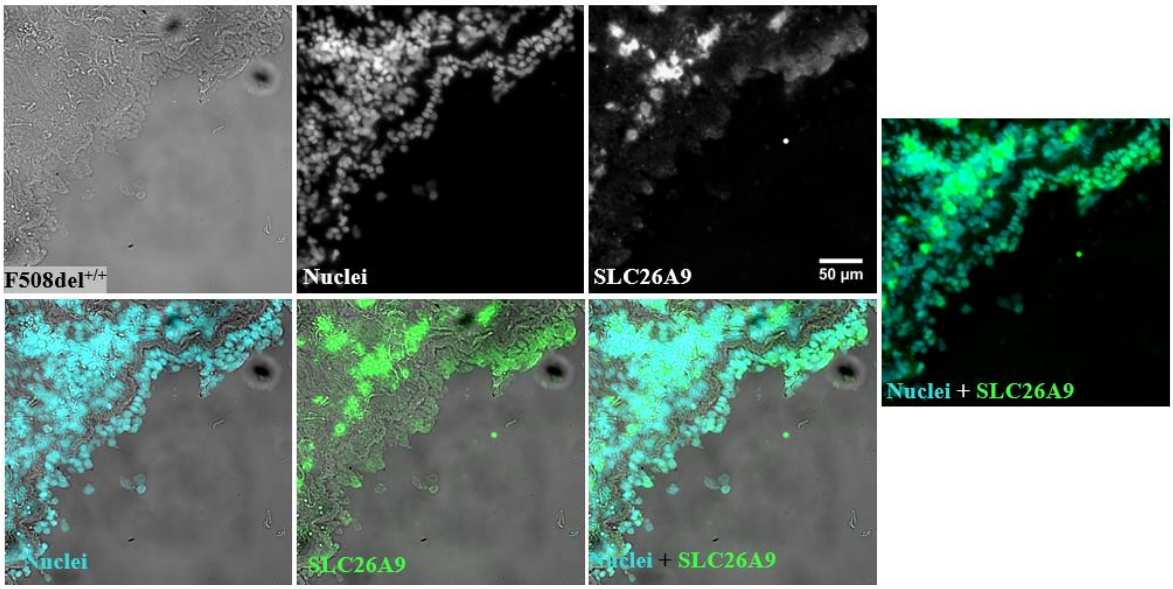

Figure 2.6. SLC26A9 pattern expression in CF lung bronchial tissue. Tissue was stained for SLC26A9, used an Ab anti-SLC26A9 (see Methods). Nuclei were stained with DAPI. In merge pictures, nuclei are depicted in cyan and protein in green. Scale bar represents 50 µm.

2.3) Generation of stable cell lines overexpressing the double-tagged SLC26A4/A9

2.3.1) Generation of the double-tagged SLC26A4 and SLC26A9

To achieve the main goal of this project, i.e, to identify new regulators of two solute carrier transporters (SLC26A4 and SLC26A9) and to study the interaction of these transporters with CFTR, it was necessary to develop novel cellular models capable of differentiating the amount of protein expressed at the PM from the total protein expressed in the cells.

With that goal, double-tagged constructs of SLC26A4 and SLC26A9 were generated. These constructs have a eGFP tagged to the N-terminus and a 3xHA (triple hemagglutinin) tag in an extracellular loop. If the protein is expressed at the PM, then the 3xHA tag is outside the cell, being thus susceptible to antibody binding without membrane permeabilization. To this end, mutagenesis was performed to insert both tags in each construct (see Appendix 2).

To generate stable cell lines, the constructs were cloned into a lentiviral vector (pLVX-TRE3G). This lentiviral vector belongs to the Tet-On 3G system, an inducible system for mammalian cells. The transduction of CFBE cells with pLVX-Tet-On 3G and pLVX-TRE3G containing the gene of interest leads to the expression of high levels of the gene of interest only when cultured in the presence of the tetracycline analogue, doxycycline (Dox).

CFBE cells were chosen as a model because they were obtained from the bronchial epithelium of a CF patient and in this way, they are a good representation of the processes occurring in CF. However, they no longer express any endogenous CFTR, as it decreased with the number of passages.

2.3.2) Study of the influence of tags in SLC26A4 expression and localization

The insertion of the two tags (eGFP and 3xHA) into SLC26A4 was successful, but this construct is still inserted in the pcDNA3.1 plasmid. Cloning of the SLC26A4 construct into the pLVX-TRE3G was not yet accomplished and consequently it was not yet possible to generate stable cells lines overexpressing eGFP-3xHA-SLC26A4.

To generate the double-constructs, the eGFP tag was inserted in the N-terminus as it was already reported that it does not affect the normal processing and trafficking of the protein (see Appendix 2, Tables 6.7 and 6.8)[125]. Nevertheless, a flexible linker was added to avoid stereo chemical impediment. The 3xHA tag was inserted in the second extracellular loop, (see Appendix 2, Tables 6.1and 6.2) because it is a glycosylated loop and therefore it is extracellular.

To study the influence of the tags in the normal processing and trafficking of the protein to the plasma membrane, CFBE 41o- were transiently transfected with the plasmid containing the eGFP-3xHA-SLC26A4 construct and an immunofluorescence assay without membrane permeabilization was performed.

Representative fluorescence images of the transiently transfected CFBE cells with the construct only with the 3xHA tag or with both tags (3x-HA and eGFP in N-terminus) are shown in Figs. 2.7 and 2.8.

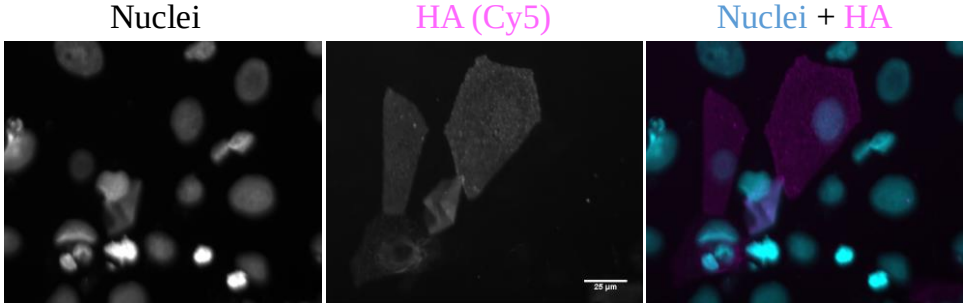

Figure 2.7. Representative immunofluorescence images of CFBE cells transiently transfected with the single tag (3xHA) SLC26A4 construct and stained with an anti-HA antibody in non-permeabilized cells. In the Hoechst channel (left), it is possible to see the cell nuclei, and the Cy5 channel image (middle) shows the anti-HA antibody (Ab) staining representing the plasma membrane localized SLC26A4. (Primary Ab – anti-HA; secondary Ab – Cy5). Images were acquired with the 20x objective. The scale bar represents 25 µm.

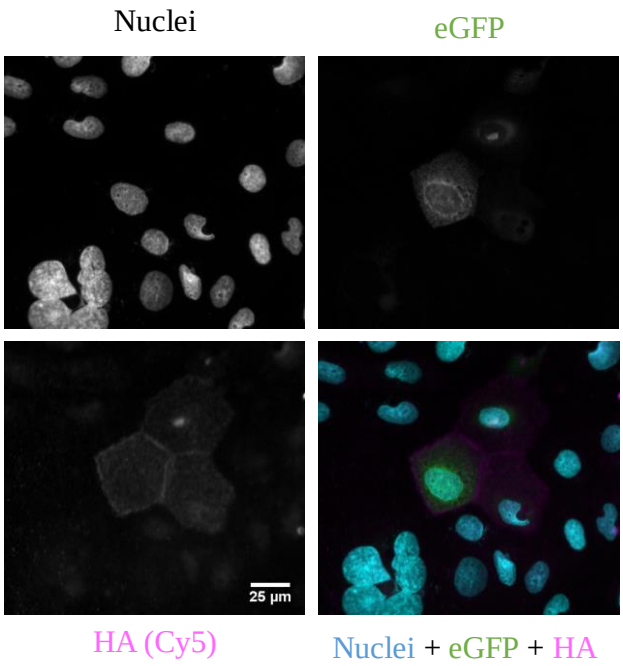

Figure 2.8. Representative immunofluorescence images of CFBE cells transiently transfected with the single tag (3xHA) SLC26A4 construct and stained with an anti-HA antibody in non-permeabilized cells. In the Hoechst channel (above-left), it is possible to see the cell nuclei, GFP channels (above-right) it is possible to see the total SLC26A4 expressed in the cell and the Cy5 channel image (below-left) shows the anti-HA antibody (Ab) staining representing the plasma membrane localized SLC26A4. (Primary Ab – anti-HA; secondary Ab – Cy5). Images were acquired with the 20x objective. The scale bar represents 25 µm.

CFBE cells transiently transfected with the single (3xHA) or double-tagged (eGFP and 3xHA) SLC26A4 construct cloned into pcDNA3.1 show a considerable membrane expression, as it is possible to observe with the anti-HA Ab (Cy5 secondary Ab – Figs.2.7 and 2.8) which indicates that neither of these tags affects the trafficking of the SLC26A4 protein to the PM.

A construct of a mutant version of SLC26A4 cloned into pcDNA3.1 was also produced. This construct has the L236P mutation (see Appendix 2- Tables 6.3 and 6.4), a natural mutant found in patients with Pendred syndrome[125]. The replacement of a leucine by a proline in the position 236 leads to the retention of SLC26A4 in the ER, so it was described as a trafficking mutation. Representative fluorescence images of transiently transfected CFBE cells with this SLC26A4 mutant construct are represented in the Fig. 2.9.

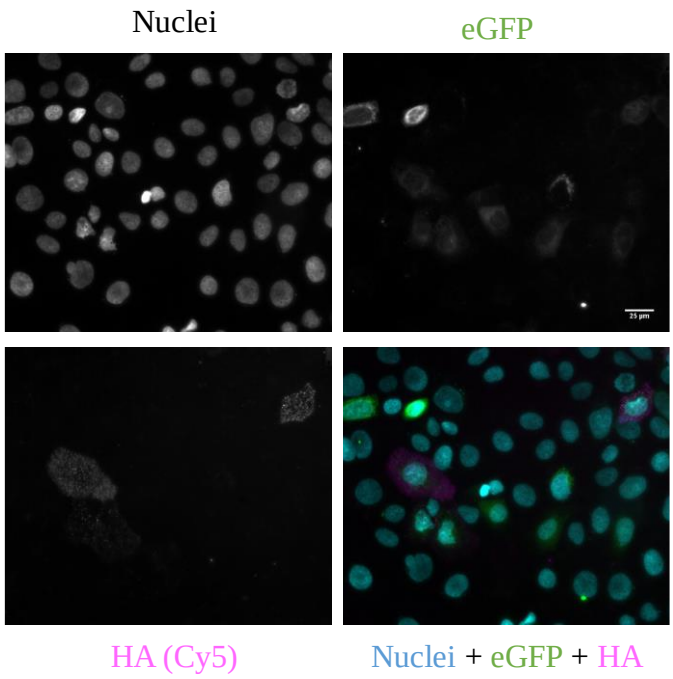

Figure 2.9 Representative immunofluorescence images of CFBE cells transiently transfected with the mutant version (L236P) of eGFP-3xHA-SLC26A4 construct in non-permeabilized cells. In the Hoechst channel (above-left), it is possible to see the cell nuclei, GFP channels (above-right) it is possible to see the total SLC26A4 expressed in the cell and the Cy5 channel image (below-left) shows the anti-HA antibody (Ab) staining representing the plasma membrane localized SLC26A4. (Primary Ab – anti-HA; secondary Ab – Cy5). Images were acquired with the 20x objective. The scale bar represents 25 µm.

Surprisingly, the traffic mutation did not completely abolish the traffic to the PM in our cellular model, as it can be observed by some Cy5 staining (Fig. 2.9, lower left panel). However, the Cy5 signal was decreased when compared to the cells overexpressing the wild-type eGFP-3xHA-SLC26A4, and not all cells that were transfected (as determined by the eGFP signal, Fig. 2.9, upper right panel) evidence membrane staining. Nevertheless, it is possible to observe that there is an increase of the amount of protein localized around the nucleus, suggesting a localization in the ER. – (Fig 2.9, upper right panel).

CFBE cells transiently transfected with wt- or L236P-eGFP-3xHA-SLC26A4 cloned into pcDNA3.1 were also characterized by Western Blot (WB) (Fig. 2.10), where the results obtained were consistent with what was shown by the immunofluorescence assays (Fig 2.8 and 2.9). Protein was extracted from the cells 48 h after transfection, and the anti-HA antibody was used to detect both versions of the protein, wt- and L236P-eGFP-3xHA-SLC26A4.

SLC26A4 follows the secretory pathway to reach the PM where it is known to be glycosylated to acquire the mature form which is trafficked to the cell surface. In this way, the lower band should correspond to the core-glycosylated from, while the upper band corresponds to the fully-glycosylated from. The absence of differences in the pattern observed in the WB (Fig 2.10) for the wt and mutant SLC26A4 proteins suggests that the mutant protein is fully glycosylated and thus has reached the cell surface. Nevertheless, additional experiments with glycosidases need to be performed to confirm that the higher molecular mass band corresponds to a glycosylated form of SLC26A4.

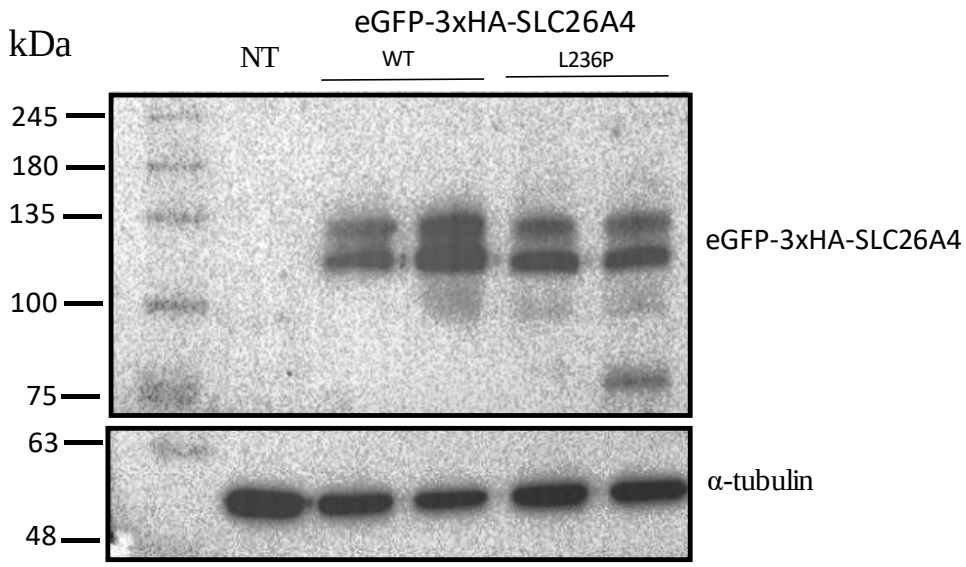

Figure 2.10. Western Blot of CFBE cells transiently transfected with wt- or L236P-eGFP-3xHA-SLC26A4, using an anti-HA antibody. Non-transfected CFBE cells (NT) were used as control for Ab specificity. α-tubulin was used as loading control and position of molecular markers are shown on the left.

Due to the difficulties found in the cloning step in the lentiviral vector pLVX-TRE3G and time limitation, CFBE cells stably expressing wt- or L236P-eGFP-3xHA-SLC26A4 were not yet produced.

2.3.3) Characterization of the cell line overexpressing the double-tagged SLC26A9

Similar, to the experiments performed for pendrin, the study of the influence of the tags in the normal processing and trafficking to the PM were also accomplished for SLC26A9 (see Appendix 5, Fig 6.10 and 6.11).

The first double-tagged construct produced had the 3xHA tag in the second extracellular loop, and an eGFP-tag in the C-terminus (see Material and Methods- 3.1.6- Mutagenesis and Appendix 6.10 and 6.11). Immunofluorescence results (see Appendix 5, Fig 6.10) revealed a complete cytoplasmic localization for this first eGFP-SLC26A9 construct, observed by the absence of co-localization with β-catenin (PM marker) and a stronger signal around the nuclei, suggesting an ER localization. Additionally, the absence of signal in the Cy5 channel (see Appendix 5, Fig 6.11) confirmed that the protein was not being expressed at the PM. Based on these results, the eGFP tag was replaced from the C-terminus to the N-terminus (work performed in collaboration with Dr. Rainer Schreiber from Dr. Karl Kunzelmann's Lab).

To study the interaction of this transporter with CFTR and to identify new regulators of SLC26A9, three cellular models were generated: CFBE stably expressing only eGFP-3xHA-SLC26A9, and CFBE stably co-expressing eGFP-3xHA-SLC26A9 and mCherry tagged wt- or F508del-CFTR.

Due to the initial heterogeneity observed in the cell population and a weak eGFP fluorescence intensity, all cellular models were sorted by flow cytometry in order to select only the cells with the highest eGFP fluorescence intensity (see Appendix 7).

Representative fluorescence images of CFBE stably overexpressing eGFP-3xHA-SLC26A9, alone or together with wt- or F508del-mCherry-Flag-CFTR - are shown in Figs. 2.11, 2.13 and 2.15, respectively. In figures 2.12, 2.14 and 2.16 it is possible to observe signal-to-noise ratio measurements of the GFP fluorescence and Cy5 (3-HA tag) signal before and after cell sorting. The signal-to-noise ratio was calculated using the following formula:

$$\text{Signal} - \text{to} - \text{noise ratio}: \frac{\text{Cell fluorescence Intensity} - \text{Background fluorescence Intensity}}{\text{Background fluorescenceIntensity}}$$

In CFBE cells expressing eGFP-3xHA-SLC26A9 together with wt- or F508del mCherry-Flag-CFTR it is possible to observe that both eGFP and Cy5 fluorescence signal-to-noise ratios were significantly increased after sorting (Fig 2.14 and 2.16). However, these results were not observed for CFBE stably overexpressing eGFP-3xHA-SLC26A9 alone (Fig 2.12). This can be justified by a higher fluorescence intensity and homogeneity between these cells before sorting when compared to the other two cell lines.

In all three cellular models, it is possible to detect a considerable PM expression of eGFP-3xHA-SLC26A9, as observed in the Cy5 panel detected by the anti-HA Ab (Fig 2.11, 2.13 and 2.15). The presence of the PM signal in cells only expressing eGFP-3xHA-SLC26A9 demonstrated that the presence of CFTR is not crucial for SLC26A9 expression at the plasma membrane. Furthermore, there is no significant difference in the Cy5 signal intensity when SLC26A9 is co-expressed with wt or F508del CFTR (Fig 2.13 and 2.15 – Cy5 panel).

However, a considerable amount of SLC26A9 also seems to be localized in the cytosol, namely around nucleus, which suggests a localization in the ER (fig 2.11, 2.13 and 2.15, eGFP panel). These results are slightly unexpected, as SLC26A9 has been identified as a membrane protein expressed in the apical side of airway epithelia. These discrepancies can be due to a weak effect of the tag in the normal protein trafficking to the plasma membrane, and/or to the effect of protein overexpression.

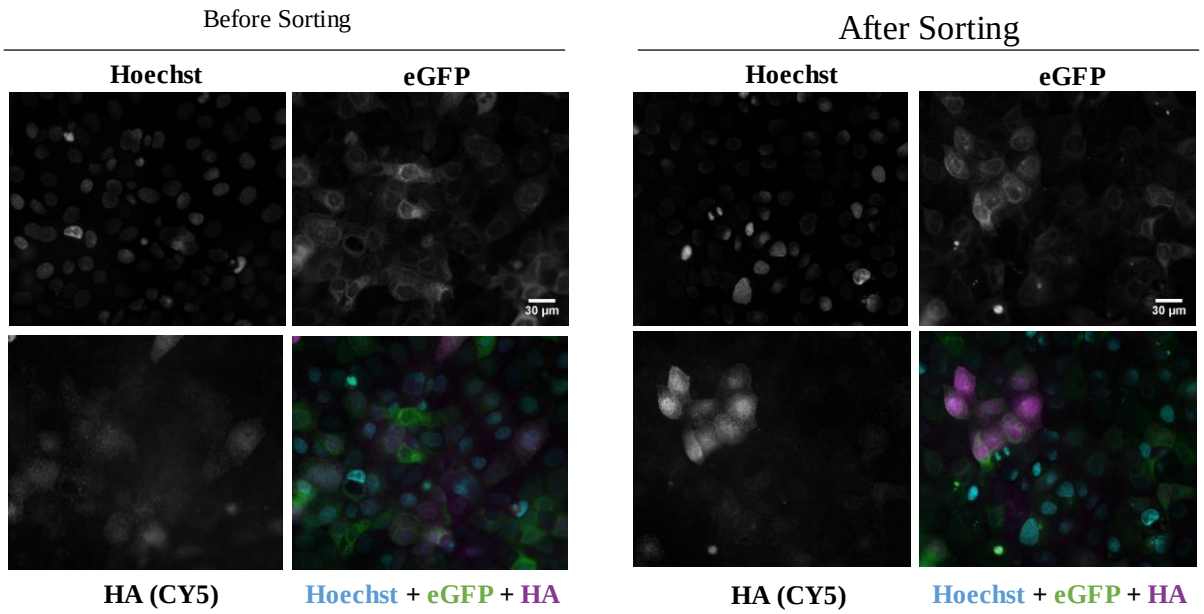

Figure 2.11. Immunofluorescence images of CFBE cells stably overexpressing eGFP-3xHA-SLC26A9 before and after sorting. The expression of SLC26A9 was induced by the addition of 1 µg/mL of doxycycline (DOX) for 48 h. Left panel – Unsorted cells; Right panel – Cell sorted. Hoechst- Nuclei; eGFP – Total SLC26A9; Cy5 (anti-HA Ab) – PM eGFP-3x-HA-SLC26A9. Images were acquired with the 20x objective in a Leica DMI 6000B microscope. Scale bar represents 30 µm.

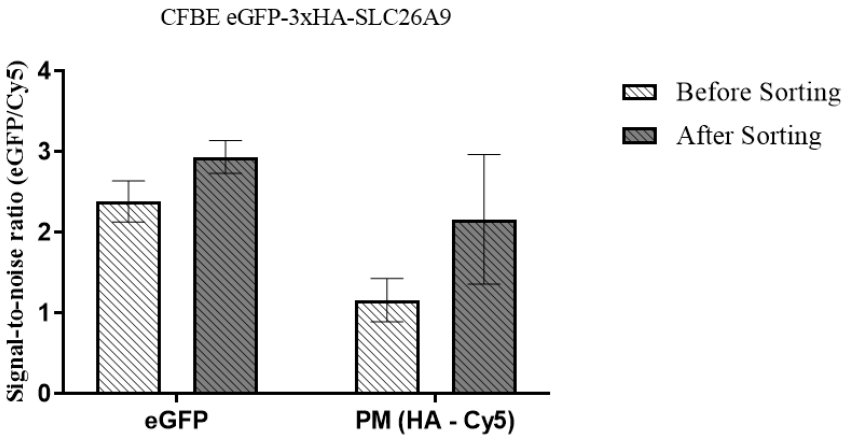

Figure 2.12. Signal-to-noise ratios of eGFP and Cy5 fluorescence in CFBE eGFP-3xHA-SLC26A9 cells before and after sorting. (n=50 for eGFP and n=40 for Cy5). The increase in the signal-to-noise ratio in both channels was not significant. P<0.05 was accepted as significant.

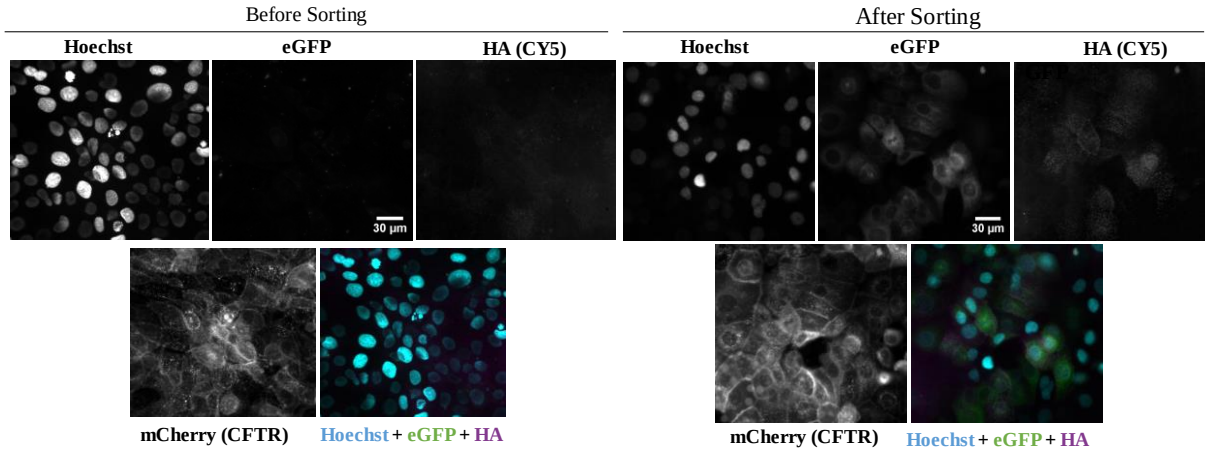

Figure 2.13. Representative immunofluorescence images of CFBE wt- mCherry-Flag-CFTR stably overexpressing eGFP-3xHA-SLC26A9 before and after sorting. The expression of both CFTR and SLC26A9 was induced by the addition of 1 µg/mL of doxycycline (DOX) for 48 h. Left panel – Unsorted cells; Right panel – Sorted cells. Hoechst – Nuclei; eGFP – Total SLC26A9; Cy5 (anti-HA antibody) – PM SLC26A9; mCherry – Total CFTR. Images were acquired with the 20x objective in a Leica DMI 6000B microscope. Scale bar represents 30 µm.

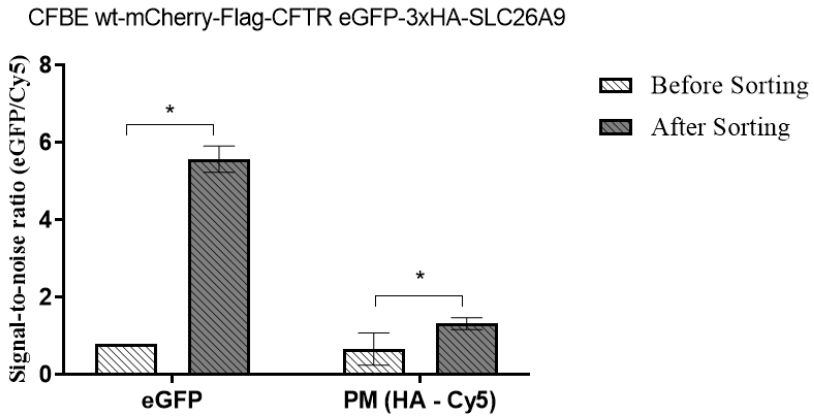

Figure 2.14. Signal-to-noise ratios of eGFP and Cy5 fluorescence in CFBE mCherry-Flag-CFTR overexpressing eGFP-3xHA-SLC26A9 cells before and after sorting. (n=50 for eGFP and n=40 for Cy5). The results showed a significant increase in the signal-to-noise of eGFP and Cy5 after cell sorting, which means that the signal can be easily distinguished from the background. P<0.05 was accepted as significant.

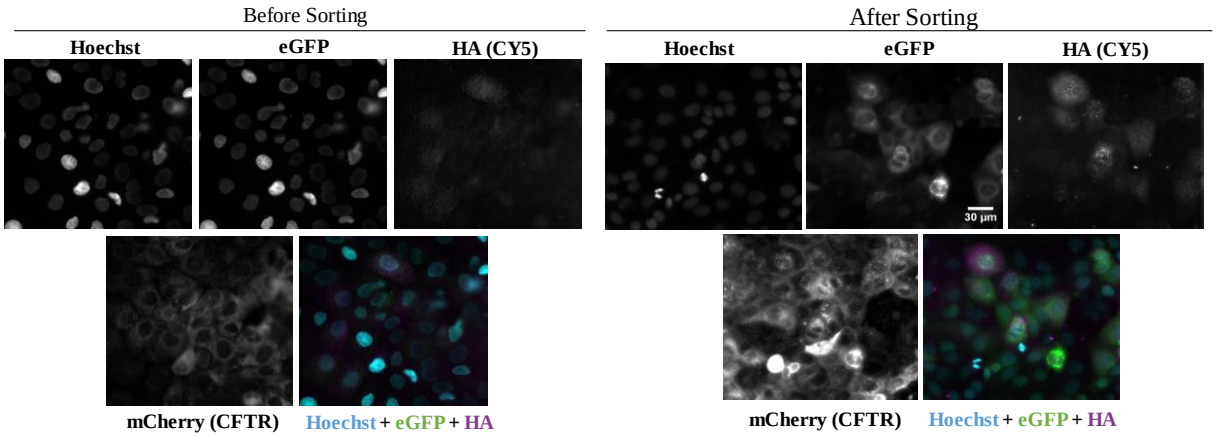

Figure 2.15. Representative immunofluorescence images of CFBE F508del-mCherry-FLAG-CFTR stably overexpressing eGFP-3xHA-SLC26A9 before and after sorting. The expression of both CFTR and SLC26A9 was induced by the addition of 1 µg/mL of doxycycline (DOX) for 48 h. Left panel – Unsorted cells; Right panel – Sorted cells. Hoechst – Nuclei; eGFP – Total SLC26A9; Cy5 (anti-HA antibody) – PM SLC26A9; mCherry – Total CFTR. Images were acquired with the 20x objective in a Leica DMI 6000B microscope. Scale bar represents 30 µm.

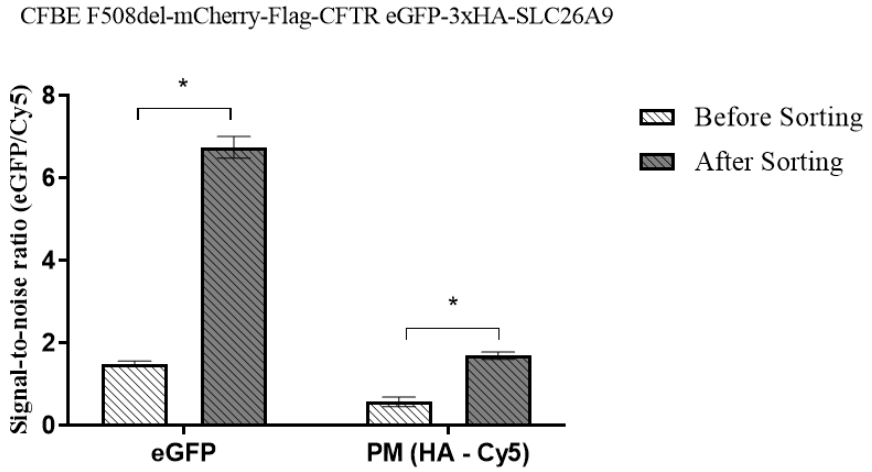

Figure 2.16. Signal-to-noise ratios of eGFP and Cy5 in CFBE F508del-mcherry-FlagCFTR overexpressing eGFP-3xHA-SLC26A9 before and after sorting. (n=50 for GFP and n=40 for Cy5). The result showed a significant increase in the signal-to-noise of eGFP and Cy5 after cell sorting, which means that the difference between signal and background is higher. P<0.05 was accepted as significant.

CFBE stably overexpressing only eGFP-3xHA-SLC26A9 or co-expressing wt or F508del-mCherry-Flag-CFTR were also characterized by Western Blot (Fig 2.17). Cells were induced for 48 h with 1 µg/ml of doxycycline (DOX) and protein was extracted as described in material and methods 3.3.1. Anti-HA antibody was used to detect SLC26A9. The analysis was performed before and after cell sorting, and the eGFP-3xHA-SLC62A9 quantification was normalized to α-tubulin (loading control). The results, in Fig 2.17 and 2.18, shown that the eGFP-3xHA-SLC26A9 expression is higher in cells after sorting, even though this difference is not significant for cells only expressing this protein, CFBE eGFP-3xHA-SLC26A9. Furthermore, the results are in concordance with what was observed the immunofluorescence assays (fig 2.12, 2.14 and 2.16). In this way, it is possible to conclude that after cell sorting the cells are a more homogenous population and a more robust model to use in further experiments.

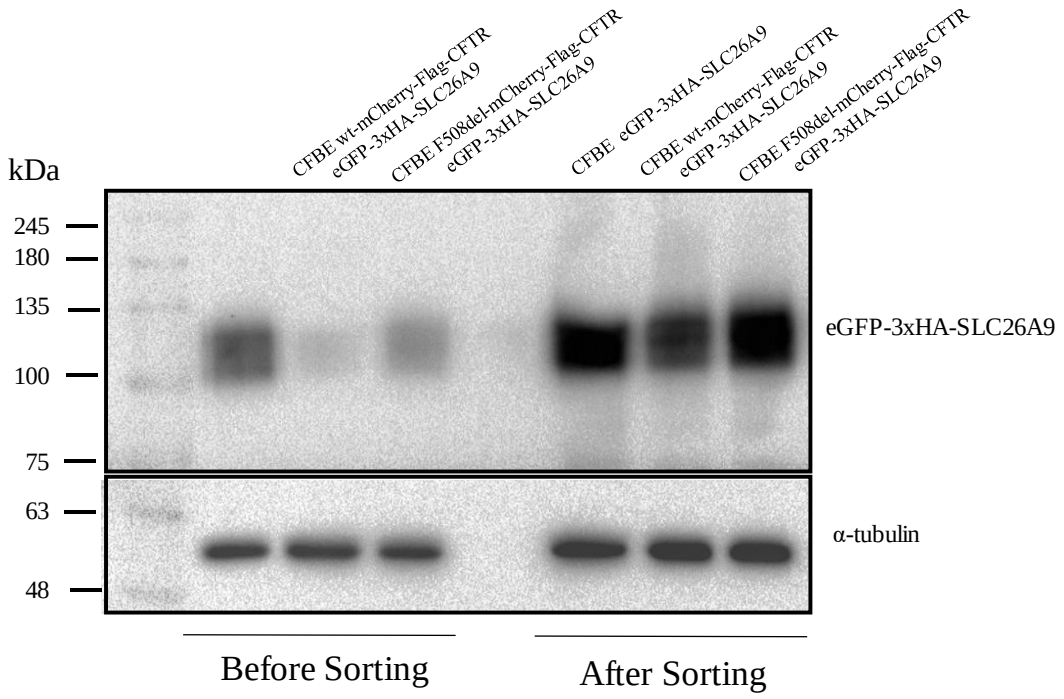

Figure 2.17. Western Blot of CFBE cells only expressed eGFP-3xHA-SLC26A9 or co-expressed with wt or F508del-mCherry-Flag-CFTR, using an anti-HA antibody. Left-cells unsorted, Right-cells sorted. α-tubulin was used as loading control and position of molecular markers are shown on the left.

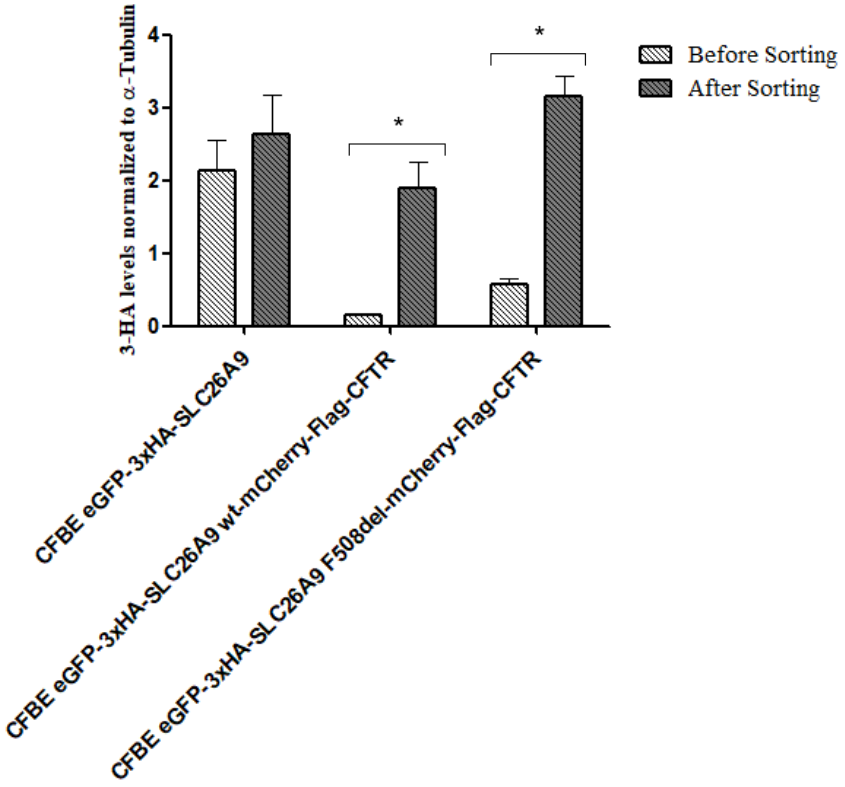

Figure 2.18. Quantification of 3xHA levels of the Westen Blot represented in fig. 2.17. After sorting it is possible to observed an increased in eGFP-3xHA-SLC26A9 expression of in all cell lines, except CFBE only expressed eGFP-3xHA-SLC26A9. * $P<0.05$ was accepted as significant.

2.1.4) Glycosylation study of SLC26A9

As membrane proteins, SLC26A4 and SLC26A9 follow the secretory pathway to reach the PM. As they go along the Golgi and traffic to the cell surface they acquire the mature form, being thus fully-glycosylated at two asparagine residues: SLC26A4 – Asn^{167} and Asn^{172}; SLC26A9 – Asn^{153} and Asn^{156}. The migration pattern observed for eGFP-3xHA-SLC26A9 (Fig 2.17) and eGFP-3xHA-SLC26A4 (Fig 2.10) in the CFBE model is typically observed in other cellular models, such as HEK 293 and Madin-Darby canine kidney (MDCK) cells[42]. The SLC26A proteins appear as multiple bands, classically as a sharp lower band and a broader upper band as observed for SLC26A4 (Fig 2.10).

To study the glycosylation pattern of tagged SLC26A9 in CFBE cells, cells overexpressing only eGFP-3xHA-SLC26A9 were induced for 48 h with DOX and the extracted protein was treated with endoglycosidase H (Endo H) which only removes the N-core-glycosylation or N-glycanase F (PNGase F) which removes both core- and full-glycosylations (see Materials and Methods – 3.3.2). Accordingly, the lower band (corresponding to the core-glycosylated form) is sensitive to Endo H while the upper band (corresponding to the fully-glycosylated form) is resistant to Endo H but sensitive to PNGase F treatment which is expected to collapse the multiple bands into a single band, corresponding to the non-glycosylated form.

As observed in Fig 2.19, treatments with Endo H or PNGase F lead to the appearance of a band of decreased molecular mass and reduction of the bands corresponding to both the fully- and core-–glycosylated forms of eGFP-3xHA-SLC26A9. However, since the PNGase F treatment did not totally abolish the presence of the upper band, it is likely that the digestion by this glycosidase was not complete. The results observed with Endo H treatment are in accordance with the immunofluorescence results showed above (Fig 2.11, 2.13 and 2.16), suggesting that part of the protein is still just core-glycosylated (thus in the ER), even though there is significant part that is Endo H resistant (i.e., fully-glycosylated) corresponding to the strong signal of the protein expressed at the PM (Fig 2.11 – Cy5 panel).

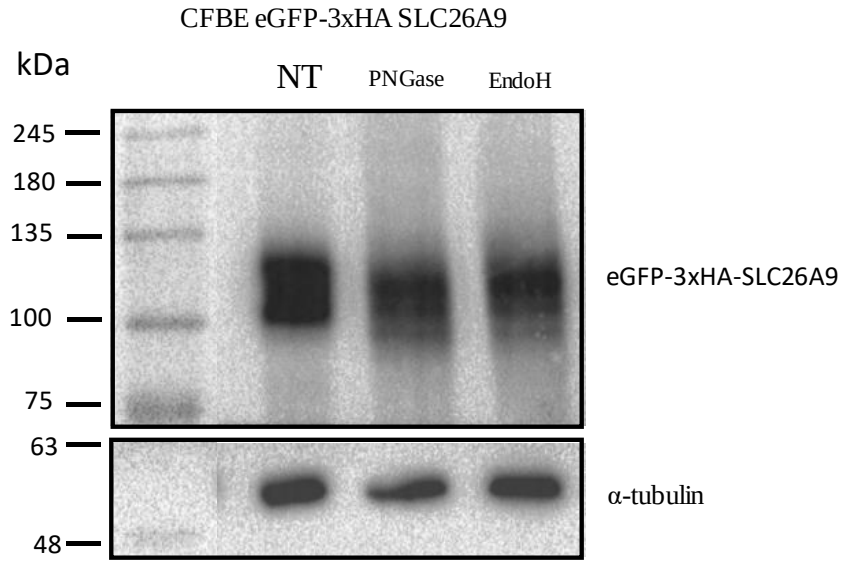

Figure 2.19. Western blot of extracts from eGFP-3xHA-SLC26A9 expressing in CFBE cells, subjected to glycosylation assays. NT- no treatment; PNGase – treatment with N-glycanase F-, Endo H – treatment with endoglycosidase H. Equal amounts of protein were loaded in each lane (10μg of protein) as demonstrated by α-tubulin control.

Due to the absence of stable cell lines overexpressing eGFP-3xHA-SLC26A4 it was not possible to study the glycosylation of this protein.

2.4) Microscopy-based siRNA screen to identify regulators of SLC26A9

To achieve the second main goal of this MSc project, i.e, to identify new regulators of SLC26A9 and to study the interaction between this anion channel and CFTR, a pilot screen using CFBE cells expressing eGFP-3xHA-SLC26A9 was performed. For this we used a siRNA library that contains siRNAs that were found to affect F508del-CFTR traffic and other siRNAs targeting genes reported as CFTR interactors (Sang Lim at Igor Stagljarlab, Univerity of Toronto, Canada). Instead of "Scrambled" non-targeting siRNA, Neg_1 was used as a negative control, since previous results in our lab have shown a positive effect in CFTR traffic by scrambled siRNA. Image acquisition and analysis were performed as described in Materials and Methods – 3.3.4 – Image acquisition, processing and analysis and 3.5.2 – siRNA screen.

The siRNA assay was performed three times to have statistically significant results. However, in two of them, the expression of SLC26A9 was significantly reduced, which may be due to experimental error in inducing cells with doxycycline (see Material and Methods – 3.5.2 - siRNA screen) or loss of expression of the cells. If the latter option is confirmed the cells will be sorted again as described in Material and Methods – 3.1.10 – Cell sorting. In this way, due to limited time, the general hits were analysed considering the assay in which the cells are expressing sufficient levels of SLC26A9. The most promising hits were selected taking into account the results obtained in all experiments.

Results from the pilot screen identified 81 siRNA hits affecting SLC26A9 traffic: 52 enhancer genes, i.e. the knock-down of these genes has an inhibitory effect on the traffic of SLC26A9 to the PM; and 29 inhibitor genes, i.e. the knock-down of these genes has a positive effect on the traffic of SLC26A9 to the PM. Among all the hits, the most promising ones were selected as describe before: two positives (DNAJC4 and SLC6A14) and two negatives (HDAC6 and YWHAQ). SLC6A14 and HDAC6 were targeted by 2 different siRNAs.

The results and deviation scores of the most promising hits selected are shown in Fig. 2.20. The scores of remaining hits, are displayed appendix 10 Tables 5.14 and 5.15, where the names of the genes affecting SLC26A9 as well as their effect on CFTR is also specified.

The gene DNAJC4 encodes DNAJ heat shock protein Family (Hsp40) member C4, which belongs to the largest group of chaperons. These heat shock proteins regulate the ATPase activity of Hsp70 proteins whose function is to reversibly bind to partially denatured protein substrates to avoid their aggregation with themselves or with other molecules[126]. This protein is also a positive hit in the F508del-CFTR traffic screen performed in our lab by Hugo Botelho[127](unpublished data), which suggests a relationship between CFTR and SLC26A9 traffic pathways.

Interestingly, the other positive hit is a membrane protein that belongs to the solute carrier family, SLC6A14. This protein mediates the uptake of a broad range of neutral and cationic amino acids in a Na^+/Cl^- dependent manner[128]. Moreover, as SLC26A9 this protein is also associated with the susceptibility to meconium ileus in individuals with CF[129].

Regarding the negative hits, we selected HDAC6 and YWHAQ. HDAC6 encodes histone deacetylase 6 which has a critical role in transcriptional regulation, cell cycle progression and development events. HDAC6 is reported to have a key role in regulation of heat-shock protein 90 (Hsp90)[130].

Curiously, it was described that knock-down of HDAC6 results in functional rescue of CFTR to plasma membrane, most likely because HDAC6 binds to polyubiquitinated misfolded species of F508del-CFTR[131]. However, in this assay we found an opposite effect in the traffic of SLC26A9 to the

plasma membrane which can mean that HDAC6 do not affect directly SLC26A9 but indirectly, by regulated other protein.

Lastly, the gene YWHAQ encodes 14-3-3 protein theta which has a crucial role in mediating signal transduction by binding to phosphoserine-containing protein. As HDAC6, there are already published data showing the effect of 14-3-3 protein theta in CFTR biogenesis. Namely, it was described that the overexpression of this protein increases the amount of CFTR at the plasma membrane by reducing retrograde retrieval transport of CFTR to the endoplasmic reticulum[132]. Accordingly, we observed that the knock-down of this protein also decreased the expression of SLC26A9 at the plasma membrane.

The remaining hits were analysed using the DAVID Database for Annotation, Visualization and Integrated Discovery) Bioinformatics Resource.

The results obtained for the most important biological processes regulated by the genes inhibiting SLC26A9 traffic include: signal transduction (30 genes), regulation of gene expression (21 genes), protein modification process (19 genes), programmed cell death (18 genes), positive regulation of cell communication (16 genes), establishment of protein localization (16 genes), PI3K-Akt signalling pathway (8 genes), and MAPK signalling pathway (6 genes).

For the genes enhancing SLC26A9 traffic, the obtained results include: signal transduction (13 genes), system development (11 genes), ion transport (8 genes), establishment of protein localization (8 genes), intracellular signal transduction (8 genes), epithelium development (5 genes), and cytoskeleton organization (5 genes).

The most significantly enriched biological processes regulated by the genes that affect the traffic of SLC26A9 to the plasma membrane are signal transduction, represented by a total of 43 genes among 82 hits. This suggests that the traffic to the plasma membrane and the activation of this anion channel are correlated.

Moreover, the results show that major pathways are involved in the regulation of this channel to the plasma membrane, namely PI3K-Akt signalling pathway (8 genes), and MAPK signalling pathway (6 genes). These results were consistent with published data: SLC26A9 activity is regulated by WNKs (serine/threonine kinases). It is thought that WNKS may act as protein scaffolds by regulating SLC26A9 through the C-terminal motifs[99]. Moreover, it is described that WNKs kinases, namely WNK1, modulate signalling through the PI3-kinase pathway and some members of the WNK kinase family have been shown to modulate MAPK signalling[133].

In the total 82 hits found in this pilot screen, 36 of them are also found as hits, enhancers or inhibitors, in the F508del-CFTR traffic screen performed in our laboratory by Hugo Botelho. This result suggests a relationship between CFTR and SLC26A9 traffic pathways as already as mentioned before.

Altogether, the results demonstrated that the cells expressing the double-tagged SLC26A9 are a robust model for future high-content siRNA microscopy screens. Moreover, the results are very encouraging to study in more detail novel regulators of this anion channel as well as to study in more detail the interaction between SLC26A9 and CFTR. Nevertheless, to achieve these goals it is essential to perform this screen assay using more replicates for each siRNA, larger siRNA libraries, to use the cells co-expressing both constructs (eGFP-3xHA-SLC26A9 together with wt- or F508del-mCherry-Flag-CFTR) and to perform a secondary validation of these primary hits.

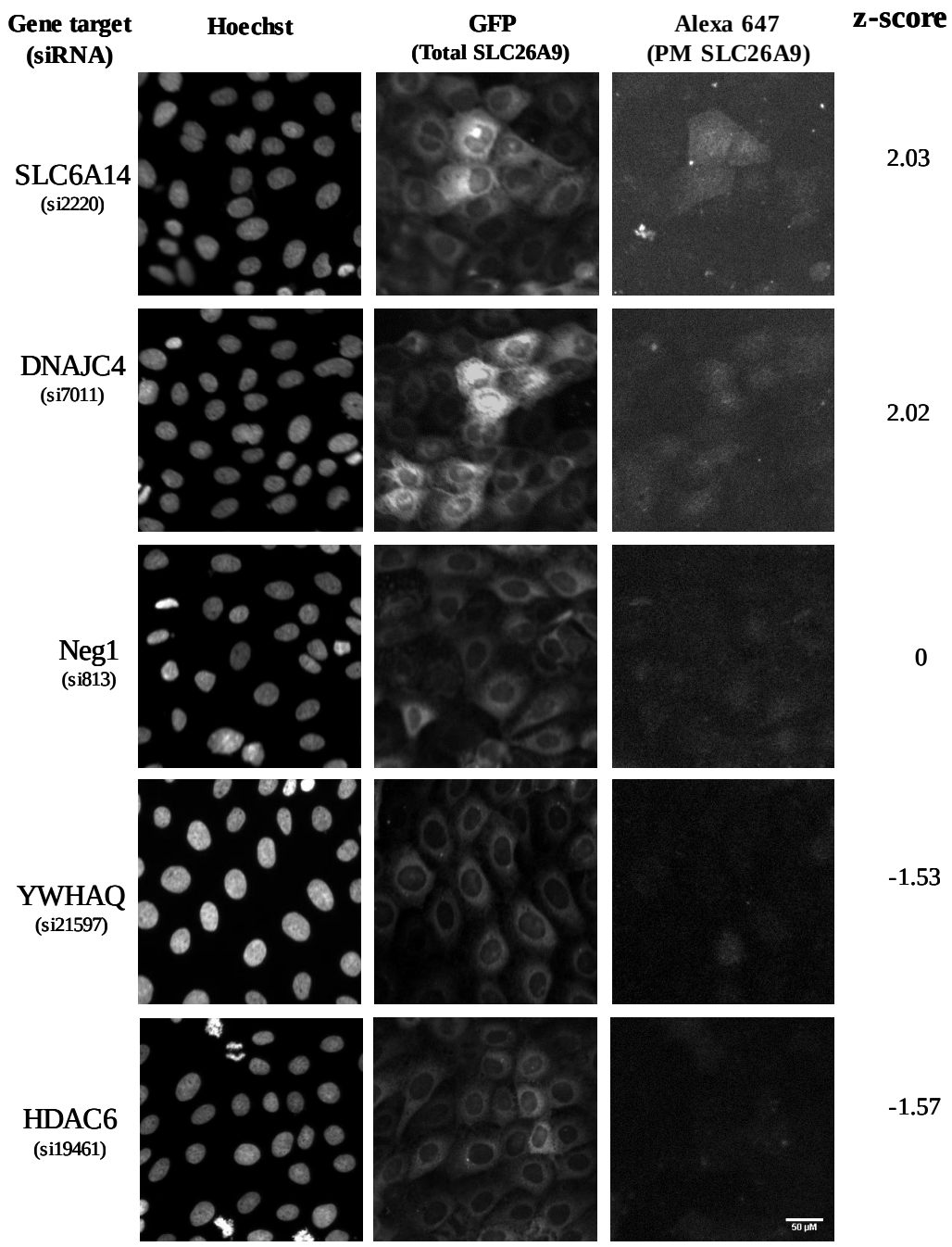

Figure 2.20 Representative images of cells under the effect of the top siRNA hits enhancing or inhibiting SLC26A9 traffic to the plasma membrane. Neg1, z-score equal 0, was represent as a control of SLC26A9 expression at the plasma membrane. Images were acquired with the 10x objective. Scale bar represents 50 µm.

3. Concluding Remarks and Future Perspectives

The results obtained in this MSc project are very inspiring to further pursue the study of identification and characterization of SLC26A4/9 regulators as well as the study of the crosstalk between these two SLC26A proteins and CFTR.

Initially, the effect of CF genotype on the transcript levels of SLC26A4 and SLC26A9 was analysed in CFBE stably overexpressing wt or F508del-mCherry-Flag-CFTR cells and also in fresh native nasal cells from CF and non-CF patients. Although mRNA levels of both transporters seemed to be slightly elevated in CF patients (and for SLC26A9 in F508del-mCherry-Flag-CFTR CFBE cells) this difference was not significant. These results indicate that the levels of SLC26A4/A9 transcripts do not seem to correlate with CFTR function nor PM expression. Further studies are necessary to achieve robust characterization of the mRNA levels, such as their expression levels in lung tissue from CF patients and healthy controls.

Then the localization of SLC26A4 and SLC26A9 was analysed in lung tissue from CF and non-CF individuals. Overall, our results demonstrated that the specific PM localization of these transporters was not altered with the loss of CFTR expression at the PM and with the loss of differentiation of the epithelium. However, these results can be further validated using CF lung tissue with different genotypes as well as with well-preserved healthy tissue, with an intact epithelial layer.

To achieve the main goal of this project, i.e. to identify new regulators of SLC26A4 and SLC26A9 and to study the interaction of these transporters with CFTR, double-tagged SLC26A4/SLC26A9 constructs were generated. These constructs have an eGFP-tag in the N-terminus and a 3xHA-tag in the second extracellular loop, which allows distinguishing between the total transporters being expressed in the cells from the fraction expressed at the PM. Our results have shown that these tags do not affect normal processing, traffic nor localization of both proteins in all cellular models tested.

Novel cellular models were generated, stably expressing the eGFP-3xHA-SLC26A9 construct alone or co-expressing it with wt- or F508del-mCherry-Flag-CFTR, being both tagged SLC and CFTR constructs under an inducible (Tet-On) promoter. These new cell lines were characterized regarding SLC26A9 cellular expression and localization and our results indicate that the expression of CFTR is not essential for the expression of SLC26A9 at the PM.

The CFBE cell line expressing eGFP-3xHA-SLC26A9 alone was then used in a pilot high-content siRNA screen (405 siRNAs, which targeting 206 genes) to identify novel genes regulating the traffic of SLC26A9 to the PM. These siRNA target 80 genes which had been previously shown to also affect CFTR traffic to the PM. Our results showed that 81 siRNA affect SLC26A9 traffic: 52 siRNAs inhibit it (enhancer genes) and 29 siRNAs enhancing it (inhibitor genes). These results suggest a strong relationship between CFTR and SLC26A9 traffic pathways.

As future work, it will be interesting to finish the cloning of eGFP-3xHA-SLC26A4 into pLVX-Tre3G and produce stable cell lines overexpressing only this construct and also co-expressing it with wt- or F508del-mCherry-Flag-CFTR, as already done for SLC26A9. In order to have a homogenous expression of SLC26A4, the cell lines will be sorted and selected for high GFP fluorescence intensity. Then the cells will be characterized regarding SLC26A4 cellular expression and localization, to validate the results from transient transfections. It will also be important to clarify whether the lower band observed in fig 2.10 corresponds to the core-glycosylated form, while the upper band corresponds to the fully-glycosylated form, by performing a glycosidase assay.

It be equally interesting to functionally characterize the cells overexpressing SLC26A4 or SLC26A9. For SLC26A9 the functional activity would be analysed by measuring its Cl^- currents in the Ussing chamber. For SLC26A4, as an electroneutral exchanger, the activity can be assessed by measuring the change in the intracellular pH due to the transport of HCO_3^- by this protein.

To further define the functional interaction between SLC26A4/A9 and CFTR it will be very of high relevance to observe the effect of these transporters on CFTR currents, also using Ussing chamber. This technique allows detecting whether CFTR function is compromised or enhanced by the overexpression of SLC26A4 or SLC26A9. Similarity, it will be highly pertinent to study CFTR function in the absence of these proteins. To this end, SLC26A4/A9 knockout (KO) cell lines (CFBE $41o^-$, CFBE wt- and F508del mCherry-Flag CFTR expressing CFBE cells) can be developed. The KO can be achieved using the CRISPR-Cas9 Gene editing system. For this technique, it will be necessary to design gRNAs specific for these proteins, and then transfect the cells with the plasmids needed for SLC26A knockout (gRNAs targeting each SLC26A and the Cas9 GFP tagged plasmid to cut the DNA). The cells can then be sorted for GFP fluorescence in order to select only the transfected cells. The KO can be confirmed by PCR and WB.

Furthermore, to study the physical interaction between SLC26A4/A9 and CFTR, co-immunoprecipitation assays of CFTR and SLC26A4/A9 can be performed. This can be achieved using cells co-expressing eGFP-3xHA-SLC26A4/A9 and wt- or F508del-mCherry-Flag-CFTR, and using anti-CFTR and anti-SLC26A4/A9 (or anti-Flag and anti-HA) antibodies.

The constructs and new cellular models of SLC26A proteins generated in this MSc project thus open many interesting possibilities in terms of studies that can be pursued. However, the first goal is to use them to perform high-content siRNA screens to identify novel genes regulating the traffic of SLC26A4 and SLC26A9. Overall, the result from the pilot screen for SLC26A traffic demonstrated that this is a robust system to such purpose. In this way, additional screens will be performed with the cells overexpressing only SLC26A4/A9 and hits will then be further classified for their effects in cells co-expressing SLC26A4/A9 and wt- or F508del-CFTR.

The data resulting from such larger-scale screens will be essential to better understand the physiology of these transporters as well as their biological relevance. In turn, the knowledge on the functional crosstalk between CFTR and these two SLC26A transports and the understanding of their regulatory pathways is crucial to possibly find an alternative pharmacological target for CF. Indeed, the design of new drugs that enhance Cl^- secretion, by modulating SLC26A9 activity (independently of CFTR activity), or drugs that mediate the HCO_3^- secretion by SLC26A4, can restore the basic defect in all CF patients, compensating for the absence of CFTR, and thus will work on all patients with CF independently of their CFTR genotype.

4. Material and Methods

4.1. Generation of cell lines overexpressing SLC26A4 or SLC26A9

4.1.1) Plasmids and cDNAs

cDNAs of human SLC26A4 and SLC26A9 were already cloned into pcDNA3.1 (+) vector and pCMV SPORT6, respectively. SLC26A9 cDNA also contained a eGFP (enhanced green fluorescent protein) tag in C-terminus. Both vectors contain an ampicillin resistance gene, which was used for selection of transformed bacteria.

A eGFP-tag was inserted in the N-terminus of SLC26A4 using the In Fusion HD Cloning Kit (Clontech, 631187). Also, a triple hemagglutinin (3xHA) tag was inserted in the second extracellular loop of both constructs (SLC26A4 and SLC26A9) to be used as a marker of these proteins' plasma membrane fraction. In this way, when an immunofluorescence experiment is performed with an antibody that binds to the 3-HA tag without plasma membrane permeabilization, only the membrane proteins are detected.

Then, the double-tagged SLC26A9 construct was cloned into pLVX-TRE3G lentiviral vector, by Dr. Rainer Schreiber from Dr. Karl Kunzelmann's Lab. This process was done in order to produce lentiviral particles to transduce cells and create stably cell lines. pLVX-tet3G (Clontech, 631358) lentiviral vector encodes a Tet-On 3G transactivor protein, which has a high sensitivity to doxycycline (Dox). The inducible promoter P_{TRE3G} was present in pLVX-TRE3G and provides very low basal expression and high maximal expression after induction with Dox. In the presence of Dox, Tet-On 3G binds specifically to P_{TRE3G} and activates the transcription of the cloned gene. The two lentiviral plasmids confer different antibiotic resistances: pLVX-TRE3G contains a puromycin resistance gene and pLVX-Tet3G contains a G418 (geneticin) resistance gene.

Vectors' maps and pLVX-TRE3G cloning sites are displayed in Appendix 1.

4.1.2) Production of competent bacterial

The bacterial strain used for this work was XL1-Blue (XLB1) (Stratagene). XL1-Blue cells are endonuclease (endA) deficient, which greatly improves the quality of miniprep DNA, and are recombination (recA) deficient, improving insert stability. XL1-Blue cells are tetracycline resistant with recA1 endA1 gyrA96 thi-1 hsdR17 supE44 relA1 lac [F′ proAB lacIq ZΔM15 Tn10 (Tetr)] genotype.

To produce competent cells, 20 µl of XL1B were grown in 3 mL of LB medium (NZYTech, MB028) supplemented with 0.075 µg/ µL tetracycline (stock 12 µg/ µL) (NZYTech, MB02201) at 37 ˚C and 220 rpm overnight. The solution was diluted in fresh LB medium (200 mL) and it was grown until a final concentration of bacteria corresponding to an absorbance between 0.45 – 0.55 at 540 nm, exponential growing phase. Then the bacteria were centrifuged at 4 ˚C, 3000 g for 12 minutes. The pellet was resuspended in RF1 solution (100 mM RbCl, 50 Mm $MnCl_2 4.H_2O$, 30 Mm Potassium acetate, 10 Mm $CaCl_2 2.H_2O$, 15 % (w/v) glycerol, pH 5.8, all from Sigma-Aldrich) with 1/3 of initial volume (approximately 33 mL) and incubated on ice for 15 minutes. Then the solution was again centrifuged at 4 ˚C, 3000 g for 12 minutes and the pellet was resuspended in RF2 (10 mM MOPS, 10 mM RbCl, 75 mM $CaCl_2 2.H_2O$, 15 % (w/v) glycerol, pH 6.8, all from Sigma-Aldrich), with 1/12.5 of initial volume (approximately 8 mL). 200 µl bacterial aliquots were rapidly frozen in liquid nitrogen and placed at – 80 ˚C to further use.

4.1.3) Transformation of competent bacterial

Competent cells were transformed by adding between 10-100 ng of DNA to a 200 µl bacterial aliquot, and then incubating for 30 minutes on ice. Then, bacterial cells suffered a heat shock for 1 min and 30 seconds at 42 ◦C followed by 2 minutes on ice. Cells were then incubated for 1 h with 600 µl of LB medium (without antibiotics). The solution was centrifuged for 2 minutes at 6000 rpm, the supernatant was discarded and the pellet was suspended with the rest of the supernatant. Finally, the suspension was plated on LB-agar plates supplemented with 100 µg/ml ampicillin (antibiotic resistance given by the plasmids used in this project) and incubated overnight at 37 ◦C.

4.1.4) Plasmid DNA extraction and quantification

Plasmid DNA purification was performed using the NZYMiniprep kit (NZYtech MB01001). NZYTech's miniprep procedure is based on the alkaline lysis of bacterial cells, followed by a centrifugation step to remove impurities, as genomic DNA, cell debris, while the plasmid DNA is selectively absorbed in the silica gel NZYTech plasmid spin column. After that, the DNA was washed and eluted with a specific buffer, buffer AE. The concentration of DNA was measure using a Nanodrop ND-1000 spectrophotometer (Thermo Scientific), by measuring the absorbance at 260 nm. The purity of the DNA was evaluated by assessment of the ratio A260/A280.

4.1.5) DNA sequencing

After purification of the plasmid DNA (as described in 3.1.4), the samples were sent for sequencing (100-200 ng/µl per reaction). The sequencing reactions were performed by StabVida using Sanger sequencing. The primers used for sequencing were ordered through StabVida, and are displayed in Appendix 5.3.1, Fig 5.10. The software Bioedit was used to analysis the results, by comparison of the obtained sequences with the reference human sequences of SLC26A4 (reference O43511, UniProt) and SLC26A9 (reference Q7LBE3, UniProt).

4.1.6) Mutagenesis

As described above, a triple hemagglutinin tag (3-HA) was inserted in the second extracellular loop of both constructs (SLC26A4 and SLC26A9) to be used as a marker of the proteins localized in the plasma membrane. For SLC26A4 the HA was inserted before the glycosylated residues, and for SLC26A9 the HA tag was insert after them. The localization was selected based on the predicted structure reported[42].

The mutagenesis reaction was performed using the KOD Hot Star Kit (Novagene, 71086) with specific primers shown in the appendix 2, table 5.1. The only difference between the mutagenesis reaction and the normal PCR reaction is the primers because they contain the 3-HA tag meant to be insert. The PCR programme and primers used are presented in appendix 2- Table 5.1 and 5.2.

The amplification of the reaction was confirmed by electrophoresis using 1% agarose gel. To eliminate the template plasmid (plasmid without the insertion), the PCR product was incubated 1 h at 37 ºC with DpnI (Invitrogen, ER1702), a restriction enzyme that specifically hydrolyses methylated DNA.

After this treatment, bacteria were transformed with PCR products as described in 3.1.3. To select bacterial colonies which have the correct insertion of the 3HA-tag, a "colony PCR" was performed using primers that bind 5´ and 3´of the insert sequence (primers and PCR programs in Appendix 2 – Tables 5.5 and 5.6). For colony PCR, the DNA was no-purified, instead, was used the DNA directly from the bacterial colony. The results were analysis by electrophoresis using 1% agarose gel. The

plasmid DNA of the colonies in which the band size was correct was extracted (3.1.3 – Plasmid DNA extraction and quantification), and the insertion was finally confirmed by DNA sequencing (3.1.7–DNA sequencing, and Appendix 5.3).

4.1.7) Cloning

After the insertion of the HA tag in the SLC26A9 cDNA, the double-tagged construct was cloned to the lentiviral vector (as already mentioned above, the cDNA of SLC26A9 already contained a GFP tag in C-terminus). However, after performing an immunostaining assay we determined that the construct with and without 3-HA was not expressed at the plasma membrane. Thus, the construct was sent to Dr. Rainer Schreiber from Dr. Karl Kunzelmann's Lab, were the localization of the eGFP tag was changed from C- to N-terminus, and this new construct was immediately cloned in the inductive lentiviral vector pLVX-TRE3G.

The eGFP tag in N-terminus of SLC26A4 was inserted using the In Fusion HD Cloning kit. First the cDNA of eGFP was amplified through a PCR reaction (primers and PCR programmes in Appendix 2- Tables 5.7 and 5.8), creating extensions of 16 bp and adding a flexible linker of five amino acids (GGGGS)[134] to avoid alterations in the normal folding of both proteins (eGFP and SLC26A4). Simultaneously, the pcDNA3.1 3xHA SLC26A4 was linearized using BamHI (Thermo Scientific ER0051) which generated ends complementary to the eGFP primers. Both products of the PCR reactions were loaded in gel with 0.5% agarose, isolated and purified using the NZYGelpure Kit (NZYTech, MB01102). The "In fusion" reaction was performed as described in appendix and the cells were transformed with the cloning reaction product. The correct insertion was confirmed by "colony PCR". The plasmid DNA of the colonies with the correct amplification size was purified and sent to sequencing through StabVida. 3.1.7 – DNA sequencing, and Appendix 5.3.)

4.1.8) Production of lentiviral particles

Lentiviral particles were produced using the protocol of calcium phosphate transfection. In this protocol, a HEPES-buffered saline solution (HBS) containing phosphate ions is combined with a calcium Cl^- solution containing the DNA to be transfected. When both solution are combined, it forms a calcium phosphate precipitate that is directly layered onto the cells.

To produce the lentiviral particles of pLVX-Tet3G and pLVX-TRE3G eGFP 3xHA SLC26A9 DNAs, HEK 293T cells were used. First, three solutions were prepared: 2,5 M $CaCl_2$; 2 x HBS (HEPES Buffered Saline) 50 mM HEPES, 280 mM NaCl and 1,5 mMm Na_2HPO_4 with the pH adjusted at exactly 7,05; 1/10 TE 1 mM tris-HCl and 0,1 mM EDTA pH 7,60.

The cells were seed at a density of 5 x 10^5 cells per well of a 6-well plate in 2 ml of EMEM + 10% FBS and were incubated for 24 h at 37º C, 5% CO_2. In the next day, two mixtures were prepared, Mix A with 5 µg of plvx-TeT-3G or plvx-Tre3G-SLC26A9), 4 µg of packaging plasmid pCMV-dR/8.74psPAX2, 0.4 µg of enveloped plasmid VSV-G/pMD2.G, 25 µl of $CaCl_2$ solution and 1/10 TE up to 250 µl; and Mix B with 250 µl of 2 x HBS solution. $CaCl_2$ was added to mix A in last to avoid DNA precipitation. Then, while vortexing, Mix B was added to the Mix A. The transfection mix was incubated for 30 minutes at room temperature, and after that added to cells.

The media was replaced 24 h after transfection and 48 later collected and used immediately for infection of cells or stored at -80 ºC for further use.

4.1.9) Lentiviral infection – Generation of stably transduced cells

CBFE 41o$^-$, wt mChrerry-Flag CFBE and F508del mChrerry-Flag CFBE cells were plated in a 6 well plate at a density of 3 x 10^5 per well in 2 ml of DMEM/ EMEM + 10 % FBS and incubated for 24 h at 37º C, 5% CO_2.

Then the cells were co-infected with 1 ml of pLVX-Tet3G, 1 ml pLVX-TRE3G-eGFP-3xHA-SLC26A9 and 4 µl of infection enhancer polybrene (8 µg/ml final concentration, Hexadimethrine bromide, Sigma-Aldrich, H9268-5G). Next, the plates were centrifuged at 220 rpm for 1 h at 25 ºC and were incubated for 24 h at 37º C, 5% CO_2.

To select the transduced cells, the media was changed 24 h after infection for EMEM/DMEM + 10 % FBS containing half of the concentration needed to kill the non-infected cells (1 µg/mL of puromycin – selection of pLVX-TRE3G- eGFP-3xHA-SLC26A9– and 200 µg/mL of G418 – selection of Plvx-Tet3G). wt mChrerry-Flag CFBE and F508del mChrerry-Flag CFBE cells have resistance for puromycin, so these cells were only selected by G418.

The media was changed for EMEM/DMEM + 10% FBS with 2 µg/mL of puromycin (Sigma-Aldrich, P8833) and 400 µg/mL of G418 (Geneticin, Sigma-Aldrich, A1720) 48h later and cells were kept in culture with these conditions, having the media changed every 48 h.

4.1.10) Cell sorting

CFBE 41 o-, wt mChrerry-Flag CFBE and F508del mChrerry-Flag CFBE stably overexpressing eGFP-3xHA-SLC26A9 SLC26A9 were sorted using BD FACSAria™ II cell sorter in IMM (Instituto de Medicina Molecular, Lisboa). The cells were induced with 1 µg/mL of doxycycline and selected according to their GFP fluorescence intensity after 48 h. First, two parameters were used: SSC-A (side scatter) and FSC-A (forward scatter), to distinguish live cells from a mixture of cells. Then, two other parameters were used: FSC-H and FSC-A to selected single cells. Finally, GFP positive cells with higher fluorescence intensity were selected and sorted. The results of the sorting are displayed in appendix 5.

4.2. Cell Culture

4.2.1) Cell lines and culture conditions

During these studies two major types of cell lines were used, Cystic Fibrosis Bronchial Epithelial cells (CFBE) and Human Embryonic Kidney 293T cells (HEK 293T) [133,134]. All cell lines were maintained in culture at 37ºC and 5% (v/v) CO_2.

Human Embryonic Kidney 293T cells (HEK 293T)[133, 134] were cultured with EMEM (Eagle's Minimum Essential Media with L-Glutamine, Lonza - BioWhittaker, BE12-611F) + 10% Foetal Bovine Serum (FBS, Gibco Life Technologies, 10270).

CFBE 41o- cells were cultured with EMEM + 10% FBS, CFBE cells stably overexpressing wt-CFTR or F508del-CFTR (CFBE wt-CFTR or CFBE F508del-CFTR)131 were grown in EMEM supplemented with 10% FBS and 2 µg/mL of puromycin.

CFBE cells stably overexpressing wt-CFTR or F508del-CFTR produced in our lab have a mcherry tag in N-terminus and a FLAG tag in the fourth extracellular loop under Tet-On promoter induction. These cells were grown in DMEM (Dulbecco's Modified Eagle Medium with high glucose and L-

glutamine, Lonza - BioWhittaker, BE12-604F) supplemented with 10 % FBS, 2 µg/mL of puromycin and 100 µg/mL of blasticidin (InvivoGEN, ant-bl-1).

CFBE and CFBE wt/F508del-mCherry-Flag-CFTR cells stably overexpressing eGFP-3xHA-SLC26A9 under Tet-On promoter induction were produced as describe above (Lentiviral infection – Generation of stably transduced cells). Cells were maintained in culture using 400 µg/mL of G418, 2 µg/mL of puromycin and 100 µg/mL of blasticidin (CFBE wt/F508del-mCherry-Flag-CFTR cells).

4.2.2) Transient Transfection

CFBE and HEK293T cells were transient transfected using lipofection, a common method for transfection. For lipofection, cationic liposomes interact with DNA forming stable complexes. These complexes can interact with anionic proteoglycans on the cell surface. Upon binding to the cell membrane, the complexes are internalized via endocytosis. Once the nucleus is reached, the DNA can be transcribed and proteins can be produced.

Lipofectamine 2000

DNA and lipofectamine were incubated separately in Opti-MEM Reduced Serum Medium (Gibco, 31985) during 5 minutes. After that, DNA mix was added to lipofectamine and incubated for 10 minutes at room temperature. This mixture was then added dropwise to attached cells seeded the day before. The ratio DNA/lipofectamine used was 1:3.

JetPEI®

JetPEI reagent and DNA were incubated individually in 150 mM NaCl. The diluted JetPEI solution was vortexed for 10 s and added to the DNA solution. The JetPEI/DNA solution was vortexed for 15 s and incubated at room temperature for 15 to 30 min. The mix was then added dropwise to attached cells.

JetPrime®

DNA was diluted in JetPrime buffer and the solution was vortexed for 5 seconds. The JetPrime reagent was added to this mixture and the resulting mixture was incubated for 10 minutes at room temperature. Finally, the mix was added dropwise to the cells. The ratio used was 1:2 DNA to jetPRIME®.

For all transient transfections, cells were seeded 24 h before transfection at 60-80 % confluency. After the transfection procedure, the medium was changed after 6 h, and the experiments were performed 48 h post-transfection. The efficiency of the transfection can be estimated when the eGFP tag is present by counting the number of fluorescence cells vs non-fluorescence cells.

4.3. Protein Analysis

4.3.1) Western Blot

Protein extraction

Protein was extracted from cells grown on 24-, 12 and 6- well plate. To extract the protein, cells were firstly washed twice with cold PBS and then lysed with sample buffer (1.5% (w/v) SDS; 5% (v/v) glycerol; 0.01% (w/v) bromophenol blue; 0.05 mM dithiotreitol; 0.095 M Tris, pH 6.8) supplemented

with benzonase 25 U/ml (Sigma-Aldrich) and $MgCl_2$ 2.5 mM. The extracts were stored at -20ºC or used immediately in SDS-polyacrylamide gel electrophoresis (SDS-PAGE).

Protein quantification

Total protein concentration was measure by a spectroscopic analytical procedure, Bradford protein assay. This is a colorimetric protein assay based on an absorbance shift of the dye Coomassie Brilliant Blue G-250. A standard curve was prepared using increasing concentrations of a standard solution, bovine serum albumin (BSA) (0 to 35µg/mL) (Sigma-Aldrich, A9647). The protein solution was incubated with Bardford reagent (BioRad, 500-0006) for 5 minutes and then the absorbance was measured at 595 nm using the spectrophotometer (Jasco V-560 UV/Vis Spectrophotometer).

SDS-PAGE

Protein was detected by Western blot analysis. Protein samples were run in 4 % stacking gels ([125 mM Tris HCl pH 6.8; 4% (v/v) acrylamide:bisacrylamide (Bio-Rad, 1610154); 0.1% (v/v) glycerol; 0.1% (v/v) SDS; 0.075% (v/v) ammonium persulphate (APS) (Bio-Rad, 1610700); 0.08% (v/v) tetramethylethylenediamine (TEMED) (Sigma, T9281)].) and 7 % separating gels [375 mM TrisHCl pH 8.8; 7% (v/v) acrylamide; 0.1% (v/v) glycerol; 0.1% (v/v) SDS; 0.075% (v/v) APS;0.06% (v/v) TEMED]. Samples were run on 1x TGS buffer (Bio-Rad, 161-0772) at 60-130 V for 90 to 160 min.

This was followed by transfer onto polivinylidene difluoride (PVDF) membranes (Merck Millipore, IPVH00010), previously activated with methanol (Fisher Scientific, 412) using 1 x TG Buffer (Bio-Rad, 161-0771) and surrounded by ice during 90 minutes at 400 mA.

The membranes were blocked with 5% (w/v) non-fat milk (Nestlé, Molico) in PBS-T [phosphate buffered saline (PBS, NaCl 137 mM; KCl 2.7 mM; KH2PO4 1.5 mM; Na2HPO4 6,5 mM, pH 7.4) and containing 0.1% (v/v) Tween] for 1 h. Then the membranes were incubated overnight with primary antibodies (appendix 9, table 5.12) at 4ºC, also diluted in 5% (w/v) milk in PBS-T. After three washing steps with PBS-T, the membranes were incubated 1 h with secondary antibodies (appendix 9, table 5.13), followed by other three washing steps in the same conditions.

Chemiluminescent detection was performed using a mixture of peroxide:luminol /enhancer solution (BioRad, 170-5061) in a ratio 1:1 on the Chemidoc XRS+ system (BioRad, 170-8265). The quantification of band intensity was performed using the Image Lab software (Bio-Rad laboratories) and normalized to an internal control.

4.3.2) Glycosylation assay

Protein was extracted and quantified was describe above. Then 10 µg of protein were incubated during 10 minutes at 99 ◦C with 1 x glycoprotein denaturing buffer (10 X). For treatment with Endo H (New England Biolabs, P0702) after initial denaturing, cell extracts were incubate during 1 H at 37 ◦C with 2 µl GlycoproteinBuffer 3 (10 X), 2 µl of enzyme (1000 U) until final volume of 20 µl. For treatment with peptide N-glycosidase F (New England Biolabs, P0704) the same conditions of incubations was performing using, 2 µl GlycoproteinBuffer 2 (10 X), 2 µl of 10 % NP-40, 1 µl of enzyme (500 U) until final volume of 20 µl. The samples were then analysed by Western Blot and described above.

4.3.3) Immunofluorescence

Non-polarized cells

CFBE or Hek 293 T cells were grown in cover slips in 24-well plates. Two different protocols were applied, one of them with permeabilization of the plasma membrane and the other without permeabilization.

For both protocols, cells were taken out from the incubator and briefly washed with PBS (137 mM NaCl (Calbiochem, 7760); 2.7 mM KCl (Sigma-Aldrich, P9541); 10 mM Na_2HPO_4 (Sigma-Aldrich, S9763); 1.8 mM KH_2PO_4 (Fluka, 60229); pH 7.4) supplemented with 0.7 mM calcium Cl- ($CaCl_2$) (Sigma-Aldrich, 223506) and 1.1 mM magnesium chloride ($MgCl_2$), designated PBS $^{+/+}$.

In the protocol with permeabilization of the plasma membrane, after washing with $PBS^{+/+}$ cells were fixed with 4% (v/v) paraformaldehyde (PFA) (Merck Millipore, 14003). Then cells were washed 3 times with $PBS^{+/+}$ and permeabilized for 10 min with 0.1% Triton X-100 (v/v). In the next step, cells were again washed with $PBS^{+/+}$ and incubated with primary antibodies for 1 hours at room temperature. Then the cells were again washed twice with $PBS^{+/+}$ (2 x 5 minutes) and incubated with a specific secondary antibody for 1 hour at room temperature and in the dark. This was followed by a new washing step with $PBS^{+/+}$ (2 x 5 minutes) and then cells were incubated with Hoechst 33342 Fluorescent Stain (Life Technologies, H3570), used to stain the nuclei, during 20 minutes at room temperature and in the dark. After two washing steps, the coverslips were mounted in glass slides with Vectashield mounting medium (Vector Laboratories, H-1000) and sealed with varnish.

To perform an immunostaining assay without permeabilization of the plasma membrane, after washing with $PBS^{+/+}$ cells were immediately incubated with primary antibodies for 1 hours on ice. Then cells were washed twice with $PBS^{+/+}$ (2 x 5 minutes) and fixed with 4% (v/v) paraformaldehyde for 10 min. After this step the protocol was the same as described above for immunostaining with permeabilization of the plasma membrane.

Primary and secondary antibodies were diluted in $PBS^{+/+}$ with bovine serum albumin (BSA) 1% (w/v). The antibodies used for immunofluorescence are displayed in appendix 9, table 5.12 and 5.13.

Immunofluorescence staining was observed in the Leica DMI 6000B fluorescence microscope which was also used to acquire the images.

Lung Tissue

Control and CF lung bronchial tissue were obtained from explanted lungs through a collaborative project between the Faculty of Sciences of the University of Lisboa and the Cardio-Thoracic Surgery Department of the Hospital de Santa Marta (Lisboa), which received approval from the hospital's Ethics' Committee.

Control and CF lung tissue was processed in the cell culture under the laminar flow hood by Verónica Felício and Nikhi A.T. A protocol to preserve the tissue and sections of interest, namely, secondary or tertiary bronchi, was applied and the samples preserved and stored in liquid nitrogen.

Tissue sections were cryocut by Luis Marques using a Leica CM1850 UV cryostat. Section were obtained with the desired thickness, 5 to 7 µm and the cryocuts were place in slides superfrost plus (Normax, M0/306). Slides with cryosection were left dry at room temperature and then the sections were separated with hydrophobic marker (PAP pen, Sigma-Aldrich, Z377821), which allow different concentrations or antibodies to be used in the same glass. The first step was hydrate slides with 1X PBS (3 x 5 minutes) and permeabilized the section with triton X-100 0.2% (v/v), already diluted in PBS.

Then other step of washed (3 x 10 minutes) with 1 x PBS was performed. To reduce the auto fluorescence of the tissue, mainly due to the amount of elastin present in the tissue, it was prepared a solution of 1mg/mL (1% m/v) of sodium borohydride ($NaBH_4$) in PBS, immediately before adding to the slide. It was applied 3 x 10 minutes to the slide and then the sections were blocked with BSA 1 % (in 1x PBS) during 30 minutes at room temperature. The next step was washed (3 x 10 minutes) with 1 x PBS and then the sections were incubated overnight at 4 ºC in a dark box with humid atmosphere, with specific antibodies, already diluted in BSA 1%. In the next day, sections were washed (3 x 10 minutes) with 1 x PBS and incubated with secondary antibodies (in BSA 1%) during 2 hours at room temperature kept in a dark box with humid atmosphere. Slides were then washed in the same conditions (3 x 10 minutes with 1 x PBS) and then immersed in a solution of DAPI (4',6diamidino-2-phenylindole dihydrochloride) (Sigma-Aldrich, D9542), 5 µg/mL in 0.1% triton/ 1 x PBS) during 2 minutes to staining the nuclei.

The antibodies used for the immunostainings are described in the Appendix 9, Table 5.12 and 5.13.

4.3.4) Image acquisition, processing and analysis

Images from non-polarized CFBE cells and HEK 293 T cells and tissues were acquired using Leica DMI6000B microscope. For non-polarized cells, a contrast-based autofocus was performed with the Hoechst channel. Then the images were acquired using the appropriate channel for each experiment. All the channels available at the microscope were used: DAPI/Hoechst, GFP, Alexa Fluor 568/mCherry and Alexa Fluor 647/Cy5.

After acquisition, the processing and analysis were done using open source software FIJI for background subtraction, contrast optimization and channel merging.

CFBE eGFP-3xHA-SLC26A9 used in siRNA screens were imaged using the Leica DMI6000B microscope for automatic imaging. The analysis was performed with open source software tools (CellProfiler and R) using specific pipelines appropriate for traffic assays.

4.4. mRNA analysis

4.4.1) RNA extraction and quantification

RNA was extracted from the cells using NucleoSpin® kit (Machery-Nagel, 740955) which allows isolation of RNA with highest integrity. Firstly, non-polarised CFBE cells were lysed with RA1 (lysis buffer) and β-mercaptoethanol. Then the samples were filtrated to clear and reduce viscosity. RNA was bound to a silica membrane followed by a desalting step using Membrane Desalting Buffer (MDB) to increase the efficacy of the next step. DNA was degraded at RT for 15 minutes using DNase. Then the silica membrane was washed and dried and in the final step eluted with RNase-free H_2O. The concentration of eluted RNA was analysed by measurement of the A260nm on a NanoDrop ND-1000 spectrophotometer and the purity was confirmed by measuring the absorbance ratio at 260/280 nm and 260/230 nm wavelengths.

4.4.2) cDNA generation

RNA was used to generate cDNA to perform qPCR and "normal" PCR. cDNA was synthesized using M-MuLV Reverse Transcriptase (Nzytech, MB08301). First, a reaction mixture was prepared on ice: 1 µg of RNA, 50 ng of random hexamer (Nzytech, MB16071), 0.5 mM of dNTPs Mix (Nzytech,

(MB08601)) and nuclease free-water up to 16 µl. This mixture was incubated for 5 minutes at 65 ºC. Then, to the tube was added: 2 µl of 10 x reaction buffer, 1 µl of NZY Ribonuclease Inhibitor (Nzytech, MB084) and 200 units of M-MuLV reverse transcriptase to a final volume of 20 µl. The final mixture was incubated at 37 ºC for 50 minutes followed by a heating step to inactivate the enzyme at 70 ºC for 15 minutes. The cDNA was used immediately for qPCR experiments or stored at -20 ºC.

cDNAs from Nasal epithelial cells from non- CF and F508del-CFTR homozygous patients were obtained at Santa Maria Hospital, Lisbon, Portugal and gently provided by Luka Clarke at the Faculty of Sciences of the University of Lisbon, Lisbon, Portugal.

4.4.3) Quantitative real-time PCR

mRNA expression was analysed using quantitative real-time PCR (q-RTPCR). cDNA from Nasal cells and lung tissue were also used to assess the mRNA expression of SLC26A4 and SLC26A9.

qPCR experiments were performed in 96 well plates (Bio-Rad laboratorieS) with Evagreen reaction mixture (Bio-Rad laboratorieS) using Cx96 real time PCR machine. The primers for SLC26A4 had already been designed by Dr. Luka Clarke using ExonMine database[135] and the primers for SLC26A9 gene had been chosen using the same database. The primers used in qPCR amplify across exon boundaries to minimise potential background amplification of products from genomic DNA.

The qRT-PCR reaction mixture was prepared adding: 5 µl of the template cDNA (diluted 1:5), 250 nM of each forward and reverse primer (Appendix 2, table 5.9), and 1x Evagreen PCR reaction mixture per well. The optimized cycle conditions for Evagreen were used: 10 seconds (sec) at 95 ºC and 30 sec at 60 ºC, and these steps were repeated for 40 cycles. To confirm amplification of specific products, melting curves were performed with a temperature gradient from 65 to 95ºC.

Relative abundance of mRNA was measured for samples run in triplicate using the Bio-Rad CFX Manager 2.0 software (Bio-Rad, 1845000).

Transcript levels of the gene of interest were calculated by normalizing to an endogenous gene, β-actin or Cap-1. The mean threshold cycle (CT) of the target genes was calculated by subtracting the mean CT of the control gene, ΔCT. The fold difference in gene expression was calculated by the relative quantification method using the mathematical equation $2^{-\Delta CT}$.

4.5) Microscopy assay for siRNA screens

4.5.1) siRNAs

The siRNAs used in this experiment belong to a library of siRNAs shown to have an effect on F508del CFTR traffic to the plasma membrane in a traffic assay perfomed by Hugo Botelho (unpublished data) or to interact with wt- and/or F508del-CFTR Negative 1" non-targeting siRNA was used as a negative control.

4.5.2) siRNA screen

A pilot siRNA screen was performed to identify genes that affect SLC26A9 traffic. To achieve this, 384-well plates coated with different siRNAs pre-mixed with lipofectamine were used. CFBE SLC26A9 3-HA GFP cells were grown to confluence and split to 50 %. In the next day, cells were trypsinized to antibiotic-free medium and seeded on siRNA coated 384-well plates (50 µl/well; 2000 cells/well) using a MultidropTM Combi peristaltic dispenser (Thermo Scientific #5840300). 24 hours after seeding, SLC26A9 expression was induced with antibiotic-free medium supplemented with 1

mg/ml doxycycline. Immunofluorescence experiments were performed 48 h after induction, 72 after seeding. The images were acquired automatically using the Leica DMI6000B microscope.

Automatic image analysis was performed with open source software tools (CellProfiler and R) using pipelines tailored for traffic assays. Firstly, an algorithm for background subtraction was applied, where the illumination correction functions are calculated for each fluorescence channel. The second pipeline includes cell segmentation, fluorescence integration, background subtraction and basic quality control. These steps allow the exclusion of cells which do not significantly express SLC26A9, have abnormal morphology (e.g apoptotic cells, cells containing too large or too small nuclei) or contain a significant number of saturated pixels.
Then, an algorithm for quantification of eGFP (SLC26A9) or Cy5 (3-HA) signal was used. This fluorescence quantification data allowed the determination of SLC26A9 traffic efficiency in each cell according to the following formula:

$$SLC26A9\ Traffic\ Efficiency = \frac{PM\ SLC26A9}{Total\ SLC26A9} = \frac{Alexa\ 647\ Integrated\ Fluorescence}{eGFP\ Integrated\ Fluorescence}$$

For each image, the SLC26A9 traffic efficiency was considered the median SLC26A9 Traffic Efficiency for all cells in the image. Then, a custom R script[136] was used in order to exclude out of focus images and images with high background fluorescence.

After averaging the SLC26A9 traffic efficiency for all images from the same siRNA treatment, the effect of different siRNAs towards SLC26A9 traffic was compared with Neg_control siRNA treatment, using the following formula:

$$Deviation\ score = \frac{Traffic\ effienciency - Traffic\ effienciency_{Neg\_control}}{2 \times SEM_{Neg\_control}}$$

Where $SEM_{Neg\_control}$ is the standard error of mean for the "Traffic Efficiency" with the treatment with Neg_control siRNA. SLC26A9 Traffic Efficiency was considered significantly affected by those whose magnitude is larger than twice the negative control SEM. Consequently, genes in which the deviation score was above +1, were considered traffic enhancers. On the other hand, genes having a deviation score below -1 were considered traffic inhibitors.

4.6) Statistical analyses

Data are presented as means ± standard error of the mean (SEM). Data were analysed using Student's *t*-test for paired or unpaired samples when appropriate. $P<0.05$ was accepted as significant.

5. References

1. Massie, J. & Delatycki, M. B. Cystic Fibrosis Carrier Screening. *Paediatr. Respir. Rev.* **872,** 6 (2013).
2. Rafeeq, M. M. & Murad, H. A. S. Cystic fibrosis: current therapeutic targets and future approaches. *J. Transl. Med.* **15,** 84 (2017).
3. Andersen, H. Cystic Fibrosis of the pancreas and its relation to celiac disease. *Am J Dis Child* **56,** 344–399 (1938).
4. Ruslan Dorfman, L.-C. T. The Cystic Fibrosis Gene: A Molecular Genetic Perspective. *Cold Spring Harb. Perspect. Med.* **2,** 1–16 (2012).
5. Schmidt, B., Haaf, J., Leal, T. & Noel, S. Cystic fibrosis transmembrane conductance regulator modulators in cystic fibrosis: Current perspectives. *Clin. Pharmacol. Adv. Appl.* **8,** 127–140 (2016).
6. Kim, S. J. & Skach, W. R. Mechanisms of CFTR Folding at the Endoplasmic Reticulum. *Front. Pharmacol.* **3,** 201 (2012).
7. Saint-Criq, V. & Gray, M. A. Role of CFTR in epithelial physiology. *Cell. Mol. Life Sci.* **74,** 93–115 (2017).
8. Donaldson, S. H. & Boucher, R. C. Sodium channels and cystic fibrosis. *Chest* **132,** 1631–1636 (2007).
9. Fajac, I. & Wainwright, C. E. New treatments targeting the basic defects in cystic fibrosis. *Presse Med.* (2017). doi:10.1016/j.lpm.2017.01.024
10. Sullivan, B. P. O. & Freedman, S. D. Cystic fi brosis. *Lancet* **373,** 1891–1904 (2009).
11. Kube, D. *et al.* Proinflammatory cytokine responses to P.aeruginosa infection in human airway epithelial cell lines. *Am J Respir. Cell Mol. Physiol* **4948,** 493–502 (2001).
12. Al, D. E. T. Interleukin-8 Concentrations Are Elevated in Bronchoalveolar Lavage , Sputum , and Sera of Children with Cystic Fibrosis. *Pediatr. Res.* **34,** 159–161 (1993).
13. Lazzarini, L., Fernando, F. & Lima, A. IL8 gene as modifier of cystic fibrosis : unraveling the factors which influence clinical variability. *Hum. Genet.* **135,** 881–894 (2016).
14. Adriaanse, M. P. M., Sande, L. J. T. M. Van Der, Neucker, A. M. Van Den & Paul, P. Evidence for a Cystic Fibrosis Enteropathy. *PLoS One* **10,** 1–15 (2015).
15. Gilljam, H., Strandvik, B., Ellin, Á. & Wiman, L. Increased mole fraction of arachidonic acid in bronchial phospholipids in patients with cystic fibrosis Increased mole fraction of arachidonic acid in bronchial phospholipids in patients with cystic fibrosis. *Scand. J. Clin. Lab. Invest.* **5513,** (2009).
16. Bhagirath, A. Y. *et al.* Cystic fibrosis lung environment and Pseudomonas aeruginosa infection. *BMC Pulm. Med.* **16,** 174 (2016).
17. Hug, M. J., Tamada, T. & Bridges, R. J. CFTR and Bicarbonate Secretion to Epithelial Cells. *News Physiol Sci* **18,** 38–42 (2003).
18. Riordan, J. R. *et al.* Identification of the Cystic Fibrosis Gene : Cloning and Characterization of Complementary DNA. *Science.* **245,** 1066 1073 (1989).
19. The cystic fibrosis mutation database. Available at: http://www.genet.sickkids.on.ca/app.
20. Johns, T. *et al.* Defining the disease liability of variants in the cystic fibrosis transmembrane conductance regulator gene Users. *Nat Genet.* **45,** 1160–1167 (2014).

21. CF Foundation Patient Registry Data. Available at: https://www.cff.org/2013_CFF_Patient_Registry_Annual_Data_Report.pdf;

22. Boeck, K. De, Zolin, A., Cuppens, H., Olesen, H. V & Viviani, L. The relative frequency of CFTR mutation classes in European patients with cystic fi brosis. *J. Cyst. Fibros.* **97,** (2014).

23. Amaral, M. D., Grande, C., Genomics, I. & Grande, C. Novel personalized therapy for cystic fibrosis: treating the basic defect in all patients. *J. Intern. Med.* **277,** 155–166 (2015).

24. De Boeck, K. & Amaral, M. D. Progress in therapies for cystic fibrosis. *Lancet Respir. Med.* **4,** 662–674 (2016).

25. Guggino, W. B. The cystic fibrosis transmembrane regulator forms macromolecular complexes with PDZ domain scaffold proteins. *Proc. Am. Thorac. Soc.* **1,** 28–32 (2004).

26. Liu, F., Zhang, Z., Gadsby, D. C. & Chen, J. Molecular Structure of the Human CFTR Ion Channel. *Cell* **169,** 85–95 (2017).

27. Farinha, C. M., Matos, P. & Amaral, M. D. Control of cystic fibrosis transmembrane conductance regulator membrane trafficking : not just from the endoplasmic reticulum to the Golgi. *Febs J.* **280,** 4396–4406 (2013).

28. Cook, D. P. *et al.* Cystic Fibrosis Transmembrane Conductance Regulator in Sarcoplasmic Reticulum of Airway Smooth Muscle Implications for Airway Contractility. *Am J Respir.* **193,** 417–426 (2016).

29. Mall, M. A. & Galietta, L. J. V. Targeting ion channels in cystic fibrosis. *J. Cyst. Fibros.* **14,** 561–570 (2015).

30. Schwiebert, E. M. *et al.* CFTR Regulates Outwardly Rectifying Chloride Channels through an Autocrine Mechanism Involving ATP. *Cell* **81,** 1063–1073 (1995).

31. Snijder, B. *et al.* A Call for Systematic Research on Solute Carriers. *Cell* **162,** (2015).

32. Hediger, M. A., Clémençon, B., Burrier, R. E. & Bruford, E. A. The ABCs of membrane transporters in health and disease (SLC series): Introduction. *Mol. Aspects Med.* **34,** 95–107 (2013).

33. Chernova, M. N. *et al.* Functional Comparison of Mouse slc26a6 Anion Exchanger with Human SLC26A6 Polypeptide Variants. *J. Biol. Chem.* **280,** 8564–8580 (2005).

34. Stern, M. *et al.* European Cystic Fibrosis Society Standards of Care : Quality Management in cystic fi brosis. *J. Cyst. Fibros.* **13,** S43–S59 (2014).

35. Marybeth Howard; Raymond A. Frizzell; & David M. Bedwell. Aminoglycoside antibiotics retore CFTR function by overcoming premature stop mutations. *Nature* **2,** 467 (1996).

36. Sala-Rabanal, M., Yurtsever, Z., Berry, K. N. & Brett, T. J. Novel Roles for Chloride Channels, Exchangers, and Regulators in Chronic Inflammatory Airway Diseases. *Mediators Inflamm.* **2015,** (2015).

37. Caputo, A., Caci, E., Ferrera, L., Pedemonte, N. & Barsanti, C. TMEM16A, A Membrane Protein Associated with Calcium-Dependent Chloride Channel Activity. *Science (80).* **322,** 590–594 (2008).

38. Schroeder, B. C., Cheng, T., Jan, Y. N. & Jan, L. Y. Expression cloning of TMEM16A as a calcium-activated chloride channel subunit. *Cell* **134,** 1019–1029 (2008).

39. Yang, Y. D. *et al.* TMEM16A confers receptor-activated calcium-dependent chloride conductance. *Nature* **455,** 2–8 (2008).

40. J., K. *Overview of the SLC26 family and associated diseases*. (2006).

41. Dorwart, M. R., Shcheynikov, N., Yang, D. & Muallem, S. The solute carrier 26 family of proteins in epithelial ion transport. *Physiology.* **23,** 104–14 (2008).

42. Li, J., Xia, F. & Reithmeier, R. a F. N-glycosylation and topology of the human SLC26 family of anion transport membrane proteins. *Am. J. Physiol. Cell Physiol.* **306,** C943-60 (2014).

43. Daniell, H. The SLC26 gene family of Anion Transporters and Channels. *Mol. Aspects Med.* **76,** 211–220 (2012).

44. Epr, C. W. Conserved structure and domain organization among bacterial Slc26 transporters. *Biochem J.* **307,** 297–307 (2014).

45. L . Aravind * † and Eugene Koonin, V. The STAS domain — a link between anion antagonists. *Curr. Biolohy* **10,** 53–55 (1994).

46. Sharma, A. K., Rigby, A. C. & Alper, S. L. STAS Domain Structure and Function. *Cell. Phisiology Biochem.* **28,** 407–422 (2011).

47. Seavers, P. R. *et al.* Structure of the Bacillus Cell Fate Determinant SpoIIAA in Phosphorylated and Unphosphorylated Forms. *Structure* **9,** 605–614 (2001).

48. Ko, S. B. H. *et al.* Gating of CFTR by the STAS domain of SLC26 transporters. *Nat. Cell Biol.* **6,** 343–350 (2014).

49. Rossmann, H. *et al.* The CFTR Associated Protein CAP70 Interacts with the Apical Cl - / HCO 3 - Exchanger DRA in Rabbit Small Intestinal Mucosa. *Biochemistry* **44,** 4477–4487 (2005).

50. Lamprecht, G. *et al.* The Down Regulated in Adenoma (dra) Gene Product Binds to the Second PDZ Domain of the NHE3 Kinase A Regulatory Protein (E3KARP), Potentially Linking. *Biochemistry* **41,** 12336–12342 (2002).

51. Lohi, H. *et al.* Isoforms of SLC26A6 mediate anion transport and have functional PDZ interaction domains. *Am J Physiol Cell Physiol* **284,** 769–779 (2003).

52. Dorwart, M. R. *et al.* Congenital Chloride-losing Diarrhea Causing Mutations in the STAS Domain Result in Misfolding and Mistrafficking. *J. Biol. Chem.* **283,** 8711–8722 (2008).

53. Detro-dassen, S. *et al.* Conserved Dimeric Subunit Stoichiometry of SLC26 Multifunctional Anion Exchangers * □. *J. Biol. Chem.* **283,** 4177–4188 (2008).

54. Ohana, E., Yang, D., Shcheynikov, N. & Muallem, S. Diverse transport modes by the solute carrier 26 family. *J Physiol* **10,** 2179–2185 (2009).

55. Mount, D. B. & Romero, M. F. The SLC26 gene family of multifunctional anion exchangers. *Eur J Physiol* **447,** 710–721 (2004).

56. Soleimani, M. The role of SLC26A6-mediated chloride/oxalate exchange in causing susceptibility to nephrolithiasis. *Physiol, J* **586,** 1205–1206 (2008).

57. Gorbunov, D. *et al.* Molecular architecture and the structural basis for anion interaction in prestin and SLC26 transporters Dmitry. *Nat. Commun.* **5,** 1–13 (2014).

58. Ohana, E., Shcheynikov, N., Yang, D., So, I. & Muallem, S. Determinants of coupled transport and uncoupled current by the electrogenic SLC26 transporters. *J. Gen. Physiol* **137,** 239–251 (2006).

59. Clark, J. S. *et al.* Species differences in Cl − affinity and in electrogenicity of SLC26A6-mediated oxalate / Cl − exchange correlate with the distinct human and mouse susceptibilities to nephrolithiasis. *J Physiol* **586,** 1291–1306 (2008).

60. Shcheynikov, N. *et al.* Coupling Modes and Stoichiometry of Cl − / HCO 3 − Exchange by slc26a3 and slc26a6. *J. Gen. Physiol.* **127,** 511–524 (2006).

61. Liebert, M. A., Sat, G., Regeer, R. R., Lee, A. & Markovich, D. Characterization of the Human Sulfate Anion Transporter (hsat-1) Protein and Gene (SAT1; SLC26A1). *DNA Cell Biol.* **22,** 107–117 (2003).

62. Satoh, H. *et al.* Functional Analysis of Diastrophic Dysplasia Sulfate Transporter. *J. Biol. Chem.* **273,** 12307–12315 (1998).

63. Hlstbacka, J. *et al.* The Diastrophic Dysplasia Gene Encodes a Novel Sulfate Transporter : Positional Cloning by Fine-Structure Linkage Disequilibrium Mapping. *Cell* **78,** 1073–1087 (1994).

64. Höglund, P. et al. Mutations of the Down-regulated in adenoma (DRA) gene cause congenital chloride diarrhoea. *Nature* **14,** 316–319 (1996).

65. Reimold, F. R. *et al.* Pendrin Function and Regulation in Xenopus Oocytes. *Cell Physiol Biochem* **28,** 435–450 (2011).

66. Shcheynikov, N. *et al.* The Slc26a4 transporter functions as an electroneutral Cl − / I − / HCO 3 − exchanger : role of Slc26a4 and Slc26a6 in I − and HCO 3 − secretion and in regulation of CFTR in the parotid duct. *J Physiol* **586,** 3813–3824 (2008).

67. Muskett, J., King, K. A. & Brewer, C. C. SLC26A4 mutation testing for hearing loss associated with enlargement of the vestibular aqueduct. *Worl J Otorhinolaryngol* **3,** 26–34 (2015).

68. Barone, S. *et al.* Regulation of the basolateral chloride / base exchangers AE1 and SLC26A7 in the kidney collecting duct in potassium depletion. *Nephrol Dial Transpl.* **22,** 3462–3470 (2007).

69. Vincourt, J., Jullien, D., Kossida, S., Amalric, F. & Girard, J. Molecular Cloning of SLC26A7 , a Novel Member of the SLC26 Sulfate / Anion Transporter Family , from High Endothelial Venules and Kidney. *Genomics* **79,** 249–256 (2002).

70. Kujala, M. *et al.* Expression of ion transport-associated proteins in human efferent and epididymal ducts. *Soc. Reprod. Fertil.* **133,** 775–784 (2007).

71. Petrovic, S. *et al.* Identification of an apical Cl ⁒ / HCO 3 exchanger in rat kidney proximal tubule. *Am J Physiol Cell Physiol* **285,** 608–617 (2003).

72. El Khouri, E. & Touré, A. Functional interaction of the cystic fibrosis transmembrane conductance regulator with members of the SLC26 family of anion transporters (SLC26A8 and SLC26A9): Physiological and pathophysiological relevance. *Int. J. Biochem. Cell Biol.* **52,** 58–67 (2014).

73. Liu, X. Z. *et al.* Prestin , a cochlear motor protein , is defective in non-syndromic hearing loss. *Hum. Mol. Genet.* **12,** 1155–1162 (2003).

74. Zheng, J. *et al.* Prestin is the motor protein of cochlear outer hair cells. *Nature* **405,** 149–155 (2000).

75. Vincourt, J., Jullien, D. & Amalric, F. Molecular and functional characterization of SLC26A11 , a sodium-independent sulfate transporter from high endothelial venules. *Faseb J.* **17,** 890–892 (2003).

76. Morin, L., Pineau, C. & Dorseuil, O. Tat1 , a Novel Sulfate Transporter Specifically Expressed in Human Male Germ Cells and Potentially Linked to RhoGTPase Signaling *. *J. Biol. Chem.* **276,** 20309–20315 (2001).

77. Lohi, H. *et al.* Functional Characterization of Three Novel Tissue-specific Anion Exchangers SLC26A7 , -A8 , and -A9 *. *J. Biol. Chem.* **277,** 14246–14254 (2002).

78. Dreier, J. P. The role of spreading depression , spreading depolarization and spreading ischemia in neurological disease. *Nat. Med.* **17,** 439–447 (2011).

79. Bassot, C., Minervini, G., Leonardi, E. & Tosatto, S. C. E. Mapping pathogenic mutations suggests an innovative structural model for the pendrin (SLC26A4) transmembrane domain. *Biochimie* **132,** 109–120 (2017).

80. Bizhanova, A. & Kopp, P. The Sodium-Iodide Symporter NIS and Pendrin in Iodide Homeostasis of the Thyroid. *Endocrinology* **150,** 1084–1090 (2015).

81. Nofziger, C., Dossena, S., Suzuki, S., Izuhara, K. & Paulmichl, M. Pendrin Function in Airway Epithelia. *Cell. Phisiology Biochem.* **28,** 571–578 (2011).

82. Lee, H. J. *et al.* Thick airway surface liquid volume and weak mucin expression in pendrin-deficient human airway epithelia. *Physiol. Rep.* **3,** 1–10 (2015).

83. Aizawa, H. & Okinami, S. Identification of Pendrin as a Common Mediator for Mucus Production in Bronchial Asthma and Chronic Obstructive Pulmonary Disease. *J. Immunol.* **108,** 6262–6269 (2008).

84. Musselmann1, K. J.A. Green1, K. S. et al. Salivary Gland Gene Expression Atlas Identifies a New Regulator of Branching Morphogenesis. *Biological* **90,** 1078–1084 (2011).

85. Meyer, G. *et al.* Functional assessment of allelic variants in the SLC26A4 gene involved in Pendred syndrome and nonsyndromic EVA. *PNAS* **105,** 18608–18613 (2008).

86. Nishio, A. *et al.* SLC26A4 expression prevents fluctuation of hearing in a mouse model of large vestibular aqueduct syndrome. *Neuroscience* **329,** 74–82 (2017).

87. Wangemann, P. Mouse Models for Pendrin-Associated Loss of Cochlear and Vestibular Function. *Cell. Phisiology Biochem.* **32,** 157–165 (2013).

88. Fong, P. Thyroid iodide efflux : a team effort ? *J Physiol* **24,** 5929–5939 (2011).

89. Azroyan, A. *et al.* Regulation of pendrin by pH: dependence on glycosylation. *Biochem. J.* **434,** 61–72 (2011).

90. Patel-chamberlin, M., Kia, M. V., Xu, J. & Barone, S. The Role of Epithelial Sodium Channel ENaC and the Apical Cl - / HCO 3- Exchanger Pendrin in Compensatory Salt Reabsorption in the Setting of Na-Cl Cotransporter (NCC) Inactivation. *PLoS One* **10,** 1–16 (2016).

91. Garnett, J. P. *et al.* Novel role for pendrin in orchestrating bicarbonate secretion in cystic fibrosis transmembrane conductance regulator (CFTR)-expressing airway serous cells. *J. Biol. Chem.* **286,** 41069–41082 (2011).

92. Wall, S. M. *et al.* NaCl Restriction Upregulates Renal Slc26a4 Through Subcellular Redistribution Role in Cl ⁻ Conservation. *Hypertension* **44,** 982–987 (2004).

93. Oliver, D. *et al.* Intracellular Anions as the Voltage Sensor of Prestin , the Outer Hair Cell Motor Protein. *Science (80).* **292,** 2340–2344 (2001).

94. Pritchard, J. B. & Renfro, J. L. Renal sulfate transport at the basolateral membrane is mediated by anion exchange. *Cell Biol.* **80,** 2603–2607 (1983).

95. Seshadri, S. *et al.* Increased expression of the epithelial anion transporter Pendrin/ SLC26A4 in nasal polyps of patients with Chronic Rhinosinusitis. *J Allergy Clin Immunol* **136,** 1548–1558 (2016).

96. Nofziger, C. *et al.* STAT6 Links IL-4 / IL-13 Stimulation With Pendrin Expression in Asthma and Chronic Obstructive Pulmonary Disease. *Clin. Pharmacol. Ther.* **90,** 399–405 (2009).

97. Adams, K. M. *et al.* IL-17A induces Pendrin expression and chloride-bicarbonate exchange in human bronchial epithelial cells. *PLoS One* **9,** 1–12 (2014).

98. Pedemonte, N. *et al.* Thiocyanate Transport in Resting and IL-4-Stimulated Human Bronchial

Epithelial Cells: Role of Pendrin and Anion Channels. *J. Immunol.* **178,** 5144–5153 (2015).

99. Dorwart, M. R., Shcheynikov, N., Wang, Y., Stippec, S. & Muallem, S. SLC26A9 is a Cl(-) channel regulated by the WNK kinases. *J. Physiol.* **584,** 333–45 (2007).

100. Chen, A.-P., Chang, M.-H. & Romero, M. F. Functional analysis of nonsynonymous single nucleotide polymorphisms in human SLC26A9. *Hum. Mutat.* **33,** 1275–84 (2012).

101. Shibagaki, N. & Grossman, A. R. The Role of the STAS Domain in the Function and Biogenesis of a Sulfate Transporter as Probed by Random Mutagenesis *. *J. Biol. Chem.* **281,** 22964–22973 (2006).

102. Chang, M., Mount, D. B. & Michael, F. Renal physiology of SLC26 anion exchangers Aleksandra Sin p ic. *Nephrol. Hypertens.* 484–490 (2007).

103. Bertrand, C. a, Zhang, R., Pilewski, J. M. & Frizzell, R. a. SLC26A9 is a constitutively active, CFTR-regulated anion conductance in human bronchial epithelia. *J. Gen. Physiol.* **133,** 421–38 (2009).

104. Phillipson, M. *et al.* Impaired mucus-bicarbonate barrier in Helicobacter pylori- infected mice. *Am J Physiol Gastrointest Liver Physiol* **291,** 396–403 (2006).

105. Anagnostopoulou, P. *et al.* Allergic airway inflammation induces a pro-secretory epithelial ion transport phenotype in mice P. *Eur Respir J* **36,** 1436–1447 (2010).

106. Anagnostopoulou, P. *et al.* SLC26A9-mediated chloride secretion prevents mucus obstruction in airway inflammation. *J. Clin. Invest.* **122,** 3629–3634 (2012).

107. Bertrand, C. A. *et al.* The CFTR trafficking mutation F508del inhibits the constitutive activity of SLC26A9. *Am. J. Physiol. Lung Cell Mol. Physiol.* (2017).

108. Salomon, J. J. *et al.* Generation and functional characterization of epithelial cells with stable expression of SLC26A9 Cl - channels. *Am. J. Physiol. - Lung Cell. Mol. Physiol.* **310,** 593–602 (2016).

109. Strug, L. J. *et al.* Cystic fibrosis gene modifier SLC26A9 modulates airway response to CFTR-directed therapeutics HMG Advance Access. *Hum. Mol. Genet.* **0,** 1–11 (2016).

110. Loriol, L., Boulukos, K. I. M., Borgese, F., Avella, M. & Ehrenfeld, J. SLC26A9 Stimulates CFTR Expression and Function in Human Bronchial Cell Lines. *J. Cell. Physiol.* **226,** 212–223 (2010).

111. Bakouh, N. *et al.* Characterization of SLC26A9 in patients with CF-like lung disease. *Hum. Mutat.* **34,** 1404–1414 (2013).

112. Pereira, S. V.-N., Ribeiro, J. D., Bertuzzo, C. S. & Marson, F. A. L. Association of clinical severity of cystic fibrosis with variants in the SLC gene family (SLC6A14 , SLC26A9 , SLC11A1 and SLC9A3). *Gene* **68,** (2017).

113. Gaitch, N. *et al.* Pancreatology Original article CFTR and / or pancreatitis susceptibility genes mutations as risk factors of pancreatitis in cystic fi brosis patients ? *Pancreatology* **21,** (2016).

114. Miller, M. R. *et al.* Variants in solute carrier SLC26A9 modify prenatal exocrine pancreatic damage in cystic fibrosis. *J. Pediatr.* **166,** 1152–1157.e6 (2015).

115. Fong, P. CFTR-SLC26 transporter interactions in epithelia. *Biophys. Rev.* **4,** 107–116 (2012).

116. Ko, S. B. H. *et al.* A molecular mechanism for aberrant CFTR-dependent HCO3 ± transport in cystic Fibrosis. *EMBO J.* **21,** (2002).

117. Williams, L. Controversies in the Role of SLC26 Anion Exchangers in Pancreatic Ductal Bicarbonate Secretion. *Pancreas* **37,** 221–239 (2008).

118. Chang, M. H. *et al.* Slc26a9 is inhibited by the R-region of the cystic fibrosis transmembrane conductance regulator via the STAS domain. *J. Biol. Chem.* **284,** 28306–28318 (2009).

119. Al., K. H. K. K. M. et. Interaction between CFTR and prestin (SLC26A5). *Biochim Biophys Acta* **1798,** 1029–1040 (2010).

120. Ousingsawat, J., Schreiber, R. & Kunzelmann, K. Differential contribution of SLC26A9 to Cl - conductance in polarized and non-polarized epithelial cells. *J. Cell. Physiol.* **227,** 2323–2329 (2012).

121. Braun, J., Mundhenk, L., Range, F. & Gruber, A. D. Quantitative expression analyses of candidates for alternative anion conductance in cystic fibrosis mouse models. *J. Cyst. Fibros.* **9,** 351–364 (2010).

122. Martins, J. R. *et al.* F508del-CFTR increases intracellular Ca 2+ signaling that causes enhanced calcium-dependent Cl - conductance in cystic fibrosis. *Biochim. Biophys. Acta - Mol. Basis Dis.* **1812,** 1385–1392 (2011).

123. Puchelle, E. *et al.* Differential Localization of the Cystic Fibrosis Transmembrane Conductance Regulator in Normal and Cystic Fibrosis Airway Epithelium. *Am J Respir. Cell Mol. Biol.* **7,** 485–491 (1992).

124. Dupuit, F. *et al.* CFTR and differentiation markers expression in non-CF and ΔF 508 homozygous CF nasal epithelium. *J. Clin. Invest.* **96,** 1601–1611 (1995).

125. Rotman-pikielny, P. *et al.* Retention of pendrin in the endoplasmic reticulum is a major mechanism for Pendred syndrome. *Hum. Mol. Genet.* **11,** 2625–33 (2002).

126. Song, L. *et al.* Genome-wide identification of Hsp70 genes in channel catfish and their regulated expression after bacterial infection. *Fish Shellfish Immunol.* **49,** 154–162 (2016).

127. Botelho, H. M. *et al.* Protein Traffic Disorders : an Effective High-Throughput Fluorescence Microscopy Pipeline for Drug Discovery. *Sci. Rep.* **5,** 1–8 (2015).

128. Karunakaran, S. *et al.* SLC6A14 (ATB 0,+) protein, a highly concentrative and broad specific amino acid transporter, is a novel and effective drug target for treatment of estrogen receptor-positive breast cancer. *J. Biol. Chem.* **286,** 31830–31838 (2011).

129. Sun, L. *et al.* Multiple apical plasma membrane constituents are associated with susceptibility to meconium ileus in individuals with cystic fibrosis. *Nat. Genet.* **44,** 562–569 (2012).

130. Mollapour, M. & Neckers, L. Post-translational modifications of Hsp90 and their contributions to chaperone regulation. *Biochim. Biophys. Acta - Mol. Cell Res.* **1823,** 648–655 (2012).

131. Kawaguchi, Y. *et al.* The deacetylase HDAC6 regulates aggresome formation and cell viability in response to misfolded protein stress. *Cell* **115,** 727–738 (2003).

132. Liang, X. *et al.* Phosphorylation-dependent 14-3-3 protein interactions regulate CFTR biogenesis. *Mol. Biol. Cell* **23,** 996–1009 (2012).

133. McCormick, J. A. & Ellison, D. H. The WNKs: Atypical Protein Kinases With Pleiotropic Actions. *Physiol. Rev.* **91,** 177–219 (2011).

134. Manuscript, A. Fusion Protein Linkers: Property, Design and Functionality. *NIH Public Access* **65,** 1357–1369 (2014).

135. ExonMine database. Available at: http://www.imm.fm.ul.pt/exonmine/.

136. R: The R Project for Statistical Computing.

6. Appendices

6.1) Appendix 1 – Vectors

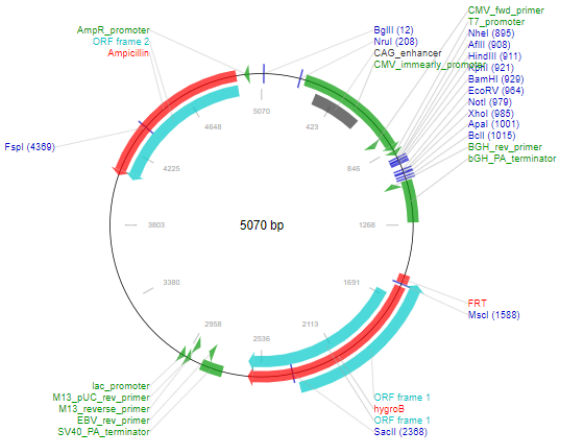

Figure 6.1. pcDNA5/FRT plasmid map, in the lab there are a eGFP insert in the multiple cloning site.

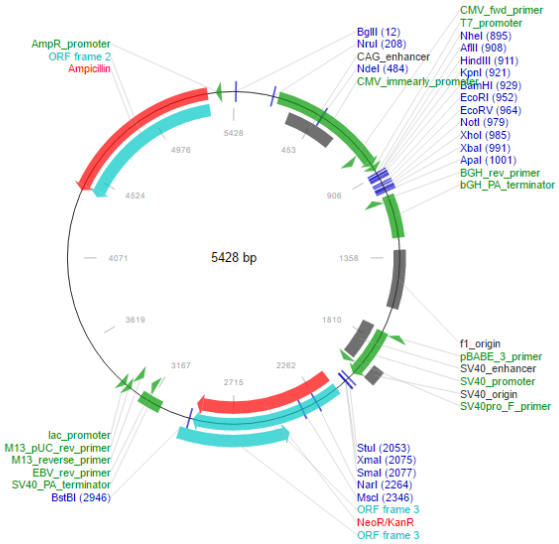

Figure 6.2. pcDNA 3.1 plasmid map

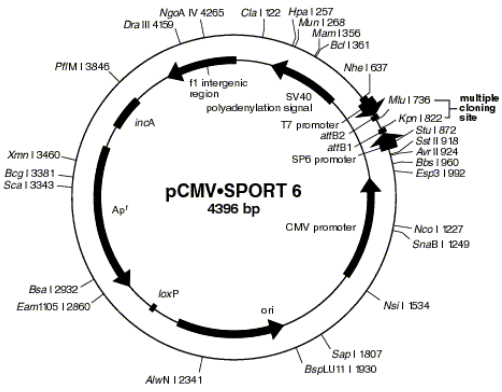

Figure 6.3. pCMV SPORT 6 plasmid map

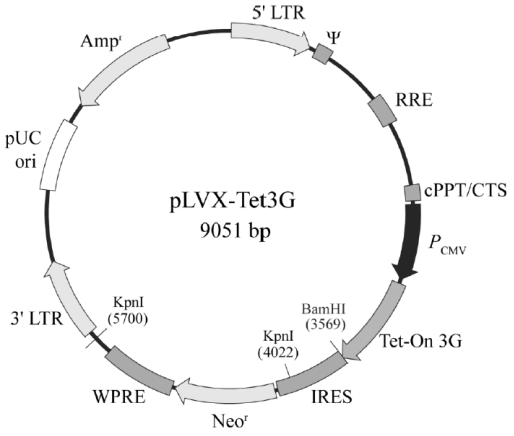

Figure 6.4. pLVX-Tet3G plasmid map

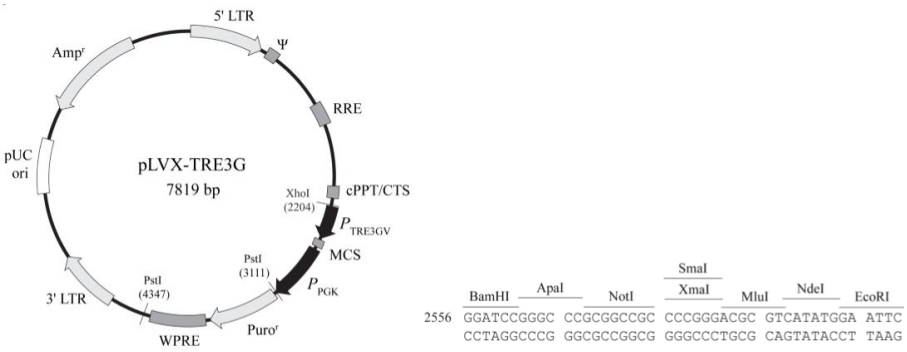

Figure 6.5. pLVX-TRE3G plasmid map and multiple cloning site

6.2) Appendix 2 – Primers and PCR programmes used

Table 6.1. Primers for mutagenesis reactions. The table presents only the forward primers. The 3xHA tag insertion is represented in bold.

Name	**Sequence**
SLC26A4_3HA_F	5‘-CTTTCTCGTATCCAGC**TACCCATACGATGTTCCAGATTACGCTTACCCATACGATGTTCCAGATTACGCTTACCCATACGATGTTCCAGATTACGCT**AGCAATGGAACTGTATTAAATAC-3‘
SLC26A9_3HA_F	5’-CTTCAACAATGCCACCAATGAG**TACCCATACGATGTTCCAGATTACGCTTACCCATACGATGTTCCAGATTACGCTTACCCATACGATGTTCCAGATTACGCT**AGCTATGTGGACACAGCAGCCATG -3’

Table 6.2. PCR programme used for the mutagenesis reactions, insertion of 3xHA tag, in each protein, SLC26A4 and SLC26A9

Programme used for:	**Temperature**	**Time**	**Number of cycles**
SLC26A4	95 ◦C	2 min	30
	95 ◦C	20 s	
	53 ◦C	10 s	
	70 ◦C	3 min 40 s	
	4 ◦C	pause	
SLC26A9	95 ◦C	1 min	30
	95 ◦C	20 s	
	53 ◦C	10 s	
	70 ◦C	6 min	
	4 ◦C	pause	

Table 6.3. Primers for mutagenesis reaction. Single mutation insertion, the nucleotide change is represented in bolt.

SLC's	**Primer Sequence**
SLC26A4	Forward: 5’-GCTGGTCTCACAGC**C**AAAGATTGTCCTC-3’
	Reverse: 5’- GAGGACAATCTTTGGCTGTGAGACCAGC-3’

Table 6.4. PCR programme used for the mutagenesis reactions, insertion of mutation L236P in SLC26A4

Programme used for:	**Temperature**	**Time**	**Number of cycles**
SLC26A4	95 ◦C	2 min	30
	95 ◦C	20 s	
	50 ◦C	10 s	
	70 ◦C	3 min 40 s	
	4 ◦C	pause	

Table 6.5. Primers for colony PCR reactions**.**

SLC's	**Primer Sequence**
SLC26A4	Forward: 5'-TAATACGACTCACTATAGGG-3'
	Reverse: 5'- GGATCTGCCAAGTACCTCACT-3'
SLC26A9	Forward: 5'-GGGAGAGAAACTTCGCAATGC -3'
	Reverse: 5'- ATCCTGGTCGAGCTGGAC-3'

Table 6.6. PCR programs used for the colony PCR reactions of SLC26A4 and SLC26A9

Programme used for:	**Temperature**	**Time**	**Number of cycles**
SLC26A4	94 ◦C	5 min	35
	94 ◦C	1 min	
	53 ◦C	1 min	
	72 ◦C	2 min	
	72◦C	5 min	
	4◦C	pause	
SLC26A9	94 ◦C	5 min	35
	94 ◦C	1 min	
	60 ◦C	1 min	
	72 ◦C	2 min	
	72◦C	5 min	
	4◦C	pause	

Table 6.7 Primers for the PCR reaction for insertion of 16 bp extension, represented in bold in pcDNA5/FRT eGFP. Linker adapted from *Fusion protein linkers: Property, design and functionality*.[134]

SLC's	**Primer Sequence**
SLC26A4 (Insertion eGFP)	Forward: 5'-**TACCGAGCTCGGATC**ATGGTGAGCAAGGGCGAG -3'
	Reverse: 5'-**TGCCATGACCGGATC**TGATCCTCCTCCTCCGGGGCCCGCGGTACCGTC -3'

Table 6.8. PCR programme used for the insertion of the 16 bp extension in eGFP necessary for cloning e-GFP into pcDNA 3.1 3xHA SLC26A4.

Programme used for:	**Temperature**	**Time**	**Number of cycles**
Insert eGFP in pcDNA3.1 3xHA SLC26A4	95 ◦C	3 min	35
	95◦C	20 s	
	60 ◦C	10 s	
	70◦C	5 min	
	4◦C	pause	

Table 6.9. Primers used for RT-PCR

SLC's	**Primer Sequence**
SLC26A4	Forward: 5'-CAGCTAGAGTCCTGATTGCCA-3'
	Reverse: 5'- GGATCTGCCAAGTACCTCACT-3'
SLC26A9	Forward: 5'- GACTACATCATTCCTGACCTGC -3'
	Reverse: 5'- AGGAGTAGAGGCCATTGACTG -3'
b-ACTIN	Forward: 5'- CTCTTCCAGCCTTCCTTCCT -3'
	Reverse: 5'- AGCACTGTGTTGGCGTACAG -3'
Cap-1	Forward: 5'- -3'
	Reverse: 5'- -3'

6.3) Appendix 3 – Result from DNA sequencing

6.3.1) Primers used for sequencing

Table 6.10. Primers used for DNA sequencing

SLC's	**Primer sequence**
SLC26A4	Forward
	5'-CAGCTAGAGTCCTGATTGCCA- 3'
	5'-GGATCTCGGTTTACTAGCTGG-3'
	Reverse
	5'-GGATCTGCCAAGTACCTCACT-3'
	5´- ACTGAACTCTCAGGACCACAG-3'
	5'-GCACAGTCGAGGCTGATCAGC-3'
SLC26A9	Forward
	5'-ACCTCTCCGAGTCCTTCAT-3'
	5'-TCGAAATGGCTATGCACTGG-3'
	Reverse
	5'-TGTGTAGGAGGGGATGGTCA-3'
	5'-ATGTCAGTGTCCATGACCTG-3'
	5'-GTCAGGGTCTCTGCGTGAAA-3'

6.3.2) Sequencing results

6.3.2.1) 3-HA tag insertion

Figure 6.6. Sequencing of 3xHA tag cloned into SLC26A4 plamid, pcDNA3.1 3xHA SLC26A4.

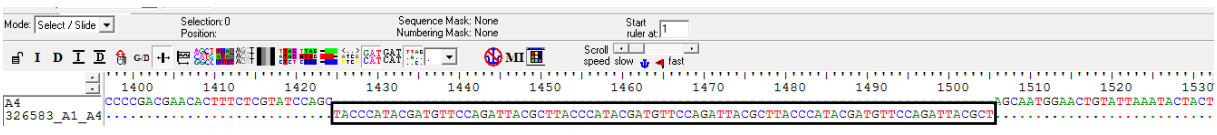

Figure 6.7. Sequencing of 3xHA tag cloned into SLC26A9 plamid, pCMV SPORT 6 eGFP-3xHA-SLC26A9.

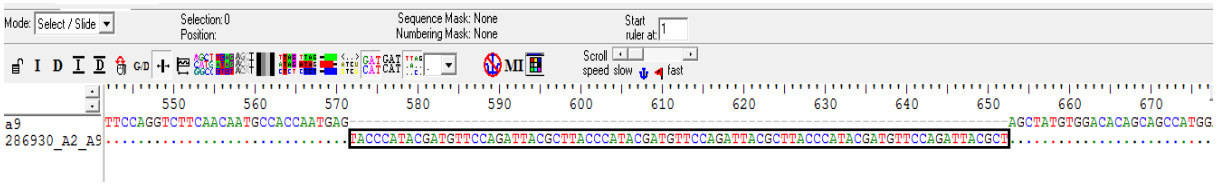

Figure 5.8 Sequencing of eGFP-tag insertion in N-terminal of pcDNA3.1 3xHA SLC26A4, in red is represented the final sequenced of eGFP, in orange is represent flexible linker inserted; at green pcDNA3.1 and at blue is represent the beginning of SLC26A4 protein

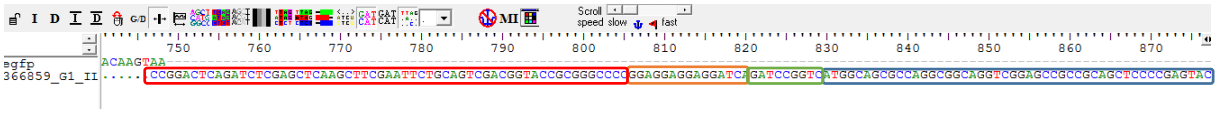

6.3.2.3) Punctual mutation insertion

Figure 6.9. Sequencing of mutation in pcDNA3.1 eGFP-3xHA SLC26A4 in black is represented the replacement of T to C.

6.4) Appendix 4 – Cloning reactions

6.4.1) Cloning reaction to insert eGFP

Table 6.11. Cloning reaction using the In-Fusion HD cloning kit to clone eGFP in pcDNA3.1 3xHA SLC26A4

GFP cDNA	200 ng
pcDNA 3.1 SLC26A4 HA linearized vector	50 ng
In fusion HD Enzyme Premix	2 µl
H20	To 20 µl

6.5) Appendix 5- Immunostaining of SLC26A9 eGFP

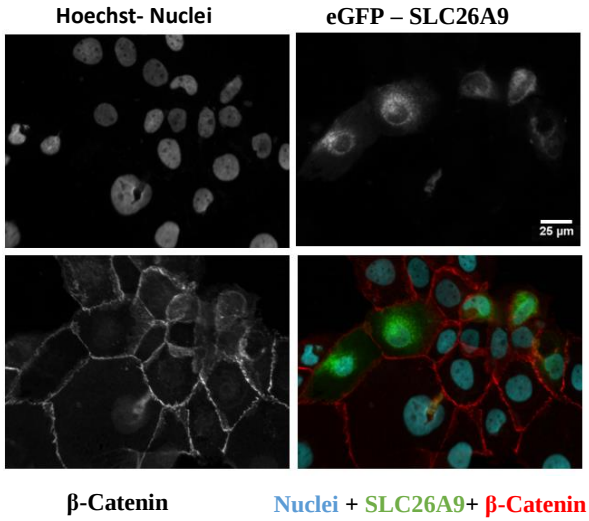

Figure 6.10. Immunofluorescence results of CFBE cells transiently transfected with SLC26A9- eGFP construct, eGFP-tag in the cytoplasmic C-terminal. The plasma membrane was not permeabilized. Markers: Hoechst- Nuclei; eGFP- SLC26A9 staining; Alexa 568- β-Catenin staining (epithelial cell plasma membrane marker). (Primary antibody – anti-β-Catenin;

secondary antibody – Alexa fluor 568) No overlap is detected between β-Catenin and SLC26A9 which mean that the construct of SLC26A9 with GFP in C-terminal is not localized at the plasma membrane. Scale bar represents 25 μm.

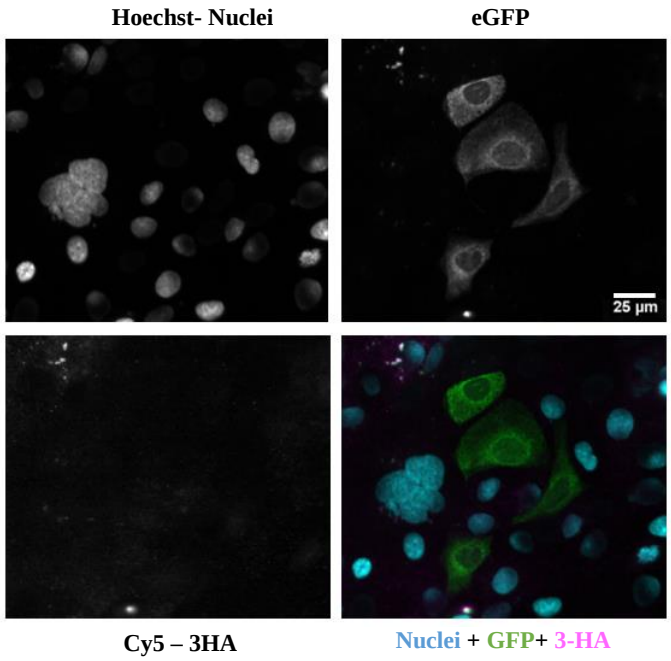

Figure 6.11. Immunofluorescence results of CFBE cells transiently transfected with the first double-tagged eGFP-3xHA SLC26A9, with eGFP-tag in the cytoplasmic C-terminal. The plasma membrane was not permeabilized. Markers: Hoechst- Nuclei; eGFP- SLC26A9 staining and Cy5 – SLC26A9 membrane staining of SLC26A9 if the 3xHA tag was exposed to the outside of the cell. (Primary antibody – anti-HA; secondary antibody – Cy5). The absence of signal at Cy5 channel mean that SLC26A9 is not expressed at the plasma membrane. Scale bar represents 25 μm.

6.6) Appendix 6 – Result from cloning and lentiviral production and transduction

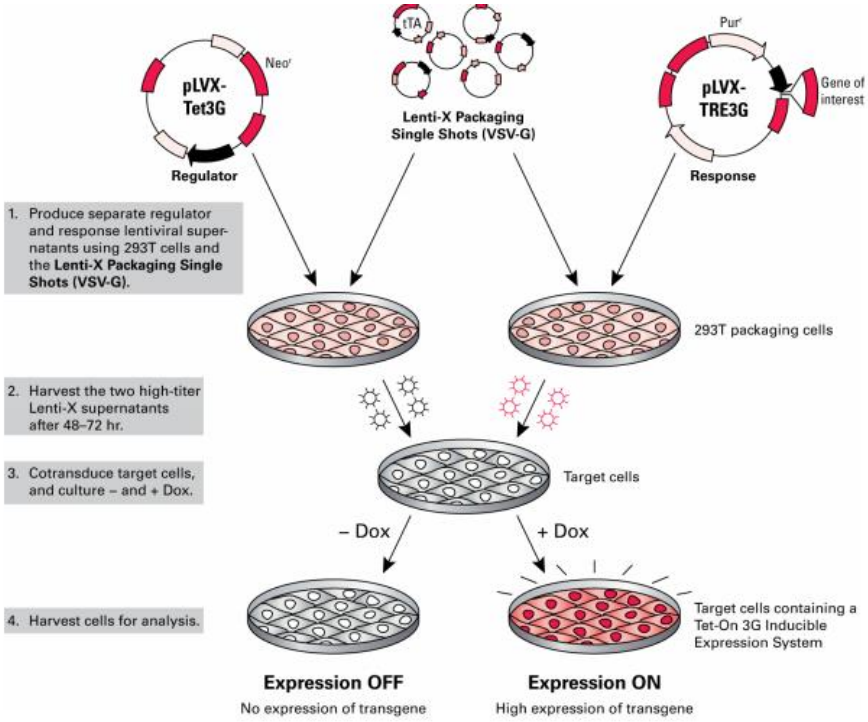

Figure 6.12. Tet-On 3G system (pLVX-TRE3G and pLVX-TET ON) allow inducible gene expression by doxycyline (Dox) in stably transduced cells

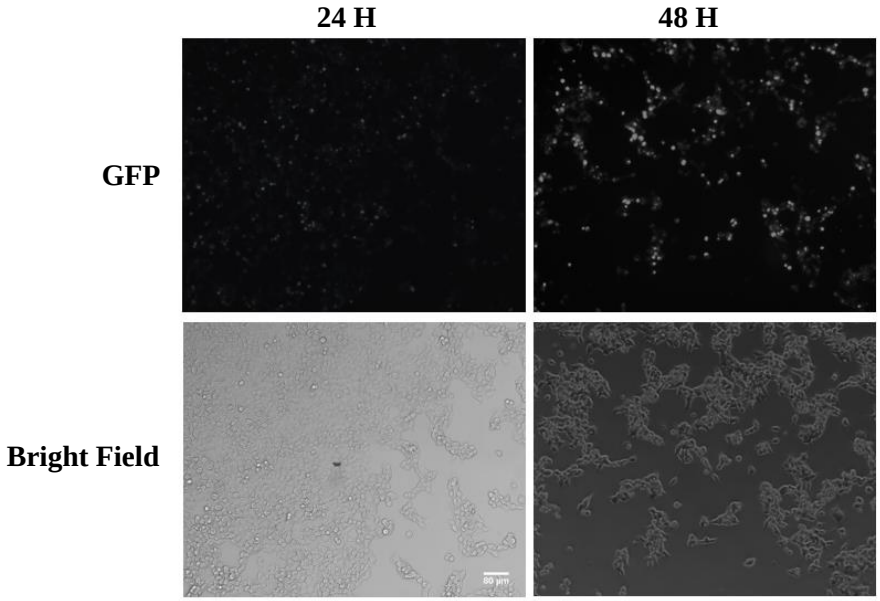

Figure 6.13. HEK 293T cells transiently transduced with lentiviral vectors (pLVX-TRE3G- eGFP-3xHA SLC26A9 and pLVX-Tet3G). On the left are represented transfected cells 24 h after doxycycline induction, while on the right are represented transfected cells 48 h after induction. It is notable the increased of the fluorescence at 48 H. The images were acquired with the 10x objective. Scale bar represents 80 µm.

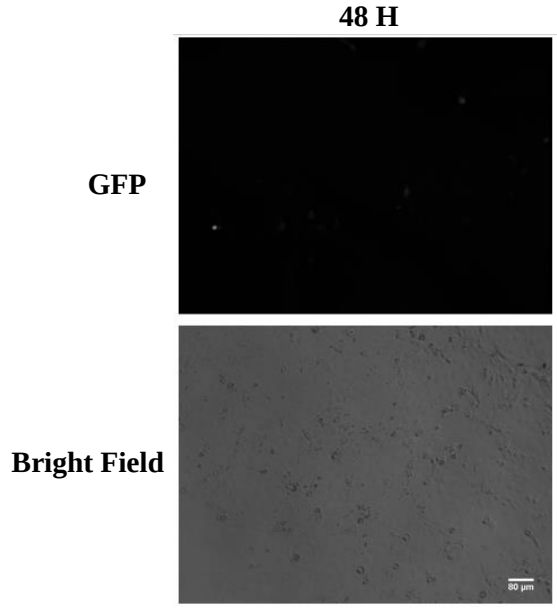

Figure 6.14. CFBE parental cells transiently transduced with lentiviral vectors (pLVX-TRE3G- eGFP-3xHA SLC26A9 and pLVX-Tet3G). Only represented cells 48 h after doxycycline induction, there is no GFP signal after 24 H. The images were acquired with the 10x objective. Scale bar represents 80 µm.

6.7) Appendix 7 – Results from Flow cytometry: cell sorting

6.7.1) CFBE eGFP-3xHA SLC26A9

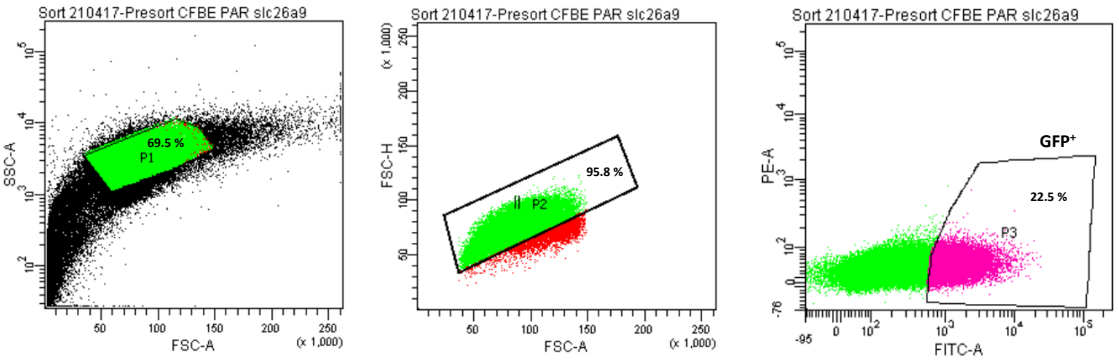

Figure 6.15. – Result from sorting CFBE eGFP-3xHA SLC26A9 cells. Fist, living cell were selected, then was selected single cells. Finally, the GPF positive cells were selected according to emission intensities.

6.7.2) CFBE wt mCherry CFTR eGFP-3xHA SLC26A9

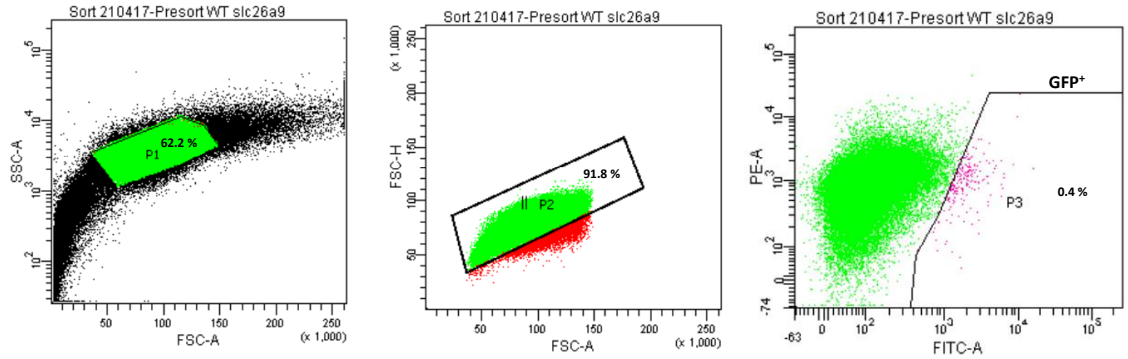

Figure 6.16. Result from sorting CFBE wt mCherry CFTR eGFP-3xHA SLC26A9 cells. Fist, living cell were selected, then was selected single cells. Finally, the GPF positive cells were selected according to emission intensities.

6.7.3) CFBE F508del-mCherry CFTR eGFP-3xHA SLC26A9

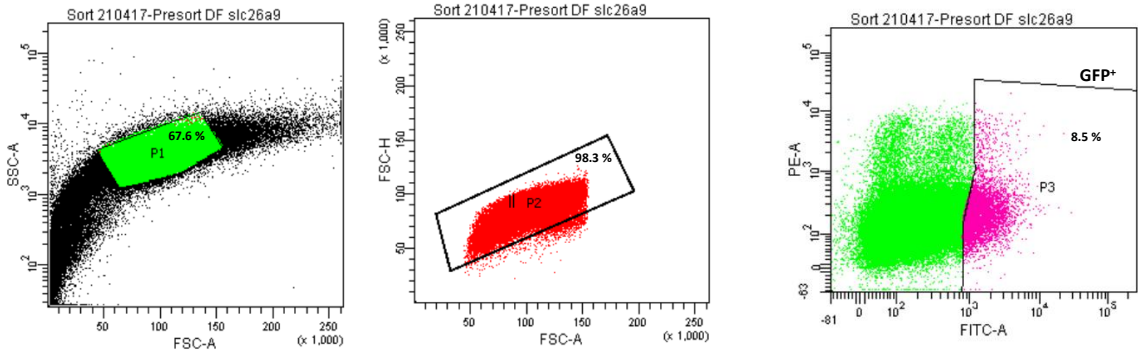

Figure 6.17. Result from sorting CFBE F508del-mCherry CFTR eGFP-3xHA SLC26A9 cells. Fist, living cell were selected, then was selected single cells. Finally, the GPF positive cells were selected according to emission intensities.

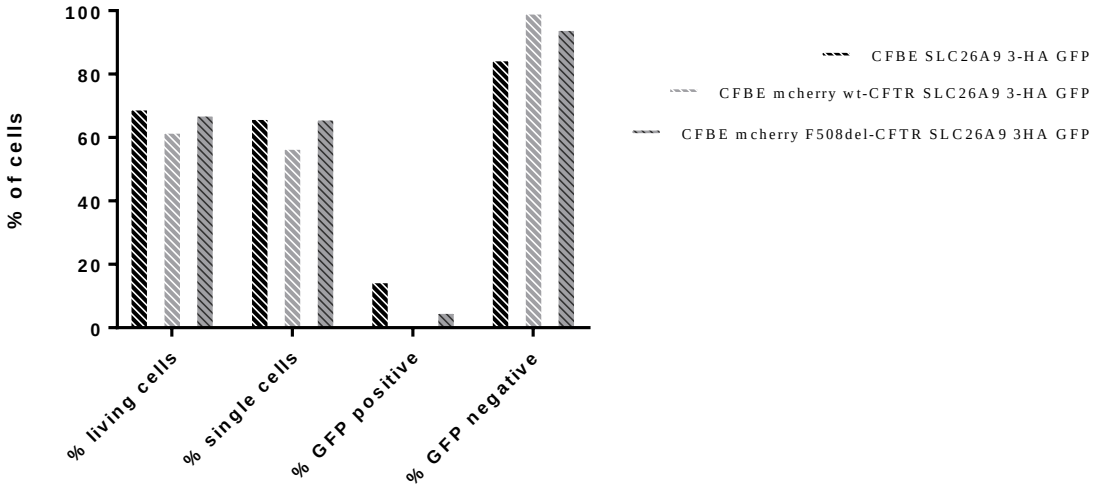

Figure 6.18. CFBE cells sorting statistics. With these results, it is possible to conclude that the quantity of cells stably expressing eGFP-3xHA-SLC26A9 was very lower after sorting.

6.8) Appendix 8 – Structure of the constructs

6.8.1) Structure of SLC26A4 construct

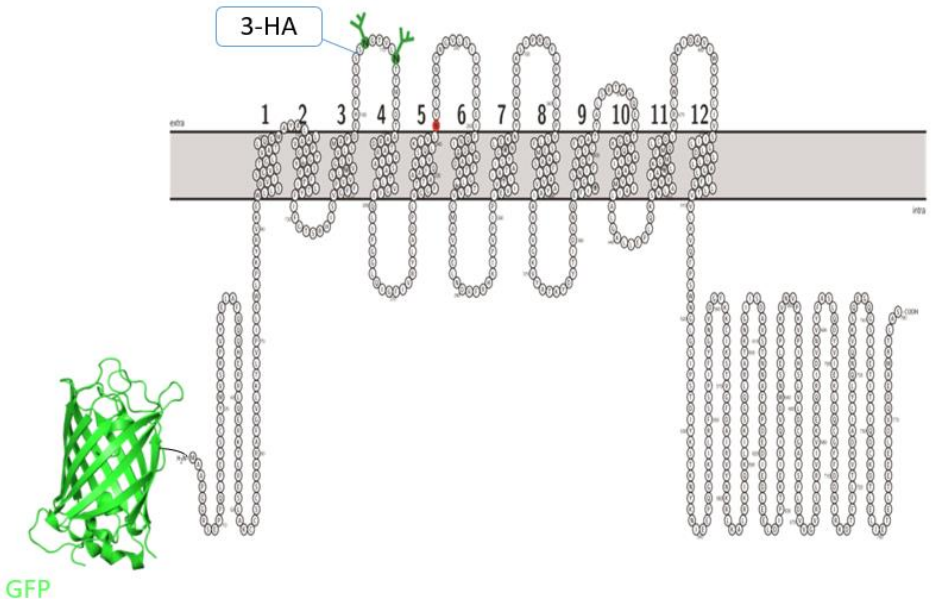

Figure 6.19. Schematic representation of SLC26A4 construct. eGFP was fused to the N-terminal of CFTR and the 3xHA tag was introduced in the second extracellular loop. Adapted from [42].5.8.2) Structure of SLC26A9 construct

6.8.2) Structure of SLC26A9 construct

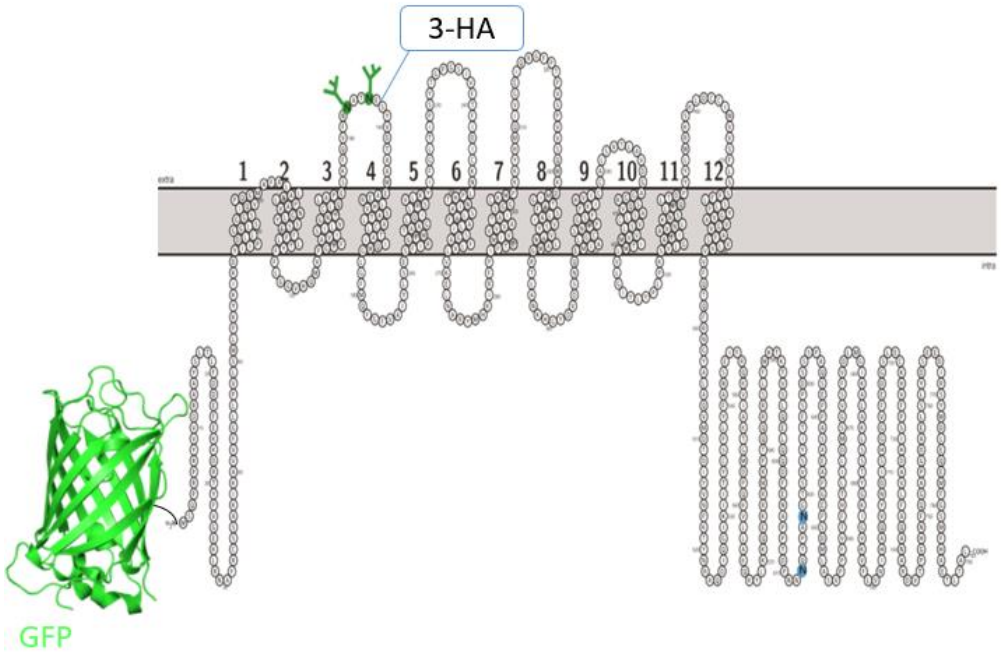

Figure 6.20. Schematic representation of SLC26A9 construct. eGFP was fused to the N-terminal of CFTR and the 3xHA tag was introduced in the second extracellular loop. Adapted from [42].

6.8.3) Structure of CFTR construct

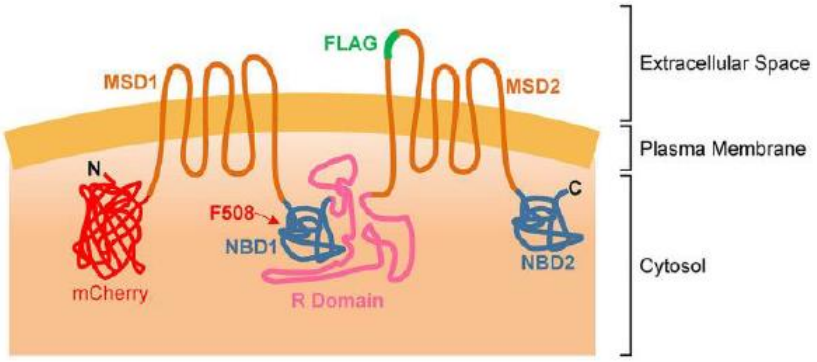

Figure 6.21. Schematic representation of CFTR construct. mCherry was fused to the N-terminus of CFTR and the Flag-tag was introduced in the fourth extracellular loop. Adapted from [127].

6.9) Appendix 9 – Antibodies

Table 6.12. Primary Antibodies used in the present work.

Target	Use	Dilution	Host	Company	Reference
SLC26A4	IF/WB/IHC	IF (1:50)	Rabbit	Abcam	Ab 98091
SLC26A9	IF/WB/IHC	If (1:200) WB(1:500)	Mouse	Novus Biologicals	H00115019-M02
HA	IF/WB	IF (1:200) WB(1:1000)		Covance)	MMS-101P-200, HA.11 16B12
Tubulin	WB	WB (1:3000)		Sigma-Aldrich	T5168
CFTR	WB	WB (1:5000)		CFF	596
E-caderin	IHC	IHC (1:200)		BD Transduction Lab	610181

Table 6.13. Secondary Antibodies used in the present work.

Antibody	**Target**	**Use**	**Dilution**	**Host**	**Company**	**Reference**
Alexa Fluor 488	Mouse IgG	IF/ IHC	1:500	Donkey	Life Technologies	A21202
Alexa Fluor 488	Rabbit IgG	IHC	1:500			A21206
Cy5	Mouse IgG	IF	1:500	Goat		A10524
(H+L)-HRP Conjugate	Rabbit IgG	WB	1:3000		Bio-Rad	170-6516
(H+L)-HRP Conjugate	Mouse IgG	WB	1:3000			170-6515

6.10) Appendix 10 – siRNA pilot screen

Table 6.14. List of siRNAs that inhibit SLC26A9 traffic to the plasma membrane. Data include the z-score and the name and it is specified if the gene is a hit in the traffic of F508del-CFTR to the plasma membrane or if is a CFTR-interacting protein (CIP).

siRNA	z-score	Gene Name	Traffic Screen (ΔF)	CIP (HEK wt)	CIP (HEK ΔF)	CIP (CFBE)
TPI1	1,016	Triosephosphate isomerase		X		
PLA2G5	1,019	Calcium-dependent phospholipase A2	X			
ARRB2	1,037	Beta-arrestin-2			X	
SEC61A2	1,04	Protein transport protein Sec61 subunit alpha isoform 2		X		
ZKSCAN4	1,045	Zinc finger protein with KRAB and SCAN domains 4	X			
BLK	1,072	Tyrosine-protein kinase Blk	X			
ALYREF	1,095	THO complex subunit 4	X			
CRX	1,1	Cone-rod homeobox protein	X			
RELB	1,105	Transcription factor RelB		X	X	
SLC9A6	1,155	Sodium/hydrogen exchanger 6		X	X	
HSF1	1,196	Heat shock factor protein 1		X	X	
MTHFD1L	1,3	Monofunctional C1-tetrahydrofolate synthase, mitochondrial	X			
EMD	1,325	Emerin		X	X	
RPS27A	1,361	Ubiquitin-40S ribosomal protein S27a			X	
TRPC3	1,367	Short transient receptor potential channel 3		X	X	
RCN1	1,37	Reticulocalbin-1		X	X	
PRKG1	1,409	cGMP-dependent protein kinase 1		X	X	
DNAH2	1,42	Dynein heavy chain 2, axonemal	X			
DHRS11	1,64	Dehydrogenase/reductase SDR family member 11	X			
AKT1	1,721	RAC-alpha serine/threonine-protein kinase		X	X	
DNAJC4	2,022	DnaJ homolog subfamily C member 4	X			
KDELR1	2,023	ER lumen protein-retaining receptor 1	X			
SLC6A14	2,025	Sodium- and chloride-dependent neutral and basic amino acid transporter B(0+)		X	X	
GRB2	2,175	Growth factor receptor-bound protein 2		X	X	
CGN	2,332	Cingulin	X			
PDPK1	2,522	3-phosphoinositide-dependent protein kinase 1		X		
DNAJB6	2,677	DnaJ homolog subfamily B member 6		X	X	
SLC6A14	2,681	Sodium- and chloride-dependent neutral and basic amino acid transporter B(0+)		X	X	
SFXN3	2,978	Sideroflexin-3		X	X	
B3GAT3	3,106	Galactosylgalactosylxylosylprotein 3-beta-glucuronosyltransferase 3	X			

Table 6.15. List of siRNAs that enhance SLC26A9 traffic to the plasma membrane. Data include the z-score and it is specified if the gene is a hit in the traffic of F508del-CFTR to the plasma membrane or if is a CFTR-interacting protein (CIP).

SiRNA	z-score	Gene Name	Traffic Screen (ΔF)	CIP (HEK wt)	CIP (HEK ΔF)	CIP (CFBE)
CDK1	-1,919	Cyclin-dependent kinase 1		X		
PLXNA1	-1,835	Plexin-A1	X			
RELA	-1,808	Transcription factor p65		X	X	X
PPP2R2B	-1,61	Serine/threonine-protein phosphatase 2A 55 kDa regulatory subunit B beta isoform		X		X
HDAC6	-1,573	Histone deacetylase 6		X		
HAX1	-1,566	HCLS1-associated protein X-1		X	X	
HDAC6	-1,564	Histone deacetylase 6		X		
YWHAQ	-1,532	14-3-3 protein theta		X	X	
LDLRAD3	-1,501	Low-density lipoprotein receptor class A domain-containing protein 3	X			
PPP2R1A	-1,485	Cellular tumor antigen p53		X	X	X
TNFRSF1A	-1,474	Tumor necrosis factor receptor superfamily member 1A		X	X	
TPM3	-1,472	Tropomyosin alpha-3 chain		X	X	
CDKN1B	-1,444	Cyclin-dependent kinase inhibitor 1B		X	X	
REPS1	-1,443	RalBP1-associated Eps domain-containing protein 1		X	X	X
GNG4	-1,432	Guanine nucleotide-binding protein G(I)/G(S)/G(O) subunit gamma-4	X			
OSBPL9	-1,425	Oxysterol-binding protein-related protein 9	X			
NCS1	-1,416	Neuronal calcium sensor 1	X			
VCP	-1,379	Transitional endoplasmic reticulum ATPase		X	X	
BAG4	-1,374	BAG family molecular chaperone regulator 4		X	X	
HSPA9	-1,347	Cellular tumor antigen p53		X	X	
LCAT	-1,319	Phosphatidylcholine-sterol acyltransferase	X			
GRN	-1,315	Granulins		X	X	
UBA52	-1,311	Ubiquitin-60S ribosomal protein L40		X	X	
ISG20	-1,285	Interferon-stimulated gene 20 kDa protein	X			
IL4R	-1,277	Interleukin-4 receptor subunit alpha	X			
CDH26	-1,266	Cadherin-like protein 26	X			
VIM	-1,251	Vimentin		X	X	
OLA1	-1,236	Obg-like ATPase 1	X			
CLDN16	-1,235	Claudin-16	X			
PAFAH1B3	-1,233	Platelet-activating factor acetylhydrolase IB subunit gamma	X			

PRSS36	-1,213	Polyserase-2	X			
DUPD1	-1,211	Dual specificity phosphatase DUPD1	X			
IL1R1	-1,203	Interleukin-1 receptor type 1	X			
MIER1	-1,197	Mesoderm induction early response protein 1	X			
COMMD1	-1,184	COMM domain-containing protein 1			X	
TM9SF2	-1,177	Transmembrane 9 superfamily member 2	X			
DNAH2	-1,17	Dynein heavy chain 2, axonemal	X			
RIPK2	-1,161	Receptor-interacting serine/threonine-protein kinase 2		X	X	
ADIPOR1	-1,146	Adiponectin receptor protein 1	X			
ACSL4	-1,143	Long-chain-fatty-acid--CoA ligase 4	X			
RAB4A	-1,137	Ras-related protein Rab-4A		X	X	
ANXA5	-1,129	Annexin A5		X	X	X
DGUOK	-1,128	Deoxyguanosine kinase, mitochondrial		X		
AHCYL1	-1,127	S-adenosylhomocysteine hydrolase-like protein 1		X	X	
MAPK12	-1,127	Mitogen-activated protein kinase 12	X			
HSPA1A	-1,113	Heat shock 70 kDa protein 1A		X	X	
GNB2L1	-1,11	Receptor of activated protein C kinase 1			X	
CAPN11	-1,078	Calpain-11	X			
ZNF274	-1,072	Neurotrophin receptor-interacting factor homolo	X			
IKBKB	-1,062	Inhibitor of nuclear factor kappa-B kinase subunit beta			X	
ZNF266	-1,058	Zinc finger protein 266	X			
CHP1	-1,037	Calcineurin B homologous protein 1		X	X	
PDIA3	-1,018	Protein disulfide-isomerase A3		X	X	